7/82

NASA

National Aeronautics and Space Administration

NASA CR-165523

R81AEG759

Recon O
8/25/82

10/82
6/14/83
8/3/83

V/STOL PROPULSION CONTROL ANALYSIS

Phase II - (Tasks 5 Through 9)

Final Draft Report

November 1981

by

General Electric Company
Aircraft Engine Business Group
Evendale, Ohio 45215

Prepared for

National Aeronautics and Space Administration
Lewis Research Center
21000 Brookpark Road
Cleveland, Ohio 44135

NASA Lewis Research Center
Contract NAS3-22057

1. Report No.	2. Government Accession No.	3. Recipient's Catalog No.
NASA CR 165523		

4. Title and Subtitle	5. Report Date
V/STOL PROPULSION CONTROL ANALYSIS - PHASE II	November 1981
	6. Performing Organization Code

7. Author(s)	8. Performing Organization Report No.
Advanced Engineering and Technology Programs Department Aircraft Engine Engineering Division	R81AEG759
	10. Work Unit No.

9. Performing Organization Name and Address	11. Contract or Grant No.
General Electric Company Neumann Way Cincinnati, Ohio, 45215	NAS3-22057
	13. Type of Report and Period Covered Contractor Report 10/1/80 thru 8/31/81

12. Sponsoring Agency Name and Address	14. Sponsoring Agency Code
National Aeronautics and Space Administration Washington, D.C., 20546	

15. Supplementary Notes

Project Manager, J.R. Mihaloew
NASA - Lewis Research Center
Cleveland, Ohio, 44135

16. Abstract

Typical V/STOL propulsion control requirements were derived for transition between vertical and horizontal flight using the General Electric RALS (Remote Augmented Lift System) concept. Steady-state operating requirements were defined for a typical Vertical-to-Horizontal transition and for a typical Horizontal-to-Vertical transition. Control mode requirements were established and multi-variable regulators developed for individual operating conditions. Proportional/Integral gain schedules were developed and were incorporated into a transition controller with capabilities for mode switching and manipulated variable reassignment. A non-linear component-level transient model of the engine was developed and utilized to provide a preliminary check-out of the controller logic. An inlet and nozzle effects model was developed for subsequent incorporation into the engine model and an aircraft model was developed for preliminary flight transition simulations. A condition monitoring development plan was developed and preliminary design requirements established. The Phase I long-range technology plan was refined and restructured toward the development of a real-time high fidelity transient model of a supersonic V/STOL propulsion system and controller for use in a piloted simulation program at NASA-Ames.

17. Key Words (Suggested by Author(s))	18. Distribution Statement
V/STOL Propulsion Control Multi-Variable Control Design	Foreign Distribution Excluded 07

19. Security Classif. (of this report)	20. Security Classif. (of this page)	21. No. of Pages	22. Price*
Unclassified	Unclassified	146	

* For sale by the National Technical Information Service, Springfield, Virginia 22161

TABLE OF CONTENTS

SECTION		PAGE
1.0	SUMMARY	1
2.0	INTRODUCTION	2
3.0	BASELINE PROPULSION SYSTEM & CONTROL REQUIREMENTS	4
	3.1 VCE/RALS Description	4
	3.2 Propulsion Control For Vertical Operations	5
	3.3 Flight Transition Control Requirements	9
4.0	STEADY-STATE OPERATION	10
	4.1 Horizontal Operating Mode	10
	4.2 Vertical-to-Horizontal Transition	10
	4.3 Horizontal-to-Vertical Transition	13
	4.4 Flight Transition Regime	16
	4.5 Remote Flow Control Valve	19
	4.6 Component Operating Characteristics	21
5.0	PROPULSION CONTROL LOGIC	28
	5.1 Control Mode Studies	28
	5.2 Controller Design	30
	5.3 Gain Schedules	33
	5.4 Overall Control Concept	42
6.0	MATHEMATICAL MODELING	45
	6.1 Inlet and Nozzle Effects Model	45
	6.2 Aircraft Model	52
	6.3 Engine Description	54
	6.3.1 Engine Components and Gas Flows	54
	6.3.2 Environmental Inputs and Outputs	56
	6.3.3 Engine and Control System Interfaces	58
	6.3.4 Operating Modes	59

TABLE OF CONTENTS (continued)

SECTION		PAGE
	6.4 Engine Model Description	61
	6.4.1 Thermodynamic Accounting	62
	6.4.2 Iteration Techniques	63
	6.4.3 Model Structure	65
7.0	SIMULATION STUDIES	65
	7.1 Flight Trajectory Simulation	65
	7.2 Engine Transient Simulation Results	71
8.0	CONDITION MONITORING	73
	8.1 Design Plan	75
	8.1.1 Identification of Condition Monitoring Objectives	76
	8.1.2 Condition Monitoring Measurements	77
	8.1.3 Engine/Control Hardware Changes	77
	8.1.4 Generalized Algorithm Development	78
	8.1.5 Evaluation of Instrumentation Sets	78
	8.1.6 Other Condition Monitoring Tasks	79
	8.2 Maximum Likelihood Estimation	80
	8.2.1 Measurement and Objective Function Models	81
	8.2.2 Estimation Model	82
	8.2.3 Optimal Filter	83
	8.2.4 Example	83
	8.3 Suboptimal Filters	86
	8.3.1 Fictitious Process Noise	86
	8.3.2 Moving Window	92
	8.4 Filter Design and Evaluation	98
	8.4.1 Truth Model and Covariance Sensitivity	98
	8.4.2 Examples	99

TABLE OF CONTENTS (continued)

SECTION		PAGE
9.0	LONG-RANGE TECHNOLOGY PLAN	101
	9.1 Control Requirements	104
	9.2 Modeling and Simulation	105
	9.3 Control Logic	106
	9.4 Condition Monitoring	106
	9.5 Propulsion Control Technology Plan	107
10.0	DISCUSSION OF RESULTS	107
11.0	APPENDICES	111
	11.1 Appendix A - Individual Regulator Response to Unit Step Demands	111
	11.2 Appendix B - Scheduled Regulator Response to Unit Step Demands	111
	11.3 Appendix C - Non-Linear Transient Model	134
	11.4 Appendix D - Nomenclature	139
	11.5 Appendix E - References	143

LIST OF FIGURES

FIGURE NO.		PAGE
1	VCE/RALS Baseline Engine	6
2	Propulsion Control For Vertical Operations	8
3	Typical Vertical-to-Horizontal Flight Transition	12
4	Typical Horizontal-to-Vertical Flight Transition	15
5	Thrust Modulation During Flight Transition	18
6	RALS & ADEN Thrust Modulation Capabilities	20
7	Effect Of RFCV On RALS Flow & Pressure	22
8	Front-Block Fan Operating Data	23
9	Rear-Block Fan Operating Data	24
10	Compressor Operating Data	25
11	High Pressure Turbine Operating Data	26
12	Low Pressure Turbine Operating Data	27
13	Four Input-Four Output Linear Engine Model (LEM)	32
14	Open Loop Model For VTH Or HTV Transition Used To Design Controller Matrix	34
15	Computer Generated Structure Of Multivariable Regulator	35
16	Structure Of Multivariable Regulator	36
17	Overall V/STOL Propulsion Control Logic	43
18	Inlet Recovery - Auxiliary Inlet Doors Open	47
19	Inlet Distortion Effects On Fan Performance	48
20	Distortion Transfer To Fan Discharge	49
21	Inlet Distortion Effects On Compressor Performance	50
22	Effects Of Cross-Wind On Nozzle Discharge Coefficient	51
23	Engine Gas Flow Paths	57
24	RALS/VCE Engine Operating Modes	60
25	RALS/VCE Engine Station Designations	66
26	Typical VTH Transition Trajectory	68
27	Typical VTH Thrust Requirements	69
28	Aircraft Pitch Acceleration Due To Forward Motion	70
29	Hybrid Simulation Response To Fan Speed Demand At Takeoff	74
30	Simple Gas Turbine Model	84

LIST OF FIGURES (continued)

FIGURE NO.		PAGE
31	Pressure Ratio Variations	87
32	Temperature Ratio Variations	88
33	Compressor Efficiency Variations	89
34	Turbine Efficiency Variations	90
35	Predicted Standard Deviation Of The Estimate Errors	91
36	Compressor Efficiency Variations With Process Noise	93
37	Turbine Efficiency Variations With Process Noise	94
38	Compressor Efficiency Variations With Moving Window Concept	96
39	Turbine Efficiency Variations With Moving Window Concept	97
40	Truth Model Sensitivity Analysis Concept	100
41	Long-Range Propulsion Control Technology Plan	108

LIST OF FIGURES

FIGURE NO.		PAGE
A-1	Response To Unit Step Demands at Takeoff	112
A-2	Response To Unit Step Demands at Start Transition	113
A-3	Response To Unit Step Demands at Activate RFCV	114
A-4	Response To Unit Step Demands at Mid Transition	115
A-5	Response To Unit Step Demands at Minimum RALS (VTH)	116
A-6	Response To Unit Step Demands at Maximum Horizontal	117
A-7	Response To Unit Step Demands at 30% RALS Flow	118
A-8	Response To Unit Step Demands at 60% RALS Flow	119
A-9	Response To Unit Step Demands at Minimum RALS (HTV)	120
A-10	Response To Unit Step Demands at 80% RALS Flow	121
A-11	Response To Unit Step Demands at Landing	122
A-12	Scheduled Regulator Response To Unit Step Demands at Takeoff	123
A-13	Scheduled Regulator Response To Unit Step Demands at Start Transition	124
A-14	Scheduled Regulator Response To Unit Step Demands at Activate RFCV	125
A-15	Scheduled Regulator Response To Unit Step Demands at Mid Transition	126
A-16	Scheduled Regulator Response To Unit Step Demands at Minimum RALS (VTH)	127
A-17	Scheduled Regulator Response To Unit Step Demands at Maximum Horizontal	128
A-18	Scheduled Regulator Response To Unit Step Demands at 30% RALS Flow	129
A-19	Scheduled Regulator Response To Unit Step Demands at 60% RALS Flow	130
A-20	Scheduled Regulator Response To Unit Step Demands at Minimum RALS (HTV)	131
A-21	Scheduled Regulator Response To Unit Step Demands at 80% RALS Flow	132
A-22	Scheduled Regulator Response To Unit Step Demands at Landing	133

LIST OF TABLES

TABLE NO.		PAGE
1	Typical Horizontal Flight Operating Conditions	11
2	Typical Vertical-To-Horizontal Operating Conditions	14
3	Typical Horizontal-To-Vertical Operating Conditions	17
4	Vertical-To-Horizontal Transition Mode Study	30
5	Horizontal-To-Vertical Transition Mode Study	31
6	Proportional And Integral Gain Constants For The Vertical-To-Horizontal Transition Controller	37
7	Proportional And Integral Gain Coefficients For The Horizontal-To-Vertical Transition Controller	38
8	Use Of Linear Regression To Determine Proportional And Integral Gain Constants For The Vertical-To-Horizontal Transition Controller	40
9	Use Of Linear Regression To Determine Proportional And Integral Gain Constants For The Horizontal-To-Vertical Transition Controller	41
10	Effects Of Cross-Wind On Nozzle Thrust Coefficient	53
11	Assumed VTH Pilot Model	55
12	Sensitivity Analysis Of Measurement Noise	102
13	Reduced State Analysis	103

1.0 SUMMARY

This report describes the results of Phase II of the V/STOL Propulsion Control Analysis Program for the development of propulsion control technologies for achieving integrated V/STOL aircraft-engine controls. The Phase I study was focused on the development of a long-range technology plan, the selection of a representative baseline V/STOL propulsion system, and the development of propulsion control design concepts for the vertical flight regime. The current Phase II program retained the Phase I baseline propulsion system and developed propulsion control design concepts for the flight transition regime between vertical and horizontal flight.

The General Electric RALS (Remote Augmented Lift System) concept was retained as a baseline engine and was used to establish typical operating conditions along Vertical-to-Horizontal (VTH) and Horizontal-to-Vertical (HTV) transition processes. Analytical studies were conducted at each selected operating condition to establish steady-state operating requirements, to define a recommended closed-loop regulator configuration, and to establish regulator gains for achieving stable control operation. Regression techniques were utilized to develop one set of gain schedules for the VTH transition and a second set of schedules for the HTV transition.

Baseline engine component performance characteristics were utilized to develop a component-level regression model of the baseline engine. Internal model aerothermo relationships were based on approximated real variable gas properties. The resulting non-linear transient engine model was combined with non-linear transient models of the actuators, augmentors, and nozzles to provide a non-linear simulation capability for evaluating the regulator gain schedules.

Additional mathematical models were developed for the inlet and nozzles and for a typical V/STOL aircraft configured for RALS. The inlet and nozzle effects model represents inlet distortion effects on the fan and compressor and nozzle deflection effects on flow coefficient.

The aircraft model was combined with a simple pilot model and used to examine typical transition trajectories and their corresponding propulsion control requirements.

The long-range propulsion control technology plan was refined to focus on those technology requirements essential for achieving a piloted-simulation capability at NASA-Ames in the 1984-85 time period.

2.0 INTRODUCTION

A V/STOL propulsion system must provide vertical thrust for takeoff and landing, horizontal thrust for conventional flight, and thrust components in each direction for achieving a controlled transition between the two flight regimes. Concurrent flight path and attitude control requirements must be provided by the propulsion system in the low-speed flight regime and by both the propulsion system and the aircraft aerodynamic control surfaces in the transitional flight regime until sufficient flight speed has been achieved for full aerodynamic control. Integrated aircraft-engine controls can be expected to be an essential requirement for achieving effective aircraft stability and control in the low flight speed and transitional flight regimes.

The current V/STOL Propulsion Control Analysis Program represents Phase II of a multi-phase program for the development of the propulsion control technologies for achieving integrated aircraft-engine controls. The overall program is aimed at the development of the propulsion control design technology base, design analysis procedures, control logic requirements, and an overall system evaluation capability through piloted aircraft-engine simulations. The initial Phase I program involved the definition of typical propulsion control requirements, the establishment of a long-range technology development plan, and the development of typical propulsion control logic requirements for the vertical flight operating regime. The results of the Phase I program were published in Reference 1. The current Phase II program represents an extension of the Phase I effort to the transitional flight regime between vertical and horizontal flight. Subsequent program phases would further extend the program to the

conventional flight regime and would address the overall problems of aircraft-engine control integration.

The General Electric RALS (Remote Augmentor Lift System) concept was selected as a baseline engine in the Phase I study in order to provide information on typical V/STOL propulsion system operational characteristics and control requirements. The baseline RALS engine was retained for the current Phase II studies so that the Phase I results could be used to establish interface requirements with the vertical flight regime.

Specific operational requirements were established for the following transitional processes:

- Vertical takeoff at maximum weight to horizontal accelerated climb at maximum power setting.
- Horizontal descent at flight idle to vertical landing at minimum weight.

A number of specific operating points were identified along each of the above trajectories and corresponding steady-state operating requirements were established. Control mode studies were conducted at each individual operating point to define closed-loop control requirements. Linear state-space models were developed for each point and were used to define a multi-variable regulator design using the K-Q Matrix technique. Regulator gain schedules were obtained by regression of the individual designs. One set of schedules was obtained for the vertical-to-horizontal transition and a second set for the horizontal-to-vertical transition.

A non-linear transient model of the baseline engine was constructed from regressions of the individual engine component operating characteristics. The component regressions were combined with regressions of variable gas property thermodynamics and with the non-linear models of the augmentors, nozzles, sensors, and actuators developed under the Phase I program to obtain a non-linear transient model of the propulsion system. The propulsion system model was used in conjunction with a mathematical model of the control logic to conduct simulation studies

of typical transition operations. Additional mathematical models of inlet and nozzle effects and of a typical RALS aircraft configuration were also developed. The inlet and nozzle effects model defines the effects of high inlet distortion and nozzle deflections on the engine and will be combined with the propulsion system model during a subsequent phase of this program. The aircraft simulation has been used to determine propulsion control requirements and operating characteristics during the transition process.

This report contains a description of typical steady-state operating requirements during the transition process, a description of recommended closed-loop control configurations and corresponding regulator gain requirements, and a discussion of the component regression process for the development of the engine model and a brief description of the resulting model. It also contains an overall propulsion control concept for integrating engine, flight, and transition control requirements and a revised long-range technology plan for achieving a piloted simulation capability.

3.0 BASELINE PROPULSION SYSTEM AND CONTROL REQUIREMENTS.

3.1 VCE/RALS Description

V/STOL propulsion systems are required to provide thrust, bleed air, and power extraction in each of the following operational modes:

- Vertical Mode - Requires vertical lift thrust over the range of takeoff and landing weights to achieve ascent, descent, and hover.
- Attitude Control - Requires direct thrust or bleed air for achieving roll, pitch, and yaw control at low speeds when aircraft aerodynamic control surfaces are ineffective.
- Transition Mode - Requires a continuous thrust vector rotation capability for achieving transitions between vertical and conventional horizontal flight.
- Horizontal Flight Mode - Requires propulsive thrust, customer bleed, and power extraction for conventional horizontal flight.

In order to achieve a high performance V/STOL capability, it will be essential to integrate each of the above operating mode requirements

into a variable cycle engine concept which can be adapted to each set of requirements and which minimizes the need for special geometry for any one mode of operation.

The General Electric Variable Cycle Engine/Remote Augmentor Lift System (VCE/RALS) was conceived for this purpose and was selected as the baseline engine for the previous Phase I Study of V/STOL Propulsion Control. It has been retained as the baseline propulsion system for the current Phase II study and is illustrated in Figure 1. The VCE consists of a single-bypass turbofan engine with the following features:

- The fan is split into a forward two-stage block driven by the low pressure turbine and a rear single-stage block driven by the high pressure turbine.
- Variable rear block fan stators and a variable low pressure turbine nozzle (VALPTN) for internal flow and pressure ratio control.
- A variable area bypass injector (VABI) for mixing fan and turbine discharge flows into the mixed-flow augmentor.
- An Augmented Deflector Exhaust Nozzle (ADEN) for varying the primary thrust vector angle.

The RALS concept adds to this VCE a remote augmentor and a vectorable remote nozzle which can be located near the nose of the aircraft in order to maximize the separation distance between the two thrust vectors. The remote system is operated by extracting most of the bypass air through a manifold and ducting it forward to the remote augmentor and nozzle. The remote system is shut down by modulating the VABI to direct all of the fan discharge air to the mixed-flow augmentor and ADEN nozzle. The current VCE/RALS concept uses both augmentors and nozzles in conjunction with engine speed modulation for vertical thrust control, mixed-flow and remote augmentor fuel-flow modulation for attitude control, remote flow modulation for transition trajectory control, and only the basic VCE for horizontal thrust control.

3.2 Propulsion Control For Vertical Operation

The propulsion control concept for the vertical operating mode was developed in the Phase I study of the current program and is illustrated

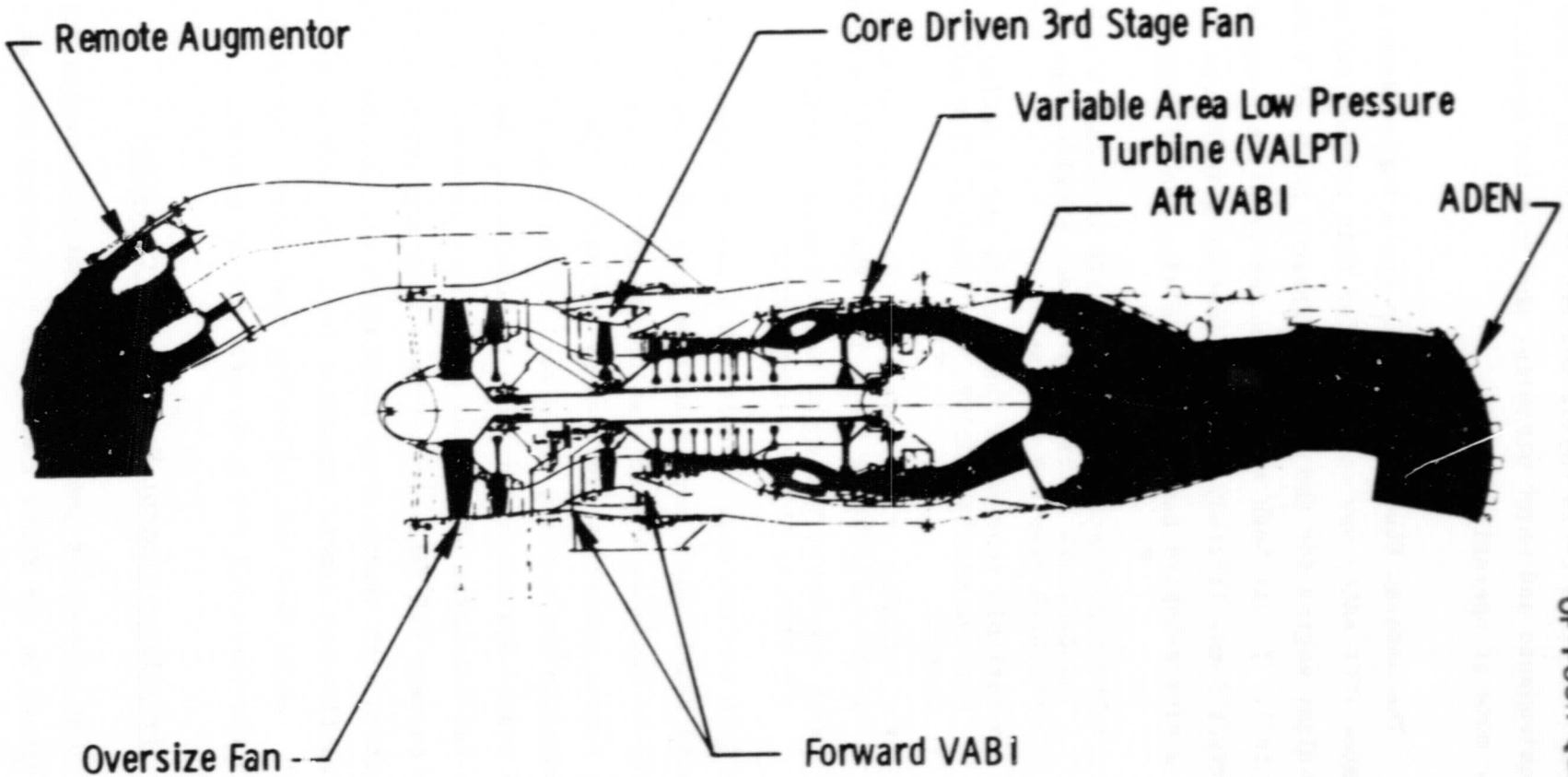

Figure 1. VCE/RALS Baseline Engine

in Figure 2. It consists of a multi-variable regulator for controlling the total engine thrust and a set of feed-forward schedules for modulating augmentor fuel-flows in response to attitude control demands.

The multi-variable regulator operates over the range of 60-100% takeoff thrust to provide total thrust control during vertical takeoff and climb, hover, and vertical descent and landing. It consists of four closed control loops which set primary fuel flow, low pressure turbine nozzle area, and primary and remote exhaust nozzle areas to achieve zero feedback errors in the fan speed, turbine temperature, compressor discharge pressure and fan discharge duct Mach number loops. Nominal mixed-flow and remote augmentor fuel-flows are scheduled open-loop along with the remaining VCE geometries (rear-block fan stators and VABI area). The regulator responds to a total thrust demand signal from the aircraft flight computer and represents the primary fuel control system. It must be integrated with accel/decel fuel schedules, limit protection schedules, bleed and power extraction compensation, etc. and these will be addressed during a subsequent phase of this program.

The feed-forward schedules operate over the range of $\pm$ 12% of nominal ADEN and remote nozzle thrust and provide the response to attitude control demands from the aircraft flight computer. These schedules provide mixed-flow and remote augmentor fuel flow modulation and ADEN and remote nozzle thrust deflections. The current VCE/RALS concept provides total thrust modulation for height control, differential thrust modulation for pitch control, differential thrust deflection for yaw control, and customer bleed extraction for roll control. It has been assumed that the aircraft flight computer demand signals will be the actual thrust magnitude and direction requirements.

The thrust and attitude control systems interact through the augmentor fuel flows and exhaust nozzle areas which are common to both systems. The interaction has, however, been minimized by the addition of gain compensation schedules to both the regulator and the feed-forward schedules. Regulator gain compensation modulates augmentor fuel flow

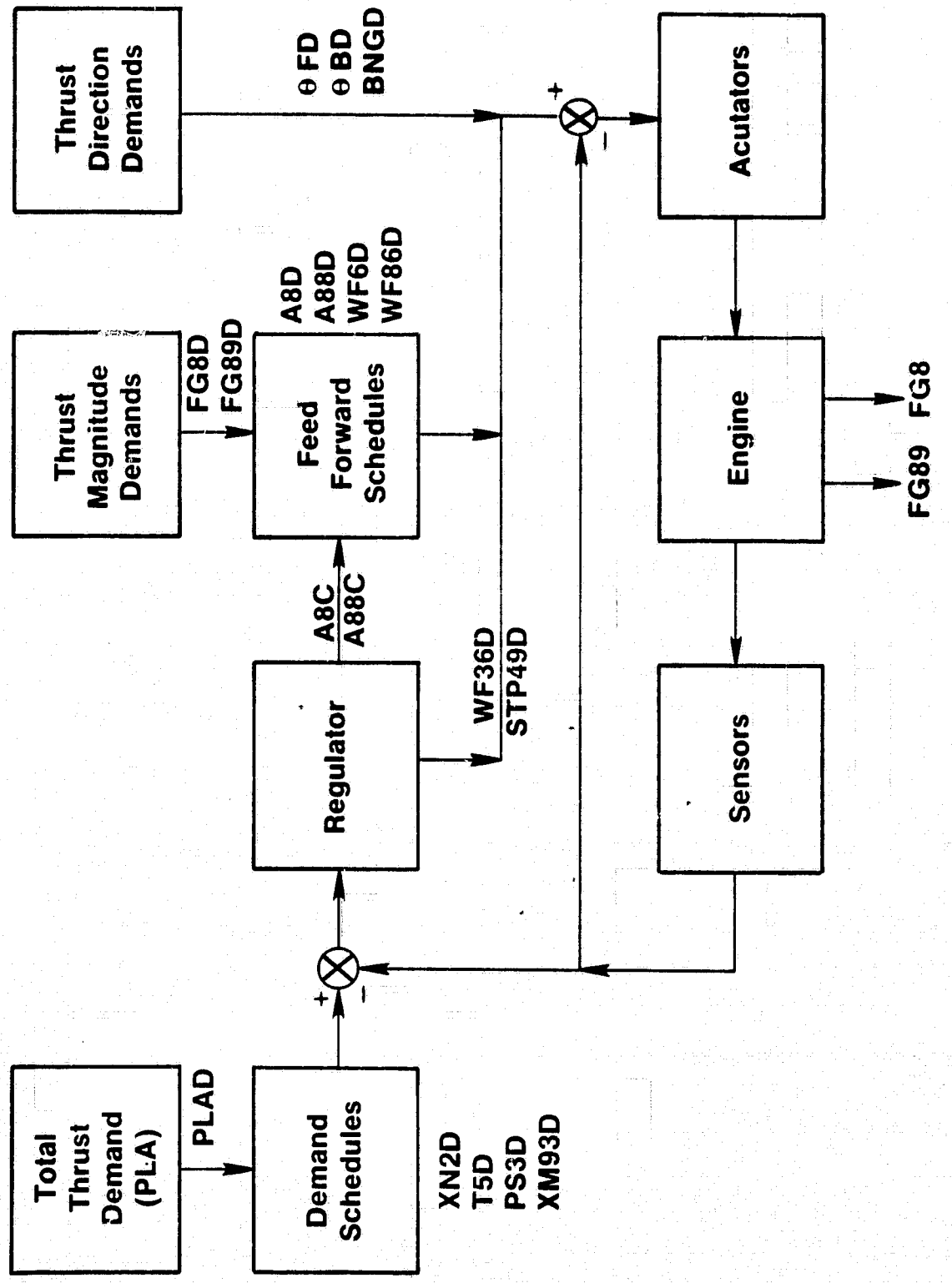

Figure 2. Propulsion Control for Vertical Operations.

and nozzle areas at constant thrust to provide gas generator regulation with no effect on attitude control. Conversely, feed forward compensation modulates augmentor fuel flow and nozzle areas to provide nozzle thrust regulation with no effect on gas generator speeds or temperatures.

3.3 Flight Transition Control Requirements

Two types of flight transitions between vertical and horizontal flight have been examined:

- Vertical-to-horizontal (VTH) transition from Vertical Takeoff to Horizontal Climb rating.
- Horizontal-to-Vertical (HTV) transition from Flight Idle Descent (FID) to Vertical Landing rating.

The VTH transition involves the rotation of the ADEN and remote nozzle thrust vectors towards the horizontal, flow-split modulation to reduce the flow to the remote system, and the shut-down of the remote augmentor. The HTV transition involves the above events in reverse order plus a throttle burst from FID to Landing and light-offs of both the mixed-flow and remote augmentors. Both transitions require the propulsion system to meet aircraft attitude control requirements during the low speed flight regime.

The following propulsion control requirements have been established for the flight transition phase:

- Pilot control of Power Lever Angle (PLA) and Thrust Vector Angle (TVA) in order to control the shape of the transition trajectory and its elapsed time.
- Aircraft flight control computer to provide individual PLA and TVA demands to the propulsion control system.
- Attitude control demands would be in the form of thrust magnitude and vector angle corrections to both the ADEN and remote nozzles.
- TVA demand establishes the applicable propulsion control regime - horizontal control for 0°, vertical control for 90° TVA, and flight transition control for all intermediate values.
- Stable mixed-flow and remote augmentor operation must be available over a broad range of PLA and TVA demands. Augmentor start-up

and shut-down must be scheduled as a function of TVA (and possibly PLA as well).

- Flow split between the VABI and the remote system must be scheduled as a function of TVA to minimize pitching moments due to the propulsion system.

- Nominal mixed-flow and remote augmentor fuel schedules must be used during flight transition in order to reserve the full ± 12% thrust modulation capability for potential attitude control needs.

The above requirements have been used as the basis for the flight transition control concept described in the subsequent sections of this report. Sea level static steady-state operating conditions were calculated for a number of operating points along a typical VTH transition and a corresponding HTV transition. These data are described in Section 4. These data were then used as the basis for the propulsion control regulator designs described in Section 5.

4.0 STEADY-STATE OPERATION

4.1 Horizontal Operating Mode

Steady-state studies of the horizontal operating mode were conducted in order to establish engine operating requirements for achieving minimum SFC over the full-throttle range from Idle to Intermediate Power Setting. Table 1 summarizes the results achieved for operation at SLS/Std. + 31°F and illustrates the variation in control parameters, potential sensed parameters, and performance parameters. These data were used to establish the starting point for the Horizontal-to-Vertical (HTV) transition and the end point for the corresponding Vertical-to-Horizontal (VTH) transition.

4.2 Vertical-to-Horizontal Transition

Figure 3 illustrates a typical VTH transition which contains the following key operating points:

1) Hover or vertical climb with the remote flow control valve (RFCV) full open, 100% of the bypass duct flow going to the RALS nozzle, and the RALS system providing 45% of the total nominal thrust. The ADEN nozzle is in the vertical position (90°).

TABLE 1 - TYPICAL HORIZONTAL FLIGHT OPERATING CONDITIONS

	POWER CODE	21	24	27	30	32	34	37	40	42	44	48	50
ENGINE PERFORMANCE	FN	1283	2054	2894	3794	4433	5108	6334	7579	8613	9696	12719	12800
	SFC	1.053	.8948	.8449	.8230	.8129	.8084	.8065	.8091	.8134	.8189	.8451	.8486
CONTROL VARIABLES	PCN2	41.55	48.4	55.4	62.2	6618	71.4	78.3	85.2	89.7	94.3	103.5	103.5
	PCN25	78.56	83.29	88.2	90.3	91.7	93.1	95.5	97.7	99.3	100.9	105.1	106
	T5	1312	1406	1498	1616	1688	1751	1854	1940	2007	2069	2230	2204
	T49	1419	1541	1662	1821	1918	2007	2152	2277	2372	2460	2675	2635
	XM13	.365	.391	.417	.424	.427	.430	.433	.435	.437	.4389	.4305	.4209
	XM93	.352	.376	.396	.405	.409	.412	.416	.418	.420	.4216	.4244	.4244
	PS3	86.7	109.1	135.8	157.8	173.0	189.8	219.9	251.0	276.4	303.3	380.8	391.9
MANIPULATED VARIABLES	WF36	1351	1838	2445	3122	3604	4129	5108	6113	7006	7940	10749	10862
	WF6	0	0	0	0	0	0	0	0	0	0	0	0
	WF86	0	0	0	0	0	0	0	0	0	0	0	0
	STP22	5.19	8.59	11.0	9.51	9.06	8.76	8.63	8.92	9.06	9.26	8.78	7.80
	STP49	109.6	101.7	98.6	89.7	85.9	83.4	80.4	79.0	78.1	77.68	78.14	81.36
	A8	262.3	246.8	247.7	253.3	257.3	263.3	272.5	281.3	287.8	294.5	304.3	303.6
	A88	---	---	---	---	---	---	---	---	---	---	---	---

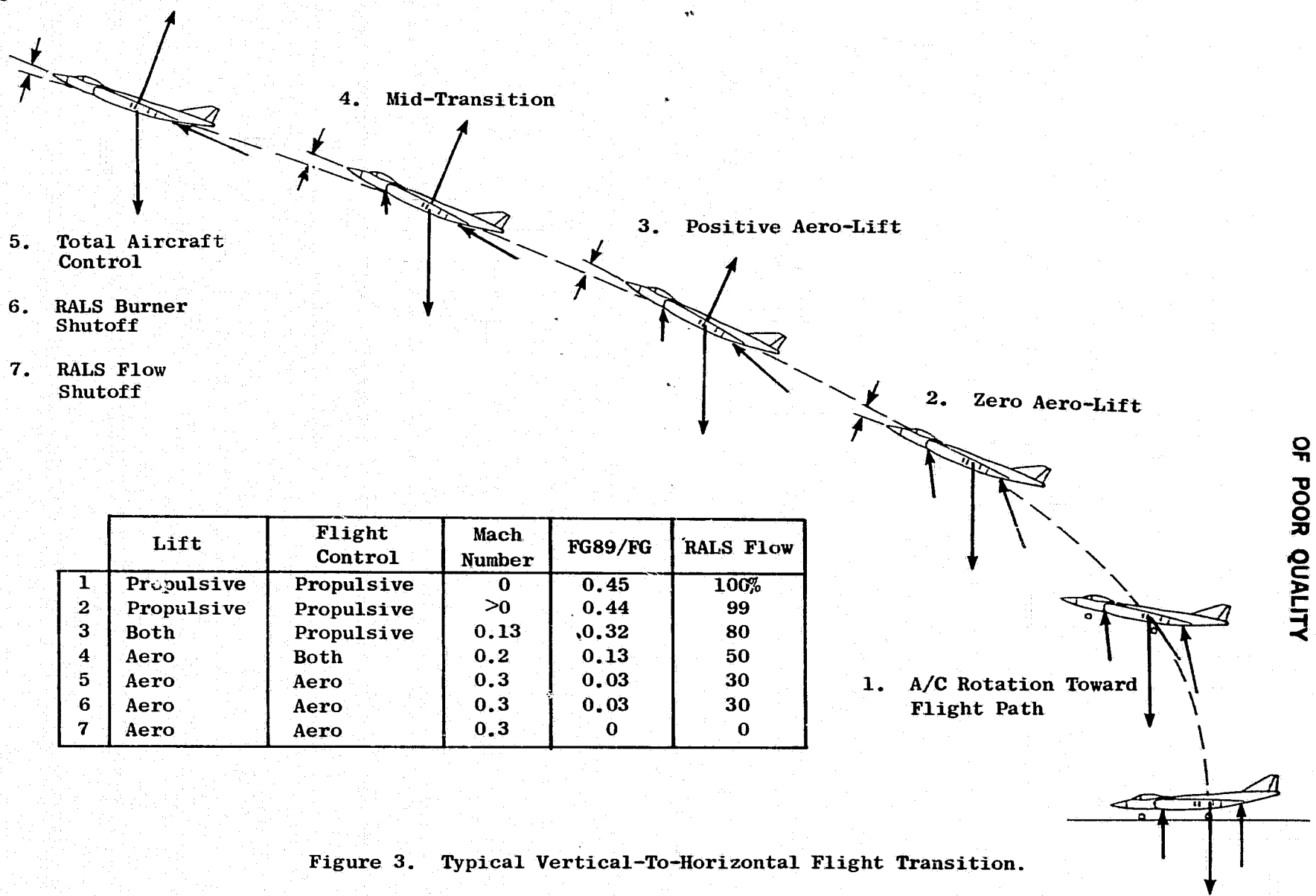

	Lift	Flight Control	Mach Number	FG89/FG	RALS Flow
1	Propulsive	Propulsive	0	0.45	100%
2	Propulsive	Propulsive	>0	0.44	99
3	Both	Propulsive	0.13	0.32	80
4	Aero	Both	0.2	0.13	50
5	Aero	Aero	0.3	0.03	30
6	Aero	Aero	0.3	0.03	30
7	Aero	Aero	0.3	0	0

Figure 3. Typical Vertical-To-Horizontal Flight Transition.

2) Start of transition with the ADEN nozzle rotated to a thrust vector angle (TVA) of 77.4° from horizontal. Remote flow transfer has been initiated by opening the rear VABI and the RALS thrust has been reduced to maintain a zero propulsive pitching moment on the aircraft. The RALS system is operating at 99% of nominal flow and producing 44% of the total thrust.

3) TVA rotation is decreased to 35.7° and the rear VABI is opened to reduce RALS flow to 80% nominal. The RFCV must be partially closed to maintain RALS burner Mach number. RALS thrust has been reduced to 32% and air speed and aerodynamic lift are increasing.

4) The TVA has been reduced to 10.8° and the remote flow to 50% of nominal. Increased throttling loss through the RFCV and reduced augmentor fuel flows reduce the RALS thrust to 13% of nominal. Air speed and aerodynamic lift continues to increase.

5) TVA has been reduced to 2.3° and the remote flow to 30% of nominal. This is the minimum flow rate at which the RALS burner can be maintained and the burner ΔT has been reduced to a minimum of 150°F in preparation for shut-off.

6) TVA has been reduced to 2.1° and the remote burner has been shut-off.

7) The RFCV has been completely shut-off and all duct flow passes through the rear VABI and ADEN nozzle completing the transition.

Table 2 contains a summary of the control, manipulated and performance variables corresponding to the above points along the VTH transition. Note that there is relatively little change in engine speed throughout the VTH transition and that the primary augmentor has been left on in order to achieve a fast acceleration to cruise speed and altitude.

4.3 Horizontal-to-Vertical Transition

The HTV transition is expected to be the most critical phase of the VCE/RALS operating envelope in that it requires a transfer of about 60% of the bypass duct flow to the RALS system before igniting the RALS burner and a substantial throttle transient from Flight Idle to at least 60% of Nominal Vertical Takeoff Thrust.

Figure 4 illustrates a typical HTV transition containing the following operating points:

TABLE 2. TYPICAL VERTICAL-TO-HORIZONTAL OPERATING CONDITIONS

	VARIABLE	VERTICAL HOVER	START TRANSITION	ACTIVATE RFCV	MID TRANSITION	MIN RALS ΔT=150°	RALS BURNER SHUT-OFF	RALS FLOW OFF
ENGINE PERFORMANCE	TVA	90°	77.4°	35.7°	10.8°	2.3°	2.1°	0°
	XM	0	.04	.08	.2	.3	.3	.3
	FRAM	0	27.	545.	1408	2197	2197	2197
	FG	16015	16040	16366	17184	18142	18092	19918
	FG89/FG	.45	.444	.323	.132	.032	.029	.0
CONTROL VARIABLES	PCN2	106.64	106.64	106.71	107.07	107.6	107.6	107.6
	PCN25	105.73	105.73	105.8	106.14	106.65	106.65	106.65
	T5	2286.5	2287.7	2312.0	2342.6	2282.2	2278.9	2234.5
	T49	2270.7	2771.4	2783.9	2799.1	2733.8	2730.7	2863.5
	XM13	.436	.436	.436	.436	.436	.436	.436
	XM93	.448	.448	.448	.448	.448	.448	.448
	PS3	336.2	336.8	351.0	378.5	398.5	398.4	398.
MANIPULATED VARIABLES	WF36	10314.	10330.	10709.	11422.	11559.	11538.	11267.
	WF6	3834.	3919.	5563.	8342.	10857.	10878.	14114.
	WF86	8981.	8783.	5530.	2019.	209.	0.	0.
	STP22	1.45	1.45	1.45	1.45	1.46	1.46	1.46
	STP49	82.7	82.6	81.2	79.8	81.7	81.5	82.5
	A8	269.1	270.2	289.5	321.4	369.1	370.0	437.
	A88	185.6	182.0	143.6	120.9	122.9	112.5	112.5

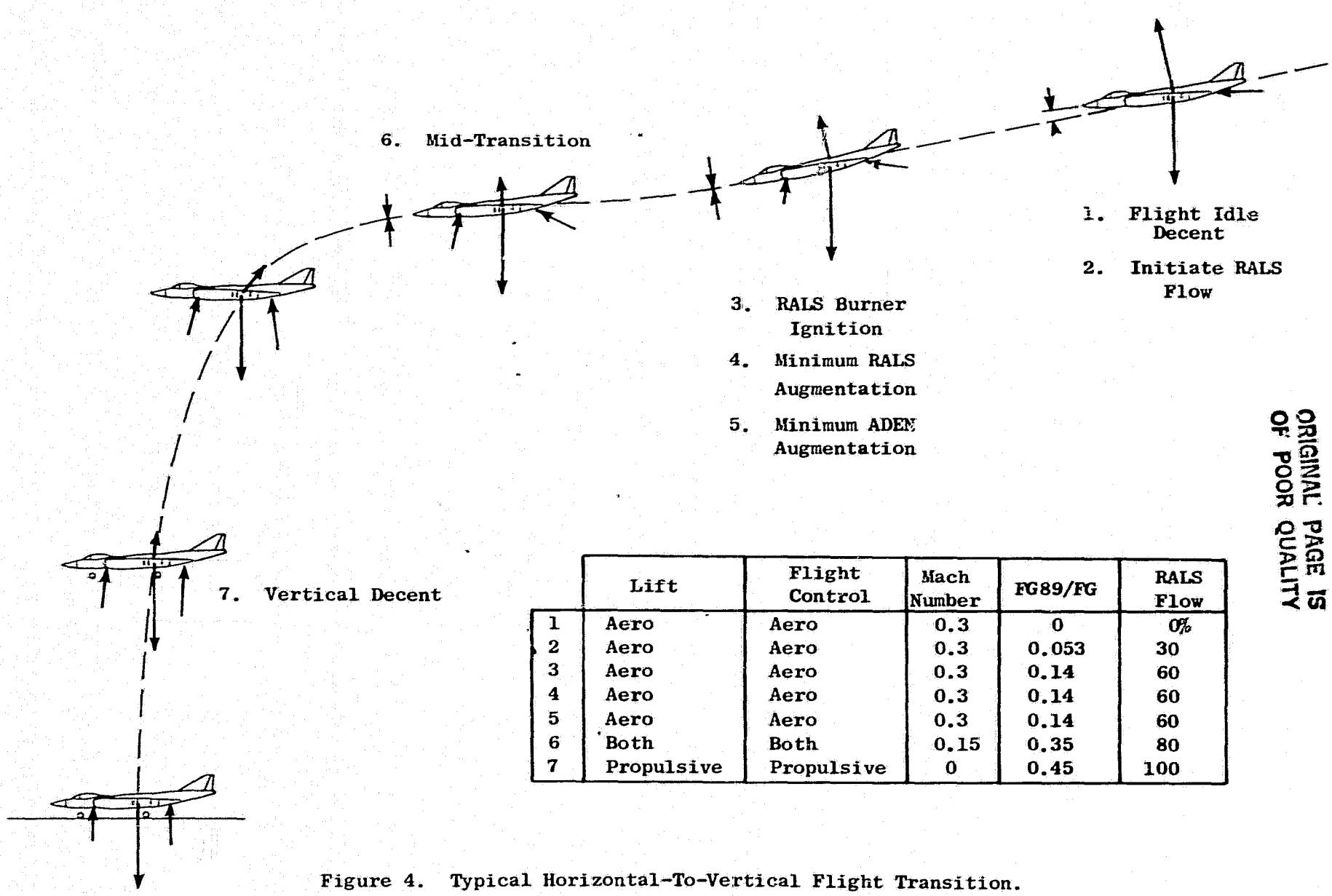

	Lift	Flight Control	Mach Number	FG89/FG	RALS Flow
1	Aero	Aero	0.3	0	0%
2	Aero	Aero	0.3	0.053	30
3	Aero	Aero	0.3	0.14	60
4	Aero	Aero	0.3	0.14	60
5	Aero	Aero	0.3	0.14	60
6	Both	Both	0.15	0.35	80
7	Propulsive	Propulsive	0	0.45	100

Figure 4. Typical Horizontal-To-Vertical Flight Transition.

1) Flight Idle Descent corresponding to low power horizontal operation with no RALS flow and both augmentors turned off. The RFCV is closed and the ADEN TVA is at 0°.

2) TVA has been increased to 3.9° and the RFCV has been opened to transfer 30% of the duct flow to the RALS system. Both augmentors are turned off and the RALS thrust is 5% of total thrust.

3) TVA has been increased to 11.5° and the RALS flow has been increased to 60% of the total flow. The RALS burner Mach number is adequate for burner ignition. RALS thrust is 14% of the total thrust.

4 & 5) The primary and RALS augmentors are ignited consecutively and brought to minimum augmentation at 150°F temperature rise.

6) The ADEN TVA has been increased to 41.2° and the RALS flow has been increased to 80% of the total flow. Fan speed has been increased and both augmentor fuel flows have been raised to achieve a RALS thrust of 35% of total. The RFCV has been opened in conjunction with the RALS nozzle area to maintain the required RALS burner Mach number.

7) The RFCV is fully open and the rear VABI is closed. RALS flow is 100% of the duct flow and the ADEN TVA is at 90° from horizontal. Fan speed has been increased to achieve 60% of the nominal VTO thrust and the RALS thrust is 45% of the total completing the transition into hover or vertical landing.

Table 3 contains a summary of the control, manipulated, and performance variable variations corresponding to the above HTV transition.

4.4 Flight Transition Regime

Figure 5 illustrates a typical flight transition regime at sea level. ADEN gross thrust has been plotted against the ADEN Thrust Vector Angle. Horizontal operation is shown from Flight Idle to Maximum Augmentation at 0° TVA. Vertical operation is shown from Minimum Weight Hover (60% Nominal Takeoff) to Maximum Weight Hover (100% Nominal Takeoff) at 90° TVA. The upper bound represents the nominal VTH transition described in Section 4.3 and the lower bound the nominal HTV transition. Lines of constant RALS thrust are indicated as functions of the ADEN thrust and TVA and correspond to zero propulsive pitch operation (no pitch rate demand). RALS and ADEN thrust modulation and deflection are available for attitude control by modulating the primary and RALS augmentor fuel flows.

TABLE 3. TYPICAL HORIZONTAL-TO-VERTICAL OPERATING CONDITIONS

	VARIABLE	FLIGHT IDLE	30% RALS FLOW	60% RALS FLOW	PRIMARY ΔT = 150°	RALS ΔT = 150°	80% RALS FLOW	LAND, 100% RALS FLOW
ENGINE PERFORMANCE	TVA	0°	3.9°	11.5°	11.5°	11.9°	41.2°	90°
	XM	.3	.3	.3	.3	.3	.15	0
	FRAM	825.	897.	972.	972.	972.	604.	0
	FG	2108.	2227.	2497.	2615.	2660.	5572.	9370.
	FG89/FG	0	.053	.14	.134	.144	.353	.45
CONTROL VARIABLES	PCN2	41.5	46.01	50.58	50.58	50.58	68.2	85.9
	PCN25	78.56	80.69	83.02	83.02	83.02	91.88	101.3
	T5	1312.7	1353.3	1419.1	1419.2	1425.6	1617.5	1783.1
	T49	1487.7	1481.0	1571.5	1571.5	1578.3	1861.6	2116.1
	XM13	.365	.378	.389	.389	.389	.410	.417
	XM93	.352	.369	.383	.383	.383	.410	.418
	PS3	86.67	97.23	110.3	110.3	110.3	161.9	235.9
MANIPULATED VARIABLES	WF36	1351.	1587.	1920.	1920.	1932.	3360.	5487.
	WF6	0	0	0	453	439	2239	4784
	WF86	0	0	0	0	219.	2243.	6056.
	STP22	5.2	2.37	1.13	1.13	1.13	4.25	11.2
	STP49	109.6	103.3	98.4	98.4	98.1	94.4	11.2
	A8	262.2	237.9	205.7	218.1	216.2	253.2	322.1
	A88	153.0	153.0	153.0	153.0	172.9	135.8	168.8

ORIGINAL PAGE IS
OF POOR QUALITY

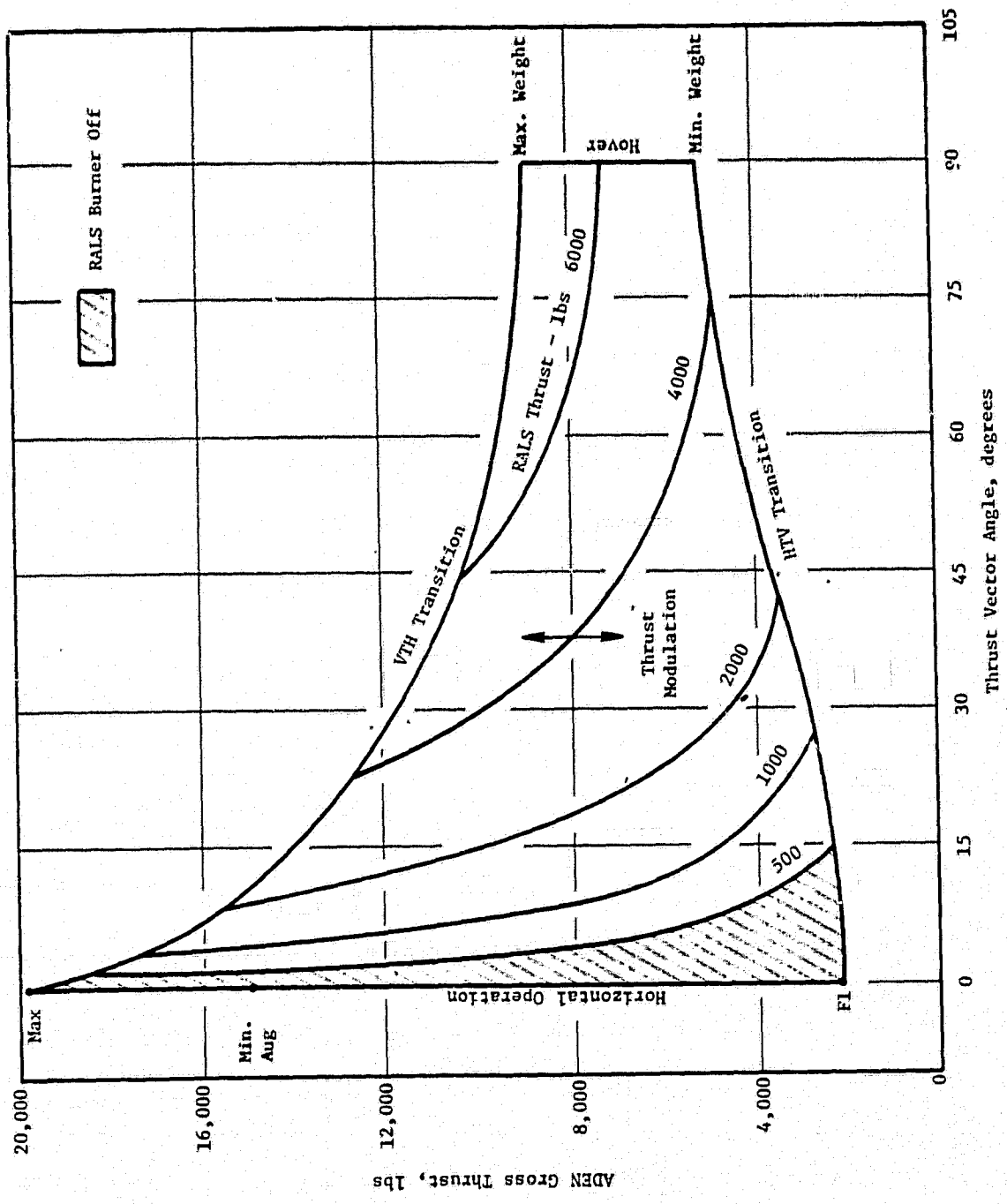

Figure 5. Thrust Modulation During Flight Transition.

The transition process and trajectory shape are controlled by the individual pilot demands:

- Power Lever Angle which sets the engine fan speed and the total thrust at nominal augmentation levels.
- Thrust Vector Angle which sets the nominal ADEN deflection and the nominal RALS thrust to achieve a zero propulsive pitch rate. TVA determines the relative accelerations parallel and perpendicular to the aircraft and, therefore, the rate of rotation of the velocity vector.
- Pitch Rate which modulates the nominal RALS thrust for zero propulsive pitch in order to achieve the required pitch rate. The Pitch Rate demand, therefore, controls angle of attack during the transition process.

Note that the nominal RALS and ADEN thrust requirements can be determined uniquely from the total Gross Thrust and Thrust Vector Angle demands. The thrust modulation requirement is defined by the Pitch Rate demand.

Thrust modulation capabilities available for height and attitude control are illustrated in Figure 6. The nominal thrust modulation capability is $\pm$.12% for both the RALS and ADEN nozzles throughout most of the flight transition regime. At maximum weight takeoff, the minimum ADEN temperature is only 765°R below the nominal temperature limiting the low side modulation to 8.9%. This capability could, however, be increased by utilizing internal speed or geometry variations in this part of the operating regime, if necessary.

4.5 Remote Flow Control Valve

The RALS burner is required to operate over a broad range of flow rates, pressures, and temperatures throughout the flight transition regime. Stable operation of the RALS burner requires an inlet Mach number in the range of .13 - .15 and the RALS geometry has been sized to operate in this range at nominal remote flow rates. The rear VABI controls the flow split between the RALS and ADEN systems and the RALS nozzle area provides the means for controlling the burner Mach number.

Operation of the Remote Flow Control Valve is required in the low flow regime associated with the mid-transition region in order to throttle

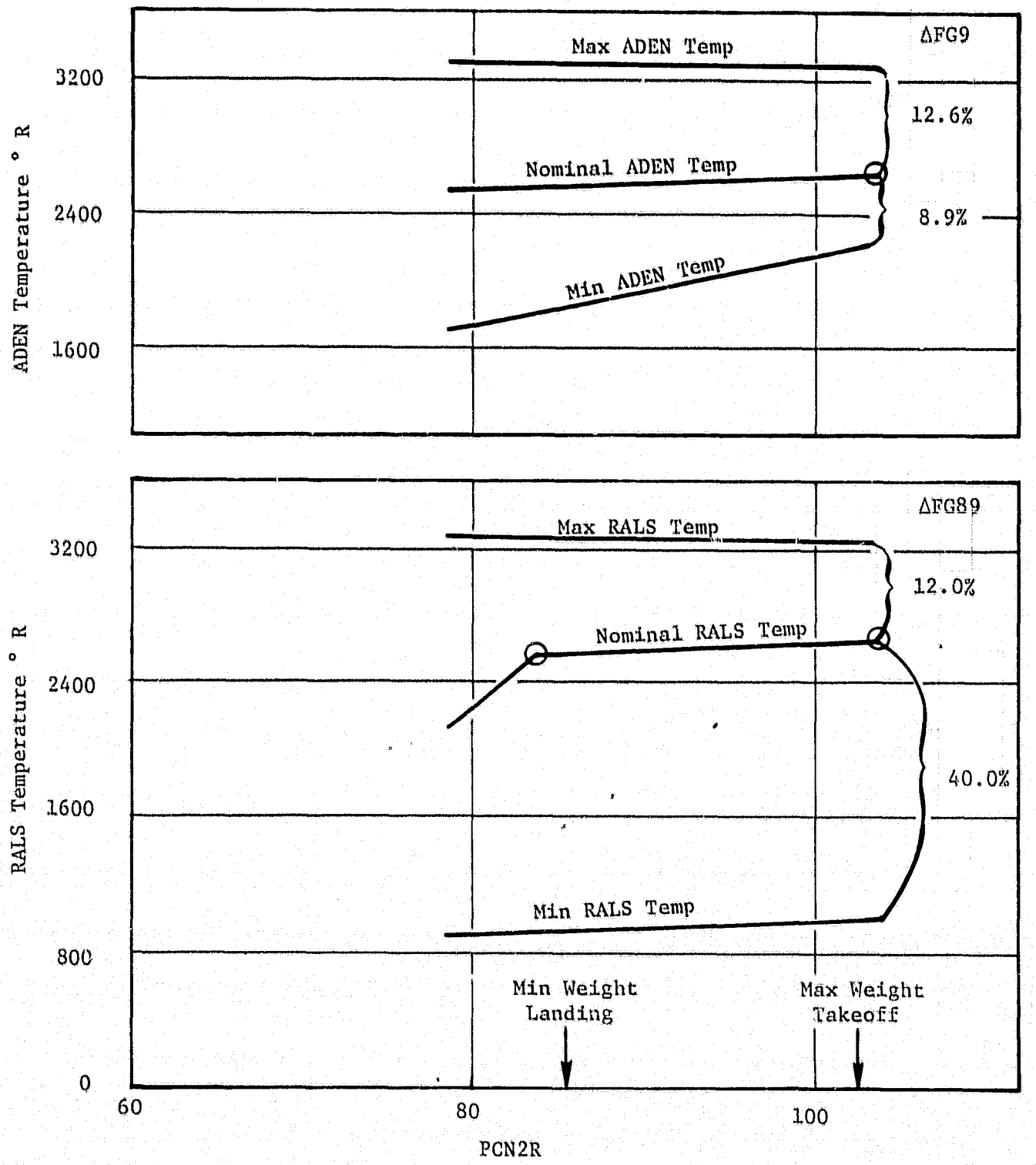

Figure 6. RALS and ADEN Thrust Modulation Capabilities.

the fan discharge pressure to maintain an acceptable burner inlet Mach number. Figure 7 illustrates the effect of the RFCV during the VTH transition of Table 2. Typical operation involves the following operating points:

1) At nominal remote flow rate, the RFCV is open and the Mach number is controlled by the RALS nozzle area. The pressure drop between fan discharge and the burner inlet is a minimum and is due to friction and the head loss associated with turning the flow forward.

2) At 80% of nominal flow rate, both the RFCV and RALS areas are reduced. Burner inlet Mach number is maintained by the additional throttling losses in the system. Note that a large reduction in RFCV area is required in this regime as the throttling losses are relatively insensitive to the area change.

3) The RFCV is choked at about 50% of nominal flow and assumes the flow control function from the rear VABI. The RALS nozzle area determines the dump pressure behind the RFCV and therefore its losses. RALS burner pressure is substantially more sensitive to the RFCV and mass flow rate at this point.

4) This point represents the minimum mass flow rate at which the required burner inlet Mach number can be maintained due to external ambient pressure limitations. The step change in RALS nozzle area corresponds to RALS burner shut-down from operation at minimum temperature rise (150°F ΔT).

5) The RFCV is closed and the duct flow has been completely transitioned from the RALS system to the ADEN nozzle.

4.6 Component Operating Characteristics

Component operating characteristics from the horizontal operating points of Table 1 and the flight transition points of Tables 2 and 3 have been used in the development of the simplified component-level transient model of the baseline engine described in Section 6. These data have been supplemented by additional steady-state operating data involving off-nominal operating schedules. Figures 8 and 9 illustrate the front-block fan and rear-block fan operating pressure ratio variations with corrected flow corresponding to the above operating data. The associated rear-block fan stator variation is also illustrated in Figure 9. Figure 10 contains similar data showing the compressor pressure ratio variation with corrected flow. Figures 11 and 12 contain the corresponding high pressure and low pressure turbine energy variations with turbine inlet corrected speed. Low

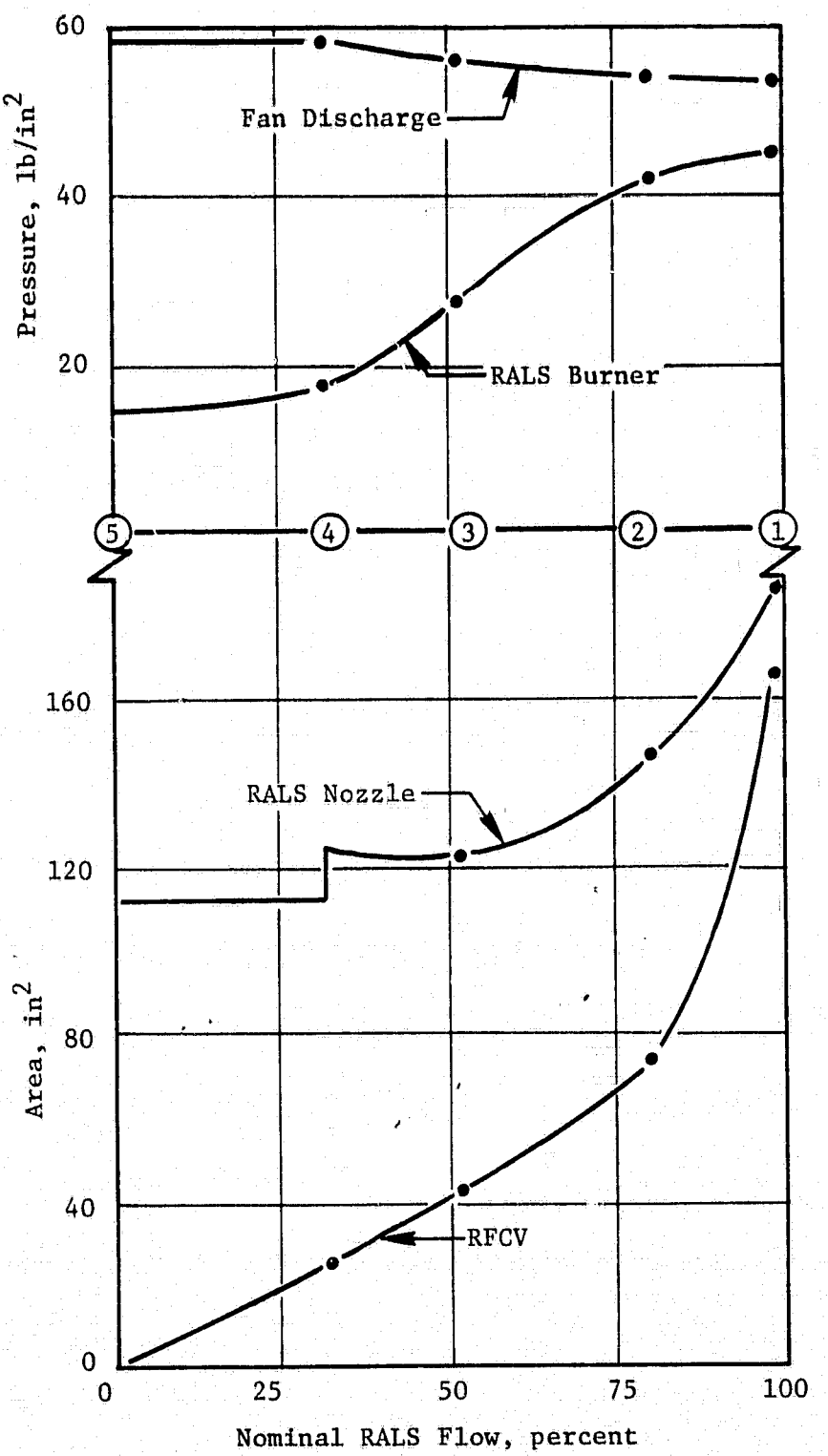

Figure 7. Effect of RFCV on RALS Flow and Pressure.

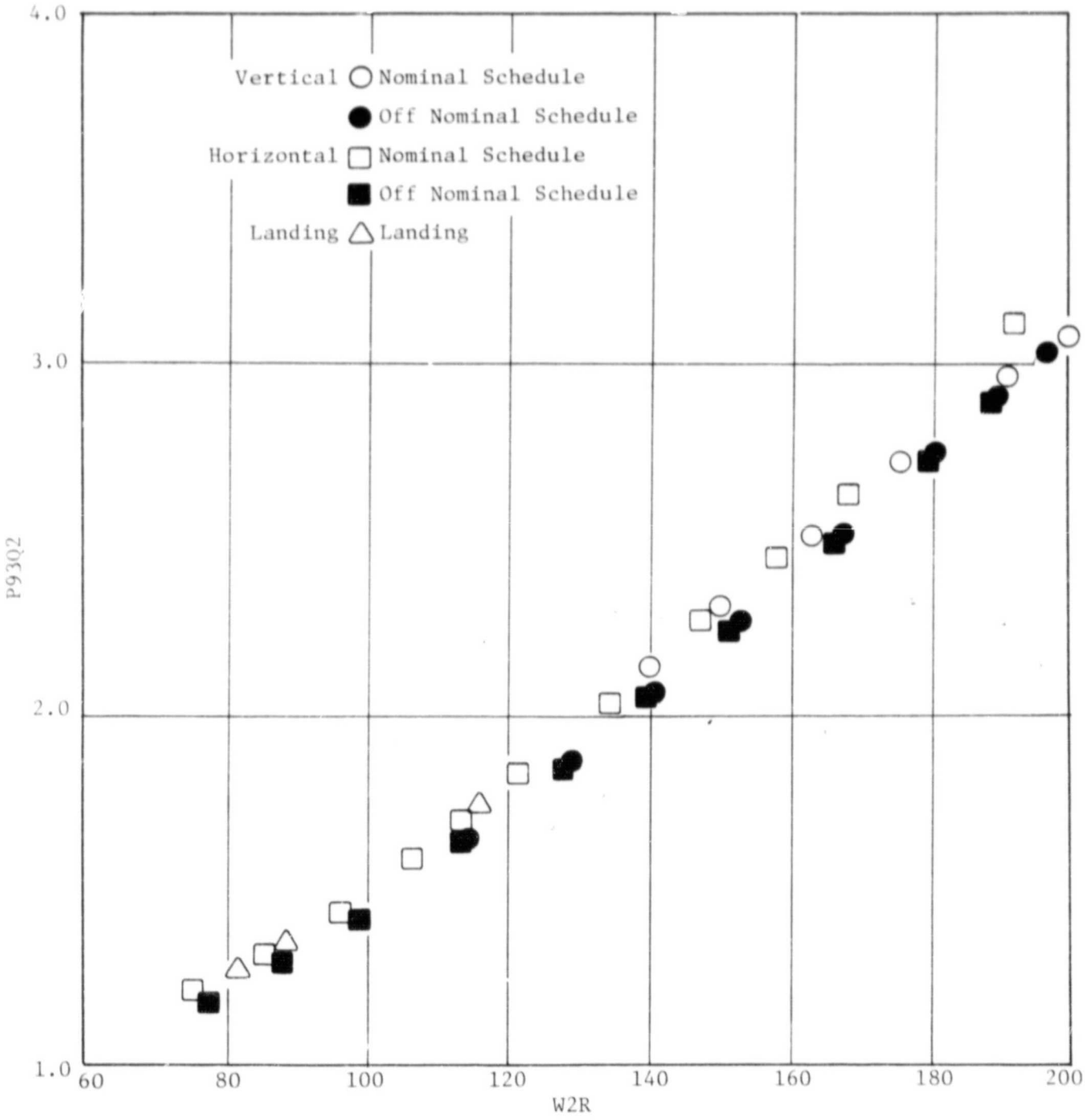

Figure 8. Front-Block Fan Operating Data.

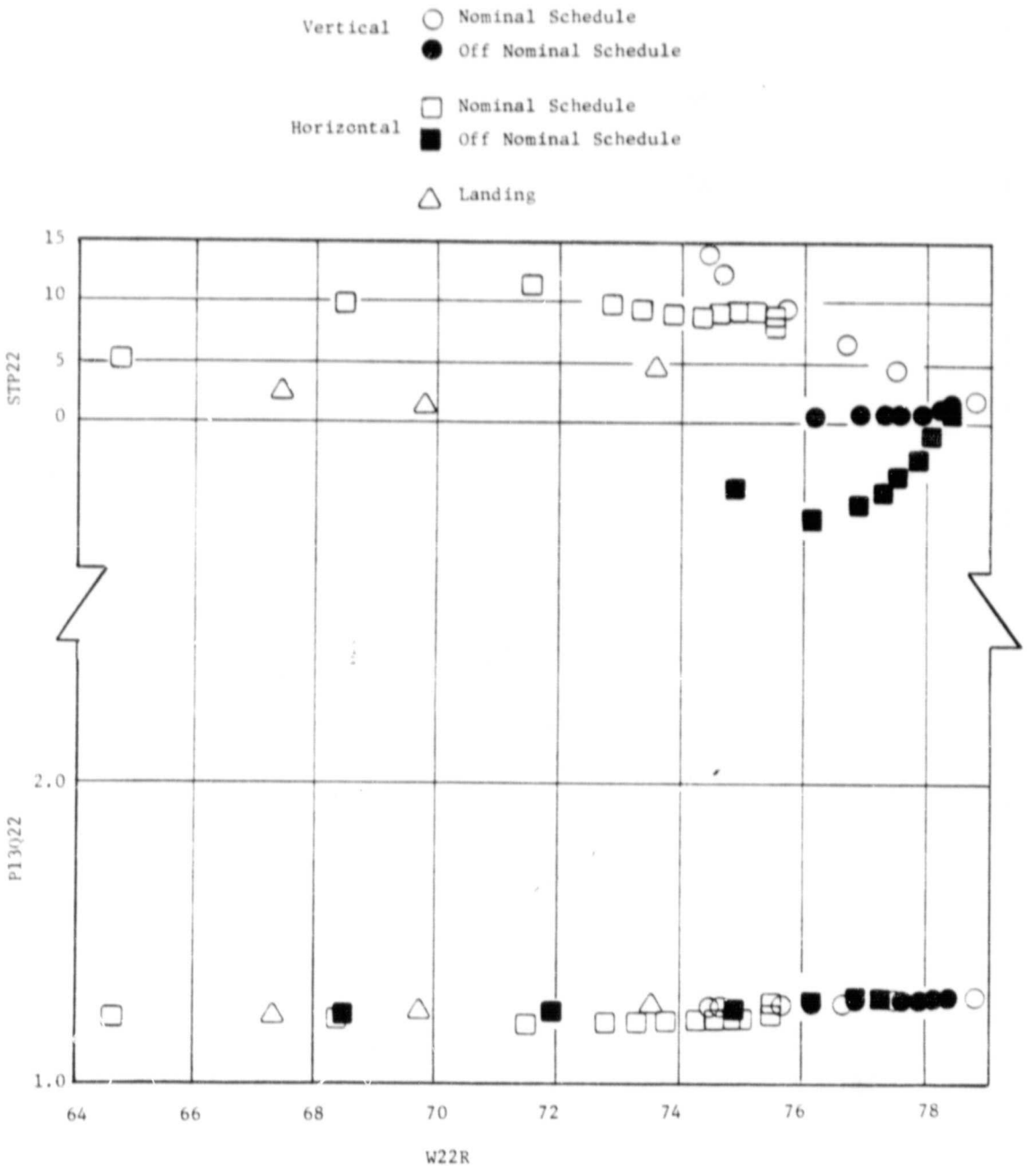

Figure 9. Rear-Block Fan Operating Data.

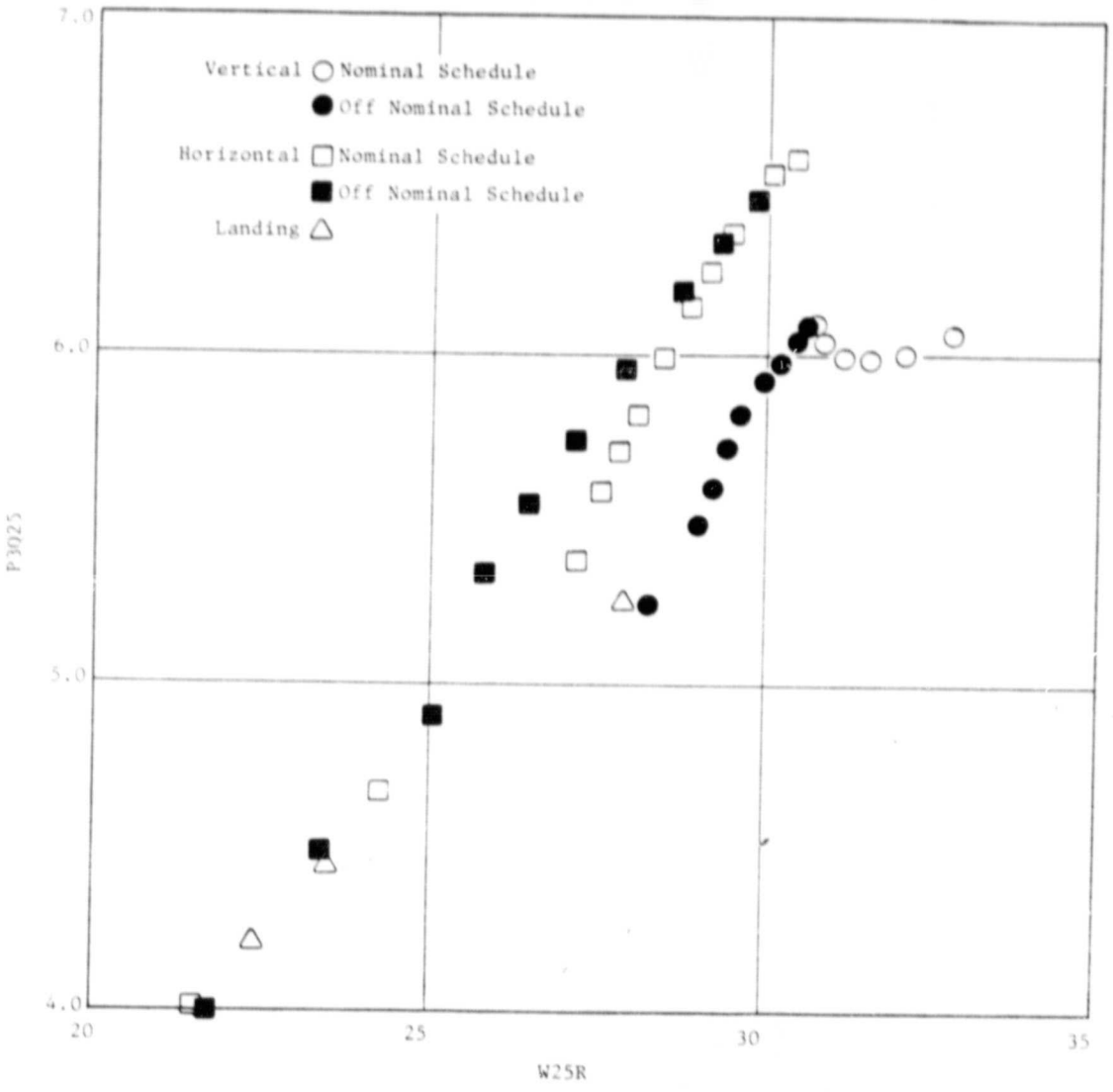

Figure 10. Compressor Operating Data.

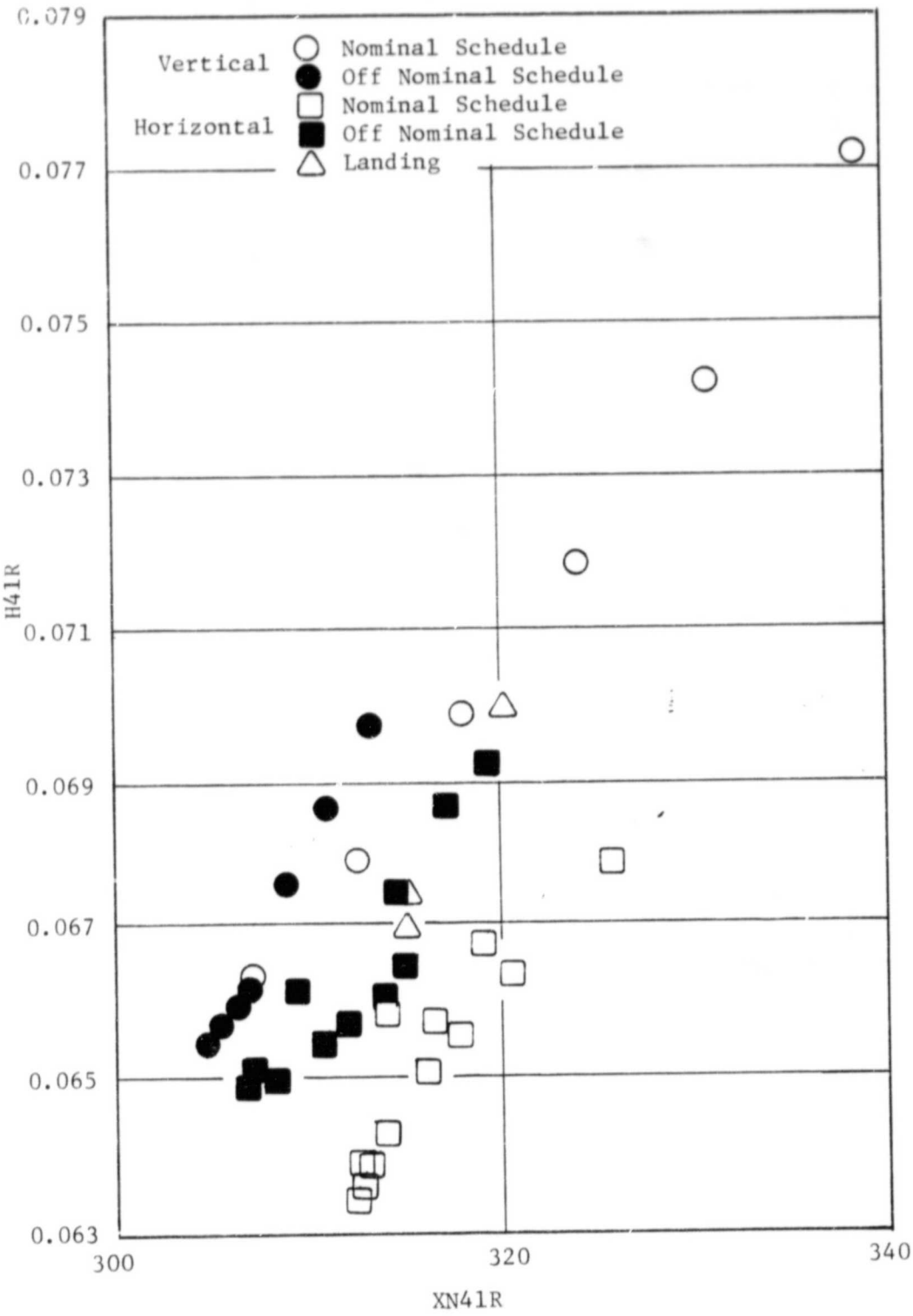

Figure 11. High Pressure Turbine Operating Data.

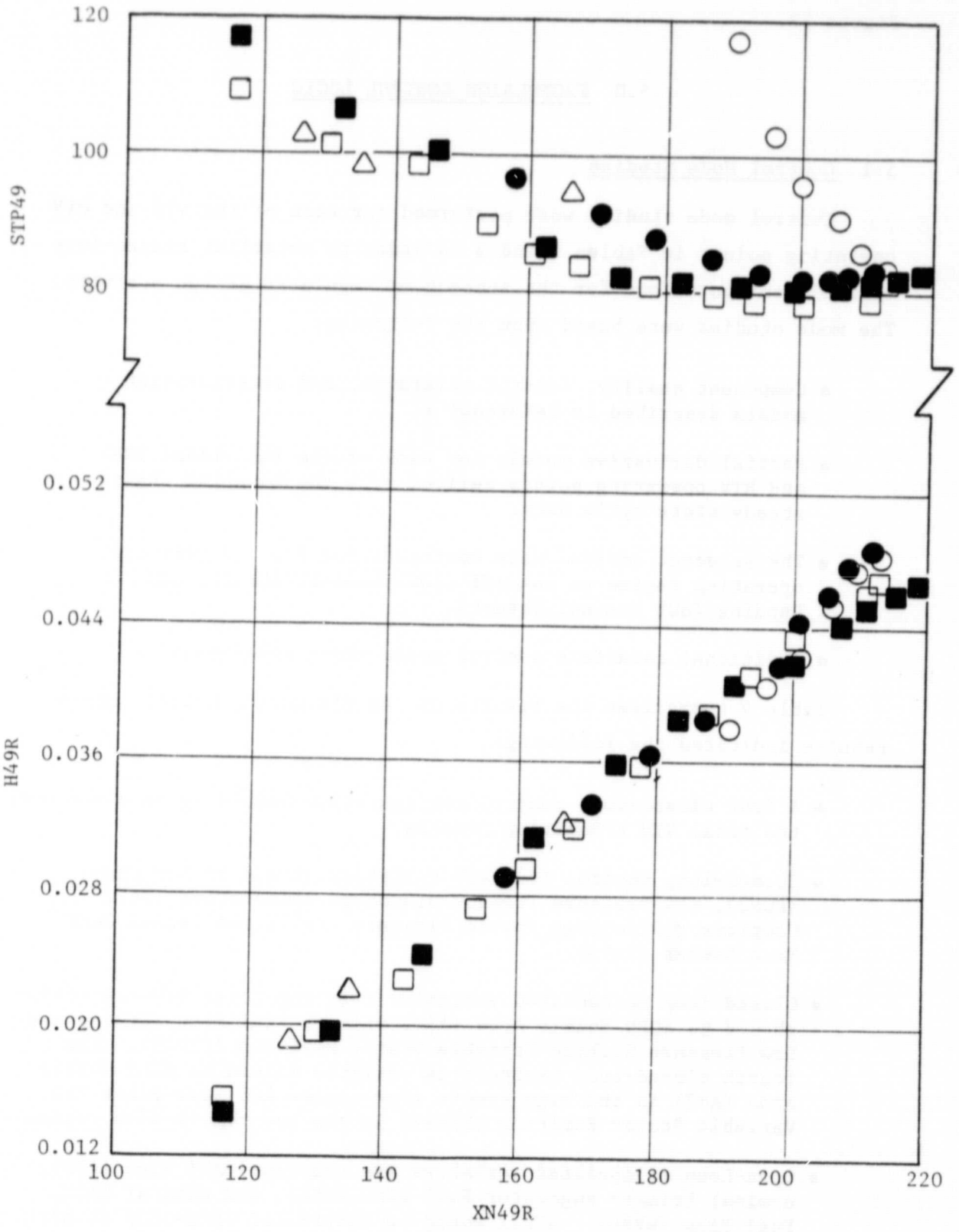

Figure 12. Low Pressure Turbine Operating Data.

pressure turbine variable stator position variation is also shown in Figure 12.

5.0 PROPULSION CONTROL LOGIC

5.1 Control Mode Studies

Control mode studies were performed for each of the VTH and HTV operating points in Tables 2 and 3 in order to establish closed-loop control configurations for the subsequent regulator design activity. The mode studies were based upon the following:

- Component quality, control tolerance, and deterioration models described in Reference 1.
- Partial derivative models for each of the individual VTH and HTV operating points derived from the baseline engine steady-state cycle deck.
- The selected control mode configuration for the vertical operating regime at Takeoff (100% Nominal Thrust) and Landing (60% Nominal Thrust).
- Additional candidate control modes where appropriate.

Table 4 summarizes the results of the VTH mode studies. These results indicated the following:

- A four closed-loop control configuration should be retained over the total VTH transition process.
- Closed-loop control (sensed) variables should be Fan Speed (PCN2), Low Pressure Turbine Discharge Temperature (T5), Compressor Discharge Static Pressure (PS3), and Bypass Duct Mach Number (XM93).
- Closed-loop manipulated variables over the total VTH transition should be ADEN Nozzle Area (A8), Primary Fuel Flow (WF36), and Low Pressure Turbine Variable Stator Position (STP49). The fourth closed-loop manipulated variable should be RALS Nozzle Area (A88) in the high remote flow regime and Rear-Block Fan Variable Stator Position (STP22) in the low remote flow regime.
- Open-Loop manipulated variables are the rear VABI area (A27), nominal Primary Augmentor Fuel Flow (WF6), and nominal RALS Fuel Flow (WF86). STP22 would be controlled open-loop at high flow rates and A88 at low flow rates.

Control of the RFCV in the mid-transition region was assumed to be open-loop but this assumption should be reviewed in more detail during subsequent studies.

Table 4 contains the expected variations in thrust, stall margin, temperature, and fuel flow corresponding to the selected control modes. These data contain no significant differences from the prior mode studies for the vertical operating mode.

Additional mode studies were conducted for 3-loop and 5-loop systems. The best 3-loop modes involved unacceptable performance variations and the best 5-loop modes did not provide sufficient improvements to warrant the added complexity of a fifth loop.

Similar mode studies were conducted for the HTV transition points of Table 3 and the results are summarized in Table 5. These results indicated the following:

- A single closed-loop control was acceptable for operation at Flight Idle Descent (FID). This control should use PCN2 as the sensed variable and WF36 as the closed-loop manipulated variable. All other manipulated variables should be scheduled open-loop.
- A four closed-loop configuration was required to achieve acceptable performance variations for each of the remaining operating points along the HTV transition. The HTV transition could use the same closed-loop control and manipulated variables as the VTH transition process.

5.2 Controller Design

The Controller design process followed the same procedure used in the prior Phase I program (Reference 1) and involved the following:

- A rectangular matrix of balanced steady-state partial derivatives was used to establish a state-space model with two states, four inputs, and four outputs for each of the VTH and HTV operating points. The state-space models were scaled and structured in the ABCD format. Figure 13 contains a schematic of the Linear Engine state-space model format.

TABLE 4 - VERTICAL TO HORIZONTAL TRANSITION MODE STUDY

OPERATING POINT		T/O	S/T	A/RFCV	M/T	M/R	MH
CLOSED LOOP CONTROL VARIABLES	PCN2	(A8)	(A8)	(A8)	(A8)	(A8)	(A8)
	T5	(WF36)	(WF36)	(WF36)	(WF36)	(WF36)	(WF36)
	PS3	(STP49)	(STP49)	(STP49)	(STP49)	(STP49)	(STP49)
	XM93	(A88)*	(A88)*	(STP22)*	(STP22)*	(STP22)*	(STP22)*
CLOSED LOOP MANIPULATED VARIABLES	A8	(PCN2)	(PCN2)	(PCN2)	(PCN2)	(PCN2)	(PCN2)
	WF36	(T5)	(T5)	(T5)	(T5)	(T5)	(T5)
	STP49	(PS3)	(PS3)	(PS3)	(PS3)	(PS3)	(PS3)
	STP22			(XM93)	(XM93)	(XM93)	(XM93)
	A88	(XM93)**	(XM93)**				
MINIMUM	%ΔFG89	-3.28	-3.74	-5.66	-9.4	-7.91	---
	%ΔFG9	-6.87	-6.67	-4.93	-3.37	-2.17	-4.28
	%ΔSM2	-1.79	-1.79	-1.79	-1.79	-1.79	-1.84
	%ΔSM22	-4.84	-4.81	-3.04	-0.19	-3.55	-0.11
	%ΔSM25	-2.14	-2.14	-2.13	-2.15	-7.10	-2.22
MAXIMUM	ΔT41(°F or °R)	47	47	48	46	36	43
	ΔT48(°F or °R)	40	40	40	40	41	38
	ΔSFC	.049	.051	.044	.042	.024	.10
	ΔWF36 (PPH)	242	240	218	241	215	229

T/O-Takeoff
S/T-Start Transition
A/RFCV-Activate Remote Flow Control Valve
M/T-Mid Transition
M/R-Min RALS (ΔT = 150°)
MH -Max Horizontal
* -Manipulated Variable Associated With XM93 For Operating Point
** -Control Variable Associated With A88 For Operating Point

TABLE 5 - HORIZONTAL-TO-VERTICAL TRANSITION MODE STUDY

OPERATING POINT		FID	30 RF	60 RF	RALS	80 RF	L
CLOSED LOOP CONTROL VARIABLES	PCN2	(WF36)*	(A8)*	(A8)*	(A8)*	(A8)*	(A8)*
	T5		(WF36)	(WF36)	(WF36)	(WF36)	(WF36)
	PS3		(STP49)	(STP49)	(STP49)	(STP49)	(STP49)
	XM93		(STP22)	(STP22)	(STP22)	(A88)	(A88)
CLOSED LOOP MANIPULATED VARIABLES	A8		(PCN2)	(PCN2)	(PCN2)	(PCN2)	(PCN2)
	WF36	(PCN2)**	(T5)**	(T5)**	(T5)**	(T5)**	(T5)**
	STP49		(PS3)	(PS3)	(PS3)	(PS3)	(PS3)
	STP22		(XM93)	(XM93)	(XM93)		
	A88					(XM93)	(XM93)
MINIMUM	%ΔFG89	---	-6.88	-7.88	-7.53	-4.00	-4.28
	%ΔFG9	-3.5	-2.42	-2.58	-2.63	-5.06	-6.36
	%ΔSM2	-1.9	-1.48	-1.5	-1.5	-1.76	-1.84
	%ΔSM22	-2.99	-1.94	-2.71	-2.55	-3.19	-4.00
	%ΔSM25	-4.17	-10.19	-10.	-9.98	-9.81	-7.09
MAXIMUM	ΔT41(°F or °R)	82	22	23	23	31	29
	ΔT48(°R or °R)	76	23	24	25	29	33
	ΔSFC	.06	.03	.035	.043	.07	.055
	ΔWF36 (PPH)	95	33	39	40	82	79

FID - Flight Idle Descent
30 RF - 30% RALS Flow
60 RF - 60% RALS Flow
RALS - RALS (ΔT = 150°)
80 RF - 80% RALS Flow
L - Landing (60% Max. T/O Power)
* - Manipulated Variable Associated With PCN2 For Operating Point
**-Control Variable Associated With WF36 For Operating Point

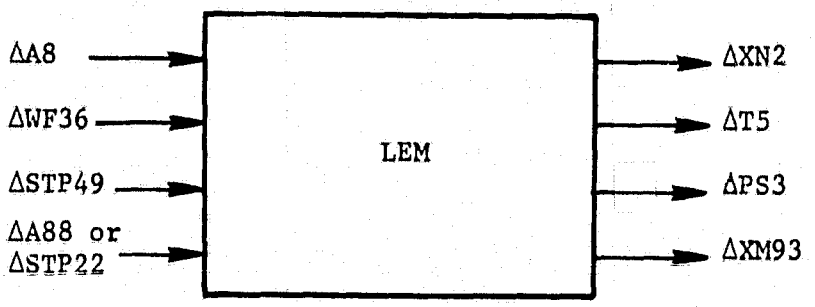

Figure 13. Four Imput-Four Output Linear Model (LEM).

- The K/Q matrix technique was then used to design Proportional/ Integral Controllers (PIC) for each individual operating point. The design technique was applied to the open-loop structure illustrated in Figure 14. Identical scale factors were used for all operating points.

- A computer generated closed-loop diagram of the system was obtained and is illustrated in Figure 15. Note that the diagram indicates the inter-relationships between the Linear Engine Model (SYS), Actuator Matrix (PRE1), Controller Matrix (PRE2), and the Seneor Matrix (F/B1). Figure 16 contains a more conventional diagram of the closed-loop structure in the standard multi-variable form.

The resulting regulator comprised the following elements:

- First Precompensator (PRE1) - A 4x4 diagonal matrix containing the dynamics of the actuators. PRE1 was the same for all transition operating points.

- Feedback Compensators (F/B1) - A 4x4 diagonal matrix containing the dynamics of the sensors. F/B1 was the same for all transition operating points.

- Controller and Second Precompensator (PRE2) - A 4x4 matrix containing Proportional/Integral Controller (PIC) Laplace Transfer functions for each of its 16 elements. Different transfer functions were obtained for each individual operating point in the VTH and HTV transitions. Table 6 contains the VTH results and Table 7 the results for the HTV transition. Note that Flight Idle Descent utilizes a single-loop control and, consequently, its PRE2 matrix contains only a single set of transfer functions.

Appendix A contains the results of a series of time domain plots for unit step demands applied simultaneously to all inputs of the closed-loop regulator for each of the VTH and HTV operating conditions. In all cases, cross-coupling occurred within the first quarter second and steady-state was achieved within two seconds.

5.3 Gain Schedules

The proportional and integral gain constants from Tables 6 and 7 were then represented by linear regression as a function of an arbitrary flight control demand (FCD) parameter. FCD values were determined in order to achieve the best fit for the major diagonal coefficients. Although FCD is a function of TVA and Power Lever Angle, no attempt has been made to define the functional relationship. Linear regressions were obtained for each of the 32 coefficients for the VTH transition and for

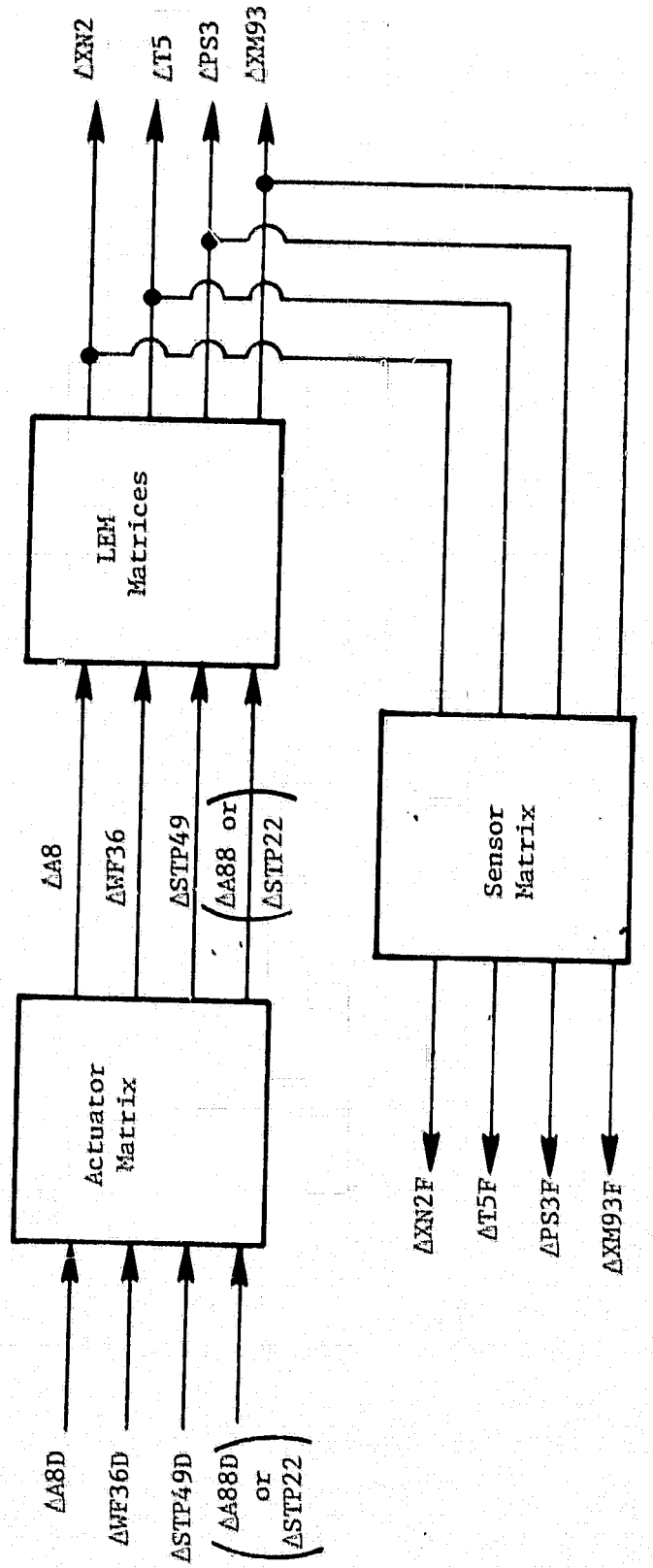

Figure 14. Open-Loop Model for VTH or HTV Transition (Used to Design Controller Matrix).

SYSTEM NAME: TKOA

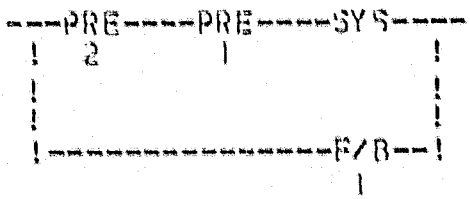

	TYP	I/P	O/P	NUM	DEN	SAMPLE-TIME
SYS 0 (TKOA)	7	4	4	2	2	0.
.LEM (LINEAR ENGINE MODEL)						
PRE 1 (TK01P)	5	4	4	4	2	1.
.ACTUATOR MATRIX						
PRE 2 (TK02P)	3	4	4	2	2	1.
.CONTROLLER MATRIX						
F/B 1 (TK01F)	5	4	4	2	1	1.
.SENSOR MATRIX						

Figure 15. Computer Generated Structure of Multivariable Regulator.

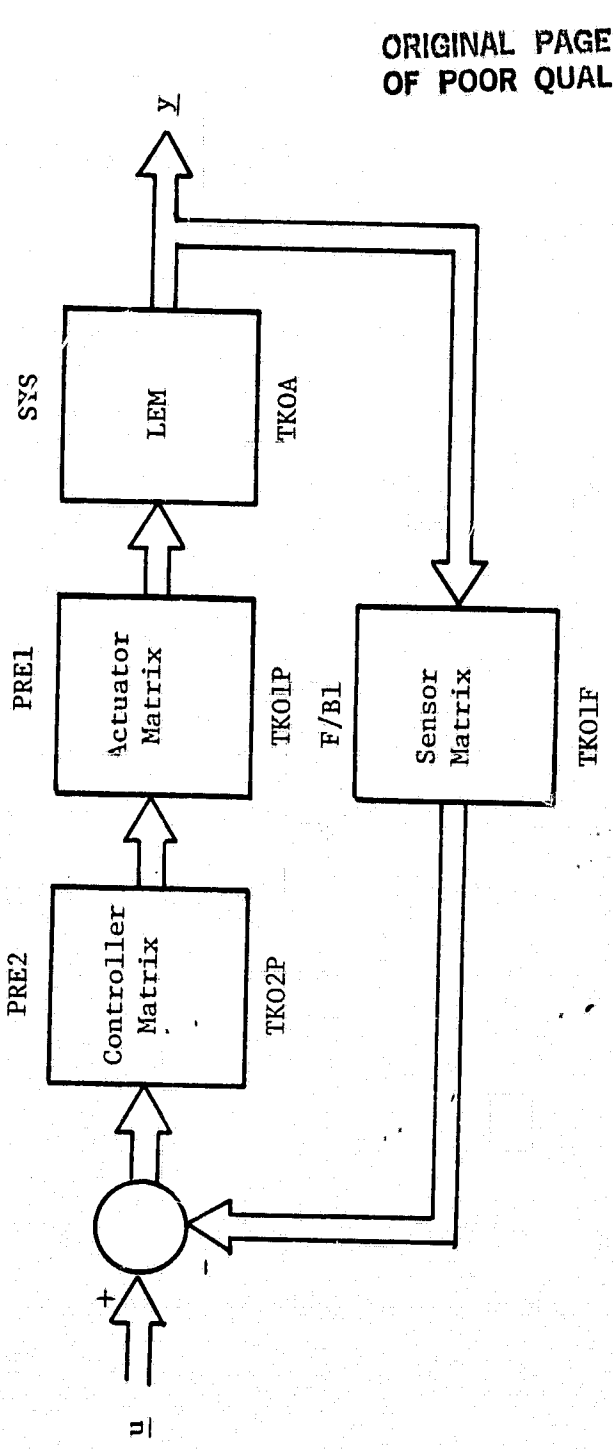

Figure 16. Structure of Multivariable Regulator.

TABLE 6 - PROPORTIONAL AND INTEGRAL GAIN CONSTANTS FOR THE VERTICAL-TO-HORIZONTAL TRANSITION CONTROLLER

OPERATING POINT		TAKEOFF TKO2P	START TRANSITION VH22P	ACTIVATE RFCV VH32P	MID TRANSITION VH42P	MIN RALS VH52P	MAX HORIZONTAL VH62P
SPECIAL MANIPULATED VARIABLE		A88	A88	STP22	STP22	STP22	STP22
PROPORTIONAL GAIN COEFFICIENTS	a11	1.51	1.42	0.92	1.44	1.53	.19
	a12	-0.69	-0.63	-0.53	-0.49	-0.59	-0.94
	a13	0.91	0.86	1.67	0.91	0.94	1.21
	a14	0.59	0.54	-0.01	0.05	0.07	-0.08
	a21	0.64	0.63	0.42	0.64	0.65	0.12
	a22	0.49	0.48	0.53	0.59	0.63	0.62
	a23	0.39	0.39	0.68	0.40	0.38	0.35
	a24	0.21	0.20	-0.01	0.005	0.008	-0.03
	a31	-0.43	-0.42	-0.86	-0.36	-0.35	-0.56
	a32	-0.47	-0.46	-0.36	-0.30	-0.32	-0.34
	a33	0.96	0.96	1.56	0.87	0.82	0.79
	a34	0.59	0.58	0.06	0.11	0.12	0.03
	a41	-0.09	-0.11	1.30	3.20	3.11	2.13
	a42	0.34	0.35	-1.55	-1.98	-2.09	-2.36
	a43	-0.19	-0.20	1.24	2.17	2.11	2.30
	a44	0.33	0.33	-0.63	-0.53	-0.50	-0.86
INTEGRAL GAIN COEFFICIENTS	b11	7.08	6.58	8.43	7.86	8.62	17.55
	b12	-0.62	-0.57	-0.37	-0.32	-0.39	-0.68
	b13	-0.54	-0.51	-3.42	-3.27	-3.37	-4.92
	b14	-0.54	-0.40	0.85	0.80	0.94	1.36
	b21	1.79	1.79	2.07	1.35	1.33	2.67
	b22	0.61	0.60	0.73	0.80	0.83	0.84
	b23	3.99	3.99	3.21	3.65	3.50	3.39
	b24	-0.39	-0.38	0.14	0.08	0.07	0.20
	b31	-1.88	-1.85	-1.09	-2.51	-2.77	-6.76
	b32	-0.37	-0.36	-0.17	-0.13	-0.15	-0.17
	b33	3.12	3.07	1.22	2.02	2.14	2.51
	b34	1.36	1.32	2.34	2.12	2.20	2.16
	b41	4.94	4.86	-8.42	7.75	8.66	8.95
	b42	0.32	0.32	-1.37	-1.65	-1.75	-1.98
	b43	-7.89	-7.86	18.95	7.27	6.90	5.34
	b44	4.45	4.47	-12.86	-11.50	-11.24	-13.43

TABLE 7 - PROPORTIONAL AND INTEGRAL GAIN COEFFICIENTS FOR THE HORIZONTAL-TO-VERTICAL TRANSITION CONTROLLER

OPERATING POINT		FLIGHT IDLE DESCENT FID2P	30% RALS IW22P	60% RALS IW32P	RALS IW52P	80% RALS IW62P	LANDING LAND2P
SPECIAL MANIPULATED VARIABLE		---	STP22	STP22	STP22	A88	A88
PROPORTIONAL GAIN COEFFICIENTS	a11	3.76	1.08	0.76	0.86	0.90	.07
	a12		-0.77	-0.58	-0.61	-1.10	-2.30
	a13		7.88	5.08	5.22	3.84	4.52
	a14		-0.0007	-0.02	-0.02	0.61	1.81
	a21		0.10	0.09	0.09	0.14	0.07
	a22		0.18	0.19	0.19	0.19	0.32
	a23		0.36	0.36	0.35	0.54	0.46
	a24		-0.005	-0.007	-0.006	0.09	0.17
	a31		-14.06	-9.59	-9.56	-4.43	-3.68
	a32		-0.43	-0.47	-0.46	-1.16	-1.56
	a33		6.91	5.30	5.18	4.60	3.80
	a34		0.20	0.14	0.14	0.76	1.49
	a41		2.97	2.67	2.90	-1.20	-1.04
	a42		-4.19	-3.88	-3.83	1.20	0.37
	a43		26.81	20.43	20.38	-1.21	-0.09
	a44		-1.27	-1.23	-1.20	0.40	0.38
INTEGRAL GAIN COEFFICIENTS	b11	4.30	5.27	4.86	5.03	5.92	4.76
	b12		-0.26	-0.22	-0.24	-0.89	-1.94
	b13		-7.12	-4.04	-4.42	0.33	4.51
	b14		3.16	2.16	2.21	-0.96	0.16
	b21		0.39	0.51	0.50	0.97	1.77
	b22		0.25	0.28	0.28	0.33	0.45
	b23		2.15	2.27	2.30	2.86	3.07
	b24		0.10	0.11	0.11	-0.07	-0.16
	b31		-34.74	-28.44	-28.51	-12.27	-18.89
	b32		-0.14	-0.12	-0.12	-0.69	-1.20
	b33		21.26	15.77	15.86	10.95	11.56
	b34		6.44	5.20	5.16	1.29	2.85
	b41		17.94	18.80	19.70	11.11	11.26
	b42		-3.04	-2.77	-2.74	0.91	0.34
	b43		16.88	13.57	12.51	-18.85	-8.99
	b44		-16.26	-15.68	-15.51	9.51	5.01

(Single Closed-Loop)

each of the 32 coefficients for the HTV transition (but with the single-loop FID case omitted). Tables 8 and 9 contain the resulting gains for each VTH and HTV operating points obtained from the results of the regression process. Comparison between Tables 6 and 8 and between 7 and 9 provide an indication of the magnitude of any resulting fitting errors.

Appendix B contains the results of a second series of time domain results for unit step demands applied simultaneously to all regulator inputs using the gains from Tables 8 and 9. The major effect of the regression errors was to increase the amount of interaction (high frequency) between control loops. The response continued to achieve steady-state although in several cases as much as five seconds was required. This was particularly true for the control variable T5.

The determination of the robustness of a multi-variable control system is one of the most dynamic aspects of advanced control theory and better methods for determining robustness continue to surface. Robustness tests are now available for parameter variations, gain variations, and frequency dependent variations for specific blocks of a closed-loop multi-variable control system. Robustness studies were conducted on the transition regulator for both sets of gain coefficients. As would be expected, the linear regression model was not as robust as its parent model but its margins were, however, adequate.

TABLE 8 - USE OF LINEAR REGRESSION TO DETERMINE PROPORTIONAL AND INTEGRAL GAIN CONSTANTS FOR THE VERTICAL-TO-HORIZONTAL TRANSITION CONTROLLER

FCD VALUE		0.0	0.1	0.7	0.75	0.8	1.0
OPERATING POINT		TAKEOFF TKO2P TKOK2P	START TRANSITION VII22P VIIK22P	ACTIVATE RFCV VII32P VIIK32P	MID TRANSITION VII42P VIIK42P	MIN RALS VII52P VIIK52P	MAX HORIZONTAL MXII2P MXIIK2P
SPECIAL MANIPULATED VARIABLE		A88	A88	STP22	STP22	STP22	STP22
PROPORTIONAL GAIN COEFFICIENTS	a11	1.59	1.52	1.06	1.02	0.98	0.83
	a12	-0.61	-0.62	-0.65	-0.66	-0.66	-0.67
	a13	0.90	0.93	1.13	1.15	1.16	1.23
	a14	0.59	0.52	0.09	0.06	0.02	-0.12
	a21	0.69	0.66	0.47	0.46	0.44	0.38
	a22	0.48	0.49	0.58	0.58	0.59	0.62
	a23	0.416	0.42	0.436	0.437	0.438	0.444
	a24	0.21	0.19	.026	.013	-2.2×10^{-4}	-0.053
	a31	-0.436	-0.447	-0.512	-0.517	-0.523	-0.545
	a32	-0.467	-0.451	-0.352	-0.343	-0.335	-0.302
	a33	1.021	1.016	.986	.984	.981	0.971
	a34	0.6	0.537	0.159	0.128	0.096	-0.029
	a41	-0.148	0.163	2.031	2.187	2.342	2.965
	a42	0.460	0.160	-1.64	-1.79	-1.94	-2.54
	a43	-0.315	-0.037	1.632	1.772	1.911	2.467
	a44	0.379	0.256	-0.485	-0.547	-0.608	-0.855
INTEGRAL GAIN COEFFICIENTS	b11	5.618	6.287	10.301	10.636	10.97	12.308
	b12	-0.558	-0.546	-0.475	-0.469	-0.463	-0.439
	b13	-0.281	-0.709	-3.278	-3.492	-3.707	-4.563
	b14	-0.563	-0.372	0.772	0.867	0.962	1.344
	b21	1.677	1.705	1.873	1.887	1.901	1.957
	b22	0.592	0.618	0.771	0.784	0.797	0.848
	b23	3.997	3.93	3.526	3.493	3.459	3.325
	b24	-0.404	-0.34	0.044	0.076	0.108	0.236
	b31	-1.204	-1.492	-3.217	-3.361	-3.505	-4.08
	b32	-0.367	-0.341	-0.189	-0.176	-0.164	-0.113
	b33	2.993	2.877	2.183	2.125	2.067	1.835
	b34	1.34	1.443	2.063	2.115	2.166	2.373
	b41	3.549	3.712	4.687	4.768	4.850	5.175
	b42	0.413	0.157	-1.382	-1.510	-1.638	-2.151
	b43	-10.768	-8.397	5.829	7.014	8.2	12.942
	b44	4.861	2.793	-9.615	-10.649	-11.683	-15.819

TABLE 9 - USE OF LINEAR REGRESSION TO DETERMINE PROPORTIONAL AND INTEGRAL GAIN CONSTANTS FOR THE HORIZONTAL-TO-VERTICAL TRANSITION CONTROLLER

FCD VALUE		0.0	0.1	0.2	0.3	0.9	1.0
OPERATING POINT		FLIGHT IDLE DESCENT FID2P	30% RALS HV22P HVK22P	60% RALS HV32P HVK32P	RALS HV52P HVK52P	30% RALS HV62P HVK62P	LANDING LAND2P LAHK2P
SPECIAL MANIPULATED VARIABLE		---	STP22	STP22	STP22	A88	A88
PROPORTIONAL GAIN COEFFICIENTS	a11	3.76	.98	.92	.86	.48	.42
	a12		-0.51	-0.65	-0.79	-1.64	-1.78
	a13		6.407	6.133	5.858	4.209	3.934
	a14		-0.187	-0.021	0.145	1.138	1.304
	a21		0.095	0.095	0.096	0.101	0.102
	a22		0.175	0.184	0.194	0.253	0.263
	a23		0.343	0.361	0.379	0.485	0.503
	a24		-0.024	-0.006	0.012	0.121	0.139
	a31		-12.150	-11.179	-10.207	-4.378	-3.406
	a32		-0.337	-0.456	-0.576	-1.295	-1.415
	a33		6.101	5.865	5.629	4.215	3.979
	a34		0.032	0.161	0.289	1.060	1.188
	a41		3.299	2.790	2.280	-0.779	-1.289
	a42		-4.507	-3.896	-3.286	0.375	0.985
	a43		25.526	22.460	19.395	1.002	-2.063
	a44		-1.422	-1.218	-1.003	0.254	0.464
INTEGRAL GAIN COEFFICIENTS	b11	4.30	5.067	5.093	5.118	5.269	5.294
	b12		-0.077	-0.235	-0.393	-1.343	-1.501
	b13		-6.337	-5.290	-4.243	2.041	3.088
	b14		2.865	2.485	2.105	-0.173	-0.553
	b21		0.334	0.458	0.581	1.322	1.445
	b22		0.251	0.268	0.285	0.385	0.402
	b23		2.143	2.239	2.336	2.917	3.014
	b24		0.134	0.105	0.076	-0.098	-0.127
	b31		-32.443	-30.474	-28.506	-16.697	-14.729
	b32		-0.02	-0.128	-0.237	-0.888	-0.997
	b33		18.650	17.757	16.865	11.51	10.618
	b34		6.032	5.571	5.110	2.344	1.883
	b41		19.58	18.626	17.671	11.944	10.989
	b42		-3.248	-2.801	-2.354	0.328	0.775
	b43		17.515	13.893	10.270	-11.467	-15.090
	b44		-18.368	-15.423	-12.477	5.196	8.142

5.4 Overall Control Concept

Figure 17 contains a preliminary block diagram of the overall V/STOL Propulsion Control concept evolving for the baseline VCE/RALS propulsion system. It indicates control inputs, outputs, and the principle interactions between the three major control sub-systems - the engine control, the thrust vector control and the flight control.

The engine control provides the basic functions such as main fuel control, internal variable geometry control, speed regulation, and engine limit protection. Engine control inputs include external sensor data (P2, T2, Mach. No.). Power Lever Angle (PLA)demand, and closed-loop sensor data (PCN2, T5, PS3, and XM93). The engine control logic includes:

- Closed-loop demand schedules for PCN2, T5, PS3, and XM93
- Open-loop demand schedules for STP22, and for STP49, A8 and A88 at reduced power operation
- Gain schedules for establishing regulator proportional/integral gains as a function of Thrust Vector Angle (TVA) and PLA demands and possibly as a function of flight condition (P2, T2, Mach. No.)
- Multivariable regulator which converts the closed-loop error signals into demand signals for the closed-loop manipulated variables (WF36, STP49, A8, and A88)
- Transition controls for limiting regulator outputs during large and/or fast throttle bursts and chops. The transition controls include fuel accel and decel schedules for stall and blowout protection; engine speed, temperature, and pressure protection; and any special logic required for augmentor light-off and shut-down protection.

The engine control logic provides output demands for primary fuel flow (WF36) and low pressure turbine stator position (STP49) to the position servos and nozzle area error signals ($\triangle$A8R and $\triangle$A88R) to the feed forward system.

The thrust vector control sets the nominal thrust split between the RALS and ADEN nozzles and the ADEN thrust vector angle. Thrust vector control inputs include sensor data (T2, PCN2), TVA demand, and Pitch Rate (PR) demand. A Thrust Ratio (TR) demand could be used in place of individual TVA and PR demands and represents the ratio of RALS Gross Thrust to

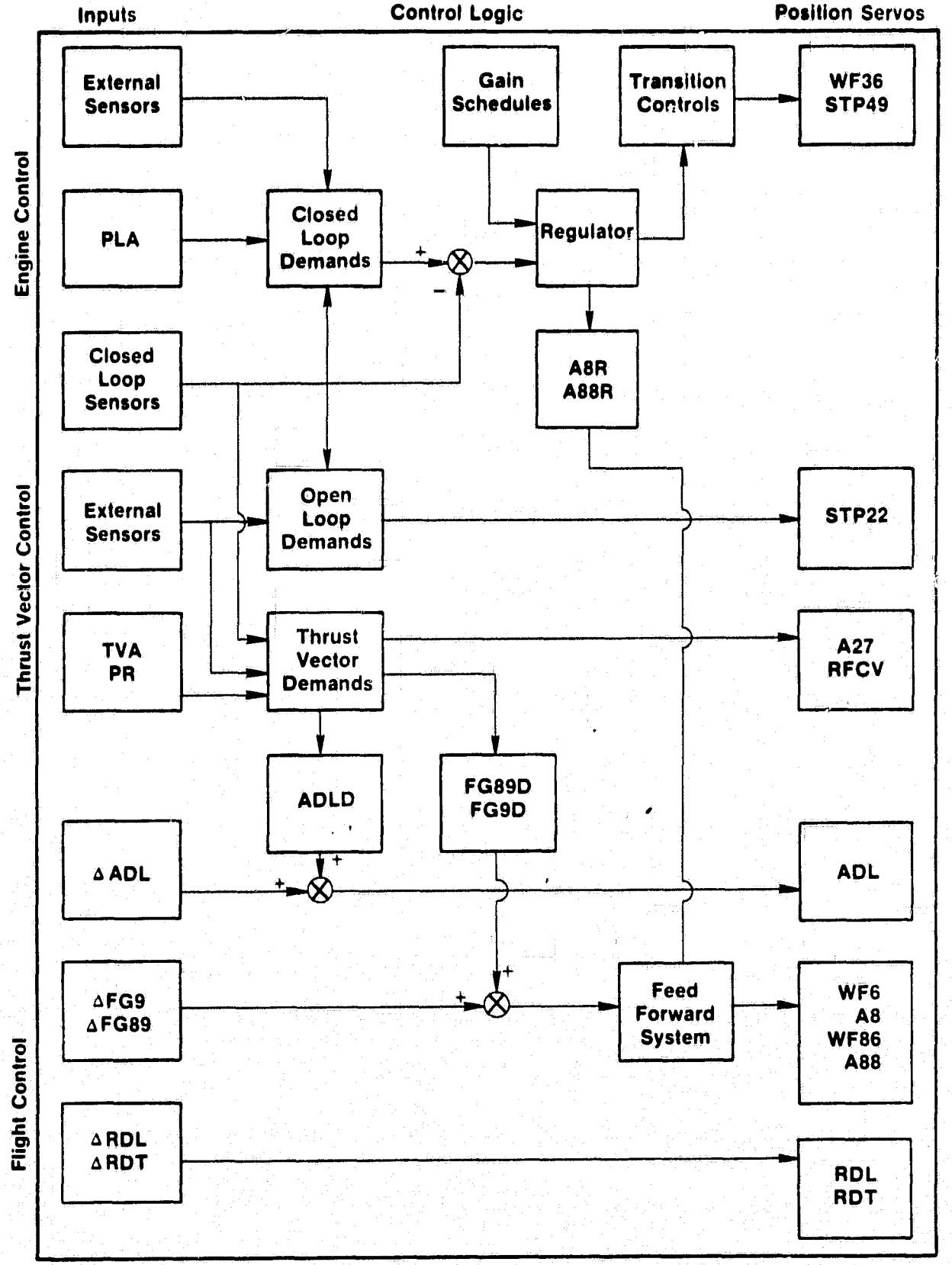

Figure 17. Overall V/STOL Propulsion Control Logic.

ADEN Gross Thrust. The thrust vector control includes:

- Open-loop demand schedules for the rear VABI (A27) and the Remote Flow Control Valve (RFCV) which sets the flow split between the primary and remote augmentors.
- The nominal ADEN deflection angle (ADL) demand which is set to the TVA demand.
- RALS and ADEN nominal gross thrust demands (FG89D and FG9D). ADEN gross thrust demand is dependent upon PLA demand, flow split demand, and the external operating condition (P2, T2, Mach. No.). RALS gross thrust demand is determined from the ADEN thrust demand and the thrust ratio demand implied by TVA and PR. Note that the individual thrust demands effectively set nominal augmentor temperatures in both the ADEN and RALS augmentors.

The thrust vector control logic provides output demands for A27 and RFCV to the positon servos and nominal demands for ADL, FG89, and FG9 to the flight control system.

The flight control responds to individual ADEN and RALS thrust magnitude and deflection demands from the aircraft height and attitude control system. It includes the following elements:

- ADEN deflection demand ($\triangle$ADL) is added to the nominal demand signal from the thrust vector control (ADLD) to establish the actual demand.
- Thrust magnitude demands ($\triangle$FG89 and $\triangle$FG9) are added to the nominal demand signals from the thrust vector control to establish the actual demands.
- RALS deflection demands in the longitudinal direction ($\triangle$RDL) and the transverse direction ($\triangle$RDT) are used to set the actual RALS deflection demands.
- The actual thrust demands and the nozzle area error signals from the engine control are input to the feed forward system to establish augmentor fuel flow and nozzle area demands to the ADEN (WF6 and A8) and the RALS (WF86 and A88) systems. Note that the feed forward system modifies all four demand signals to trim nozzle area errors at constant thrust and to trim thrust corrections at constant engine operating point.

The flight control logic provides demand signals directly to the corresponding positon servos.

Control logic has been defined under the Phase I and II study efforts for the regulator gain schedules, the regulator, and the feed-forward system. Additional control logic must be developed under subsequent study programs to define the following:

- Closed-loop and open-loop demand schedules
- Thrust vector control demand schedules
- Transition control schedules and logic
- Gain schedules for the feed-forward system, if required

Each of the above schedule requirements need to be examined over their respective operating regimes to determine scheduling requirements with PLA, TVA, and any external operating effects due to P2, T2, and flight Mach number. Control stability and robustness studies must be conducted at selected operating conditions to establish any additional control logic requirements for full range-full power operation.

6.0 MATHEMATICAL MODELING

6.1 Inlet and Nozzle Effects Model

A realistic evaluation of V/STOL steady-state and transient performance characteristics over the total vertical and horizontal flight operating regime will require the addition of inlet and nozzle environmental effects peculiar to the V/STOL system to the conventional engine simulation. These effects include the following:

- The effects of high angles of attack on inlet recovery and distortion during the flight transition between vertical and horizontal operation.
- The effects of the above inlet distortion on internal fan and compressor performance and stall tolerance.
- The effects of large exhaust system deflections on nozzle performance.
- The effects of flow re-ingestion and associated inlet temperature distortion associated with operation in-ground effect or at low flight speeds.

It is expected that the supersonic V/STOL aircraft will operate with an open auxiliary inlet during vertical operations and at low forward speeds and that the auxiliary inlet characteristics will dominate the level of

inlet recovery and distortion. Figure 18 illustrates the effects of flight Mach number and mass flow ratio on the inlet recovery characteristics of a representative auxiliary inlet. Examination of an inlet distortion pattern measured with an open auxiliary inlet indicates that the inlet distortion parameter which is defined by:

$$ID = (PAV - PMIN)/PAV$$

is equal to approximately three times the inlet revovery loss. It has been assumed that this relationship would be approximately valid over the entire range of flight Mach numbers and inlet mass flow rates such that:

$$ID = 3(1.0\text{-Inlet Recovery})$$

Figure 19 illustrates the effects of this inlet distortion on the fan mass flow, efficiency, and stall pressure ratio and Figure 20 contains the distortion transfer effects through the front and rear block fans to fan discharge.

Compressor inlet distortion will depend upon the portion of the fan exit distortion which is ingested by the compressor and can be approximated by the relationship:

$$(ID)_{comp} = (ID)_{fan} \frac{\text{Compressor Mass Flow}}{\text{Fan Mass Flow}}$$

Figure 21 illustrates the resulting inlet distortion effect on compressor mass flow, efficiency, and stall pressure ratio for the baseline VCE/RALS engine.

The engine exhaust nozzles will be subject to significant crosswind effects at the low flight speeds associated with the flight transition region. The crosswind velocity will be the resultant of the aircraft motion and the unsteady environmental air velocity. Figure 22 illustrates the effect of the crosswind velocity on the nozzle discharge coefficient. Note that the effect is dependent upon the effective nozzle aspect ratio.

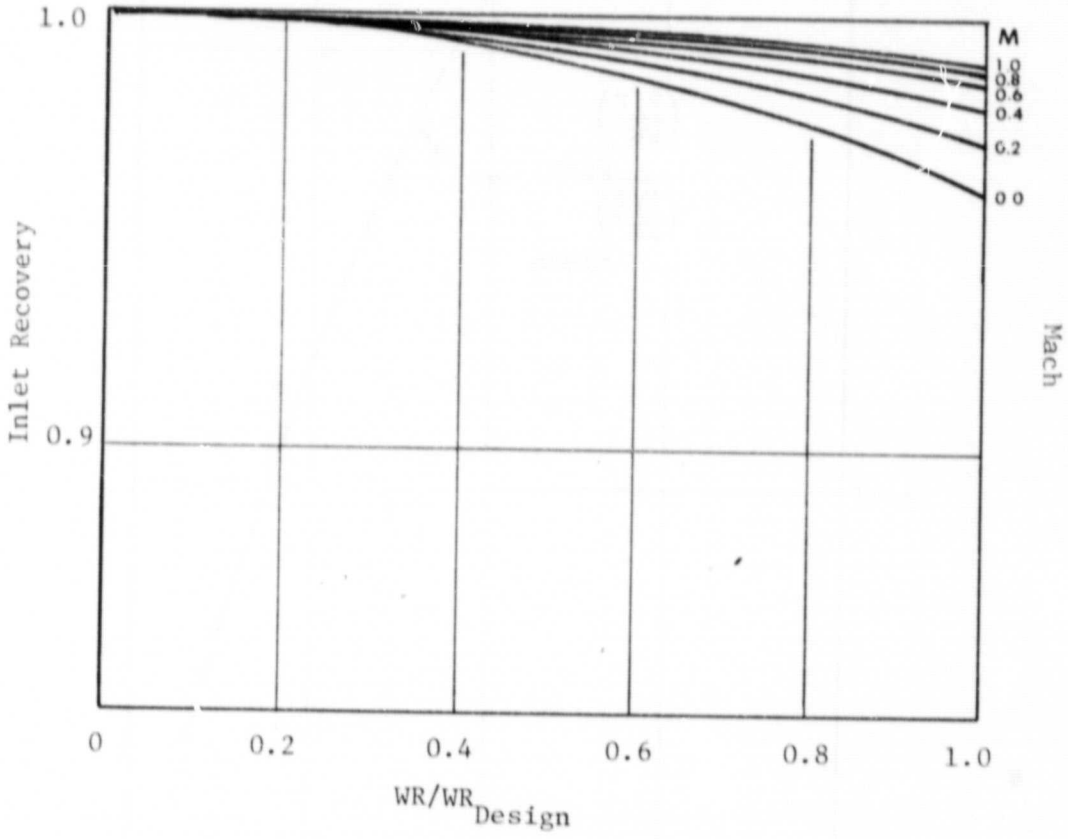

Figure 18. Inlet Recovery-Auxiliary Inlet Doors Open.

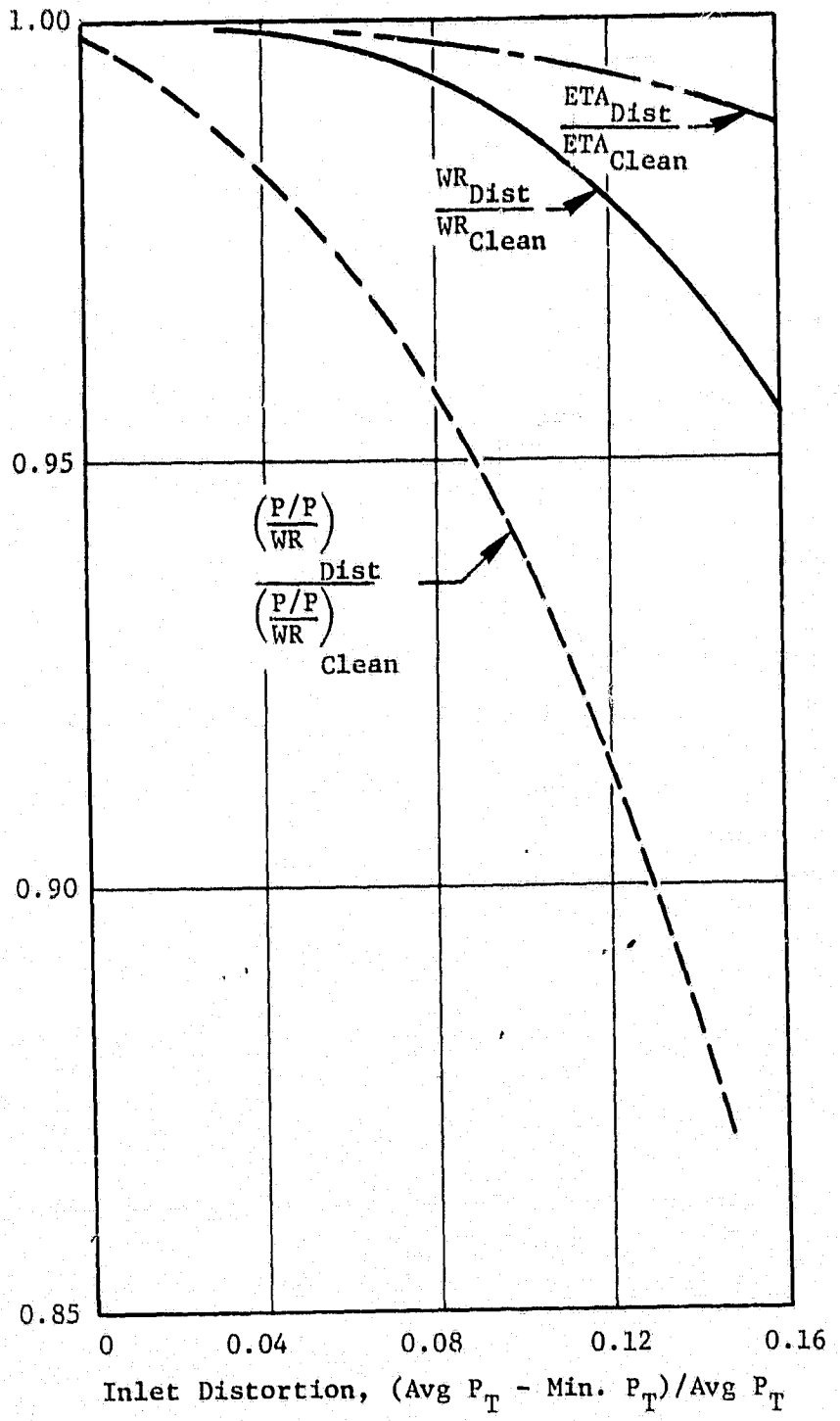

Figure 19. Inlet Distortion Effects on Fan Performance.

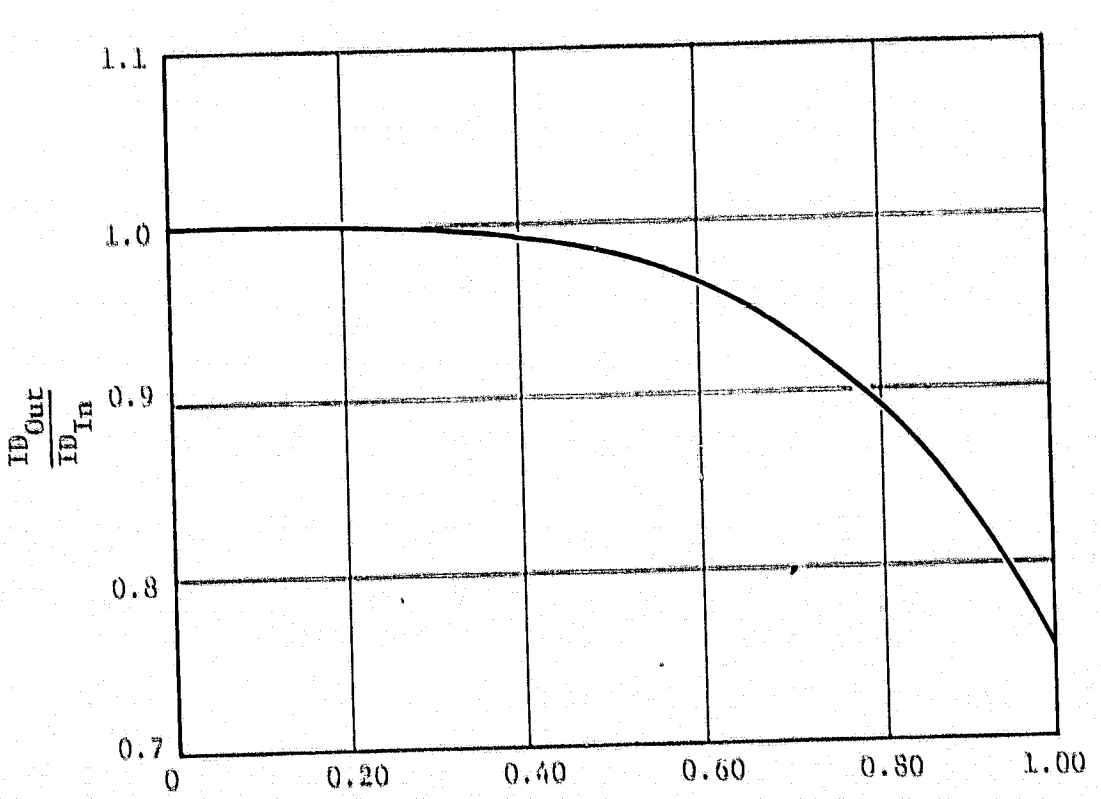

Figure 20. Distortion Transfer to Fan Discharge.

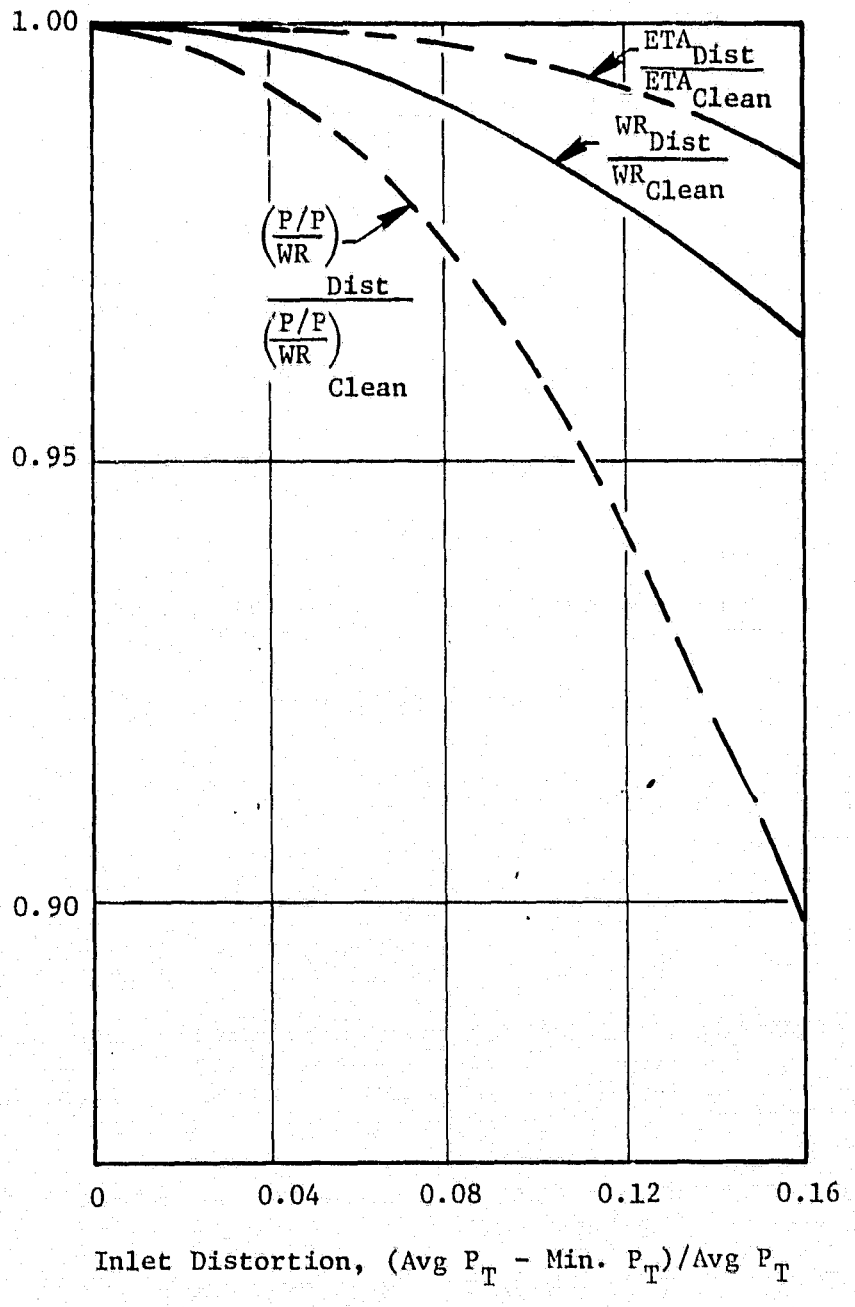

Figure 21. Inlet Distortion Effects on Compressor Performance.

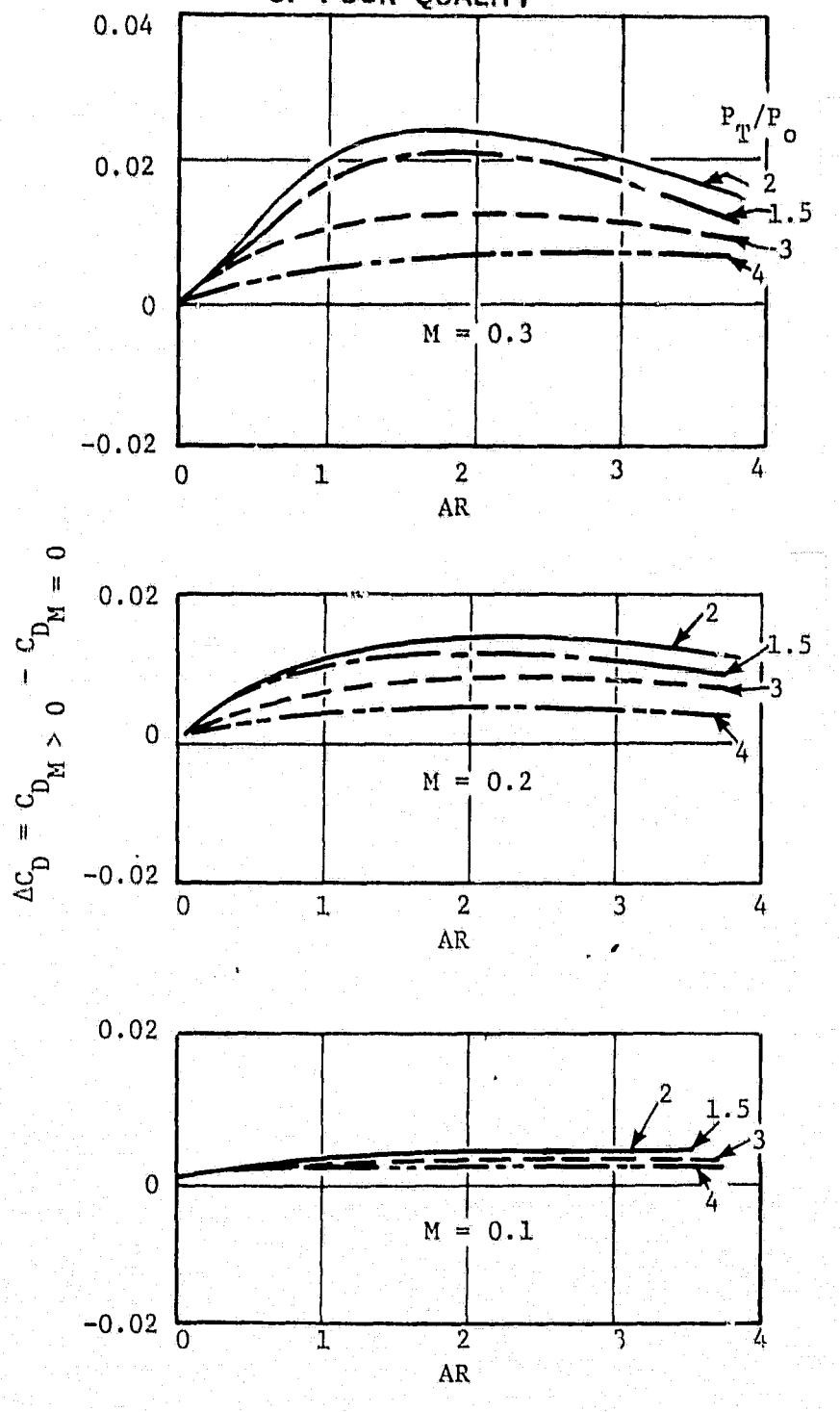

Figure 22. Effects of Crosswind on Nozzle Discharge Coefficient.

Corresponding crosswind effects on nozzle thrust coefficient are shown in Table 10. Note that these effects are relatively small.

The inlet and nozzle effects model will be added to the component-level engine transient model in order to provide a capability for more realistic simulation studies in the hover and low-speed transitional region.

6.2 Aircraft Model

A simplified dynamic model of a V/STOL aircraft has been modified to fit the baseline VCE/RALS propulsion system for use in studying the flight transition process. The model uses aircraft stability derivatives obtained from Reference 2. Assistance in the development of the dynamic model was provided by the McDonnel Douglas corporation.

The aircraft is controlled aerodynamically during conventional horizontal flight by ailerons, rudder and stabilator. Aerodynamic control is augmented by thrust control during the hover and low flight speed operating regime. The thrust control system assumes a two-engine installation and consists of the following:

- Pitch control is provided by modulating the fuel flow to the primary and remote augmentors about nominal levels which are scheduled throughout the vertical and transition flight regimes. The nominal augmentor fuel flow schedules are designed to produce a zero propulsive pitching moment about the aircraft pitch axis.

- Yaw control is provided by longitudinal vectoring of the ADEN and RALS nozzles and by side vectoring of the RALS nozzle. Side vectoring of the ADEN nozzle is not available with the current ADEN nozzle configuration.

- Roll control is provided by vertical wing-tip jets supplied by continuous compressor bleed air. The flow distribution between the two jets is modulated to respond to roll control demands. The continuous bleed level is scheduled throughout the vertical and transition flight regime to maintain the required level of roll control.

The present model configuration is limited to flight simulations initiated at zero forward speed (hover) and terminated at an air speed of about 105 knots. Aerodynamic control has not yet been integrated with

TABLE 10 - EFFECTS OF CROSS-WIND ON NOZZLE THRUST COEFFICIENT

M	PT_j/P_o	ΔCFGR AR =.38	ΔCFGR AR =1.0	ΔCFGR AR =3.6
.1	1.5	.0005	.0005	.0005
	2.0	0	.0005	.0008
	3.0	0	0	0
	4.0	0	0	0
.2	1.5	.0005	.0016	.0015
	2.0	.001	+.001	+.001
	3.0	0	-.0002	-.0005
	4.0	0	0	0
.3	1.5	.001	.0023	.0016
	2.0	.001	.0015	.0013
	3.0	-.0002	-.001	-.001
	4.0	0	-.0005	-.0002

the model thrust control system and thrust roll and yaw controls have not yet been added. The current model is, therefore, currently applicable only to the simulation of Vertical-to-Horizontal transitions and only to the above flight speed limit. Additional limitations on the current model include the omission of ram drag and crosswind effects on aircraft motion.

Preliminary VTH transition trajectories were simulated. The results indicated the need for some form of pilot model to control the rate of transition from vertical to horizontal flight and the corresponding aircraft attitude during the transition. Table 11 contains a simple pilot model which was defined and incorporated with the dynamic aircraft model for this purpose. Note that this pilot model is applicable only to the VTH transition. The pilot model involves the following:

- Total thrust is held constant at 110% of the aircraft weight
- Thrust vector angle rotation rate is dependent upon the normal acceleration, normal velocity, forward velocity, and pitch attitude
- Pitch acceleration is dependent upon actual and desired final pitch attitude, forward velocity, and the pitch rate
- Thrust vector angle and pitch rate are obtained by integration of the above rates

The VTH pilot model was utilized in conjunction with the aircraft model to conduct simulation studies of the initial phase of the VTH transition process. The results of these studies are described in Section 7.1.

6.3 Engine Description

6.3.1 Engine Components and Gas Flows

The baseline engine consists of the following turbo-machinery components - a front block fan, a rear block fan, a compressor, a high pressure turbine, and a low pressure turbine. Additional components include a main burner, two augmentors, and two nozzles. Front block fan discharge air can be split between the rear block fan and an outer duct which bypasses the air around the second block fan. Second block fan discharge air is similarly split between the compressor and an inner duct which bypasses the rest of the turbomachinery. The outer

TABLE 11. ASSUMED VTH PILOT MODEL

THRUST = 1.1* AIRCRAFT WEIGHT
$\frac{\partial(TVA)}{\partial t} = 1/2^* \left[ZIVEL - PITCH^*XIVEL + \frac{\partial(ZIVEL)}{\partial t} \right]$
$\frac{\partial^2(PITCH)}{\partial t^2} = \frac{XIVEL}{100} \left[FINAL\ PITCH - PITCH \right] - 1/2^* \frac{\partial(PITCH)}{\partial t}$
where: TVA is the ADEN Thrust Vector Angle ZIVEL is the Normal Velocity XIVEL is the Forward Velocity PITCH is the Pitch Attitude Angle

bypass from the front block is mixed with the inner bypass air from the rear block. The resulting bypass air can be directed to the remote burner and nozzle, to the rear mixer for mixing with the hot stream from the low pressure turbine, or split between the two systems. Remote burner discharge is exhausted through the RALS nozzle and the mixed stream from the rear mixer is exhausted through the afterburner and ADEN nozzle. Current propulsion control studies have been restricted to single bypass operation of the baseline engine with no outer bypass flow around the second block fan.

Gas flow paths are shown schematically in Figure 23. Major components are identified by the shaded areas. Stations are identified at the boundaries of each component where there is an interface with another component. Thermodynamic accounting is accomplished at each station (or node) and includes accounting for pressure, temperature, enthalpy, gas flow, and air flow. In addition to the major gas flows, there are secondary flows for fuel flow, cooling air from the compressor to the hot engine parts, and customer bleed flow to airframe systems. All flow paths are indicated and labeled. The cooling flows are designated as WACLi where i is the station number where the flow is assumed to be returned to the primary system. The bleed flows are designated as WBi where i is the station where the flow is removed from the engine. The fuel flows are designated as WFi where i is the last station before the fuel flow is introduced into the primary system. Combustion is assumed to be completed before the next station.

A more conventional description of the station designations can be obtained from Figure 25.

6.3.2 Environmental Inputs and Outputs

The environmental inputs to the engine from the atmosphere and the air frame are:

P2	Inlet Total Pressure
T2	Inlet Total Temperature

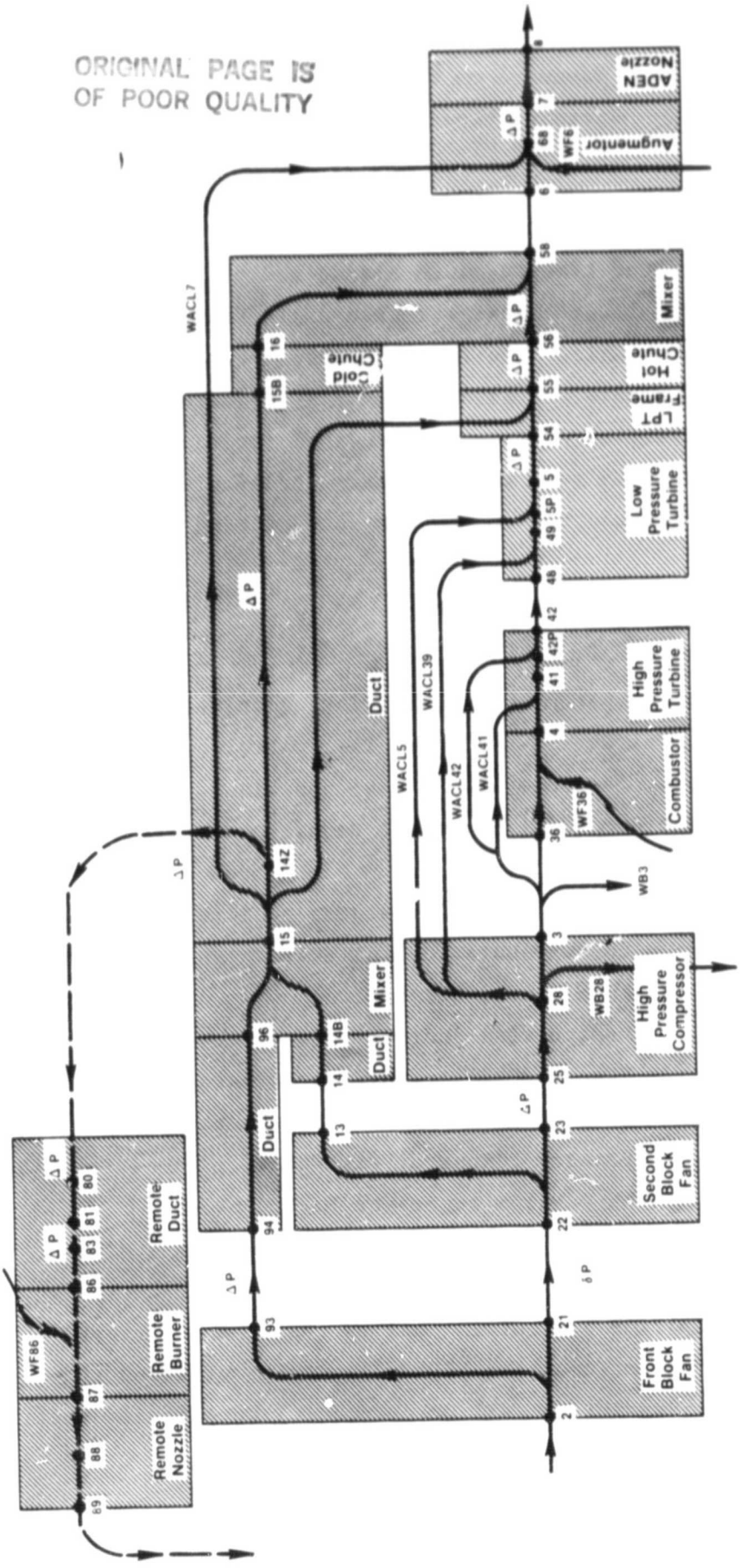

Figure 23. Engine Gas Flow Paths

PAMB	Ambient Static Pressure assumed to be the back pressure on the nozzles
WB28, WB3	Customer bleed air extracted from the compressor for use by air frame systems

The engine outputs are the two thrust vectors. The rear thrust vector is obtained from the ADEN nozzle and is defined by a gross thrust magnitude and a longitudinal rotation angle from the horizontal direction around the pitch axis. The remote thrust vector is obtained from the remote (RALS) nozzle and is defined by a gross thrust vector and two orthogonal rotation angles - longitudinal rotation and a transverse rotation around the roll axis. A corresponding ram drag vector parallel to the aircraft velocity vector has been omitted from the initial modeling process.

6.3.3 Engine and Control System Interfaces

The control system outputs provide additional inputs to the engine model and its evaluation process. The control outputs include the individual fuel flows, variable stator vane positions, and any variable flow areas. The current baseline engine requires the following control outputs:

STP22	Second block fan stator position (angle)
STP49	Low pressure turbine stator vane angle
A8	ADEN nozzle throat area
AE80	Remote flow control valve area
A88	Remote (RALS) nozzle throat area
AE16	Rear VABI cold-stream discharge area
WF36	Primary combustor fuel flow
WF6	Mixed-flow augmentor fuel flow
WF86	Remote augmentor fuel flow

The transition controller obtains the demands for WF36, A8, A88 (at high remote flow rates), and STP22 (at low remote flow rates) from the multivariable regulator. All other control outputs are obtained directly from open-loop schedules.

Internal engine variables sensed by the control system include the following:

N2	The front block fan and low pressure turbine rotor speed
N25	The rear block fan, compressor, and high pressure turbine rotor speed
M93	The gas Mach number at front block fan discharge
PS3	The compressor discharge static pressure
T5	The total temperature at low pressure turbine discharge
T25	The total temperature at compressor inlet

N25 and T25 are used to calculate the corrected compressor speed which is used for open-loop scheduling of the variable compressor vanes which have been assumed to track their nominal schedule and, consequently, have been omitted from the transient studies. The remaining sensed variables provide inputs for the regulator in determining the closed-loop demands.

External sensed variables and inputs to the control system include the following:

T2	Engine or front-fan inlet total temperature
PLA	Power Lever Angle
FCD	Flight Control Demand or its equivalent (thrust vector angle or thrust ratio demands)

These inputs define the external environment and the current thrust management demands on the engine.

6.3.4 Operating Modes

The engine and the model are capable of the following modes of operation:

- Horizontal (H) Mode - The H mode is used for conventional horizontal flight and has the remote system shut down. All bypass duct flow is mixed with turbine discharge flow in the VABI and the resulting flow exhausted through the ADEN. The top sketch in Figure 24 illustrates the major gas flow paths for the H mode of operation.

- Vertical (V) Mode - The V mode is used for vertical takeoff and landing. All bypass duct flow is diverted to the remote system and discharged through the RALS nozzle. The cold side of the VABI

Horizontal (H) Mode of Operation

Vertical (V) Mode of Operation

Figure 24. RALS/VCE Engine Operating Modes

is closed and the turbine discharge flow passes through the hot side of the VABI and is discharged through the ADEN. The bottom sketch in Figure 24 illustrates the major gas flow paths for the V mode of operation.

- Transition (T) Mode - The T mode is used for flight transition between the H and V modes. The bypass duct flow is split between the remote system/RALS nozzle and the VABI/ADEN. The T mode is further subdivided into T1 and T2 modes as follows:

  T1 - the remote system flow is controlled by the RALS nozzle

  T2 - the remote system flow is controlled by the Remote Flow Control Valve (RFCV)

The T1 mode is used for high remote flow rates (the initial phase of the V to H transition and the final phase of the H to V transition) where the RALS nozzle is capable of adequate flow control. The T2 mode is used for low remote flow rates (the final phase of the V to H transition and the initial phase of the H to V transition) where the RALS nozzle is set at minimum area and the RFCV must be used to control the flow.

The engine model reflects each of the above modes of operation and uses different iteration logic for each individual mode. The accounting sequence for the remote and bypass systems is also switched for each mode.

6.4 Model Description

The engine model represents a non-linear model of the baseline engine which has been combined with non-linear models of sensors, actuators, augmentors, and nozzles developed under the Phase I study. The model represents the steady-state and transient performance of the engine. The engine dynamics, and corresponding time constants, can be classified as follows:

• Gas Momentum Conservation	.003 seconds (time constant)
• Gas Mass and Entropy Conservation	.003 to .03 seconds
• Rotor Dynamics	.25 to 2.5 seconds
• Heat Storage	5 seconds and up

The current function of the engine model is to develop the engine control concept and to demonstrate by simulation that its dynamics are suitable for the aircraft control and flight transition processes. The gas dynamics effects are about an order of magnitude outside of the

desired range and have, therefore, been omitted from the model. Conversely, the heat storage effects have been shown to effect mainly acceleration and deceleration rates and some long term thrust transients. These dynamics interact very little with the control system and have also been omitted. The rotor dynamics have a significant effect on the control system and have been included in the model.

The gas flow and thermodynamic model is a quasi-steady-state model with each of the major engine components (fan, compressor, burners, turbines, mixer, nozzles and ducts) represented as discrete elements of the model. Mass flow, pressure, temperature, and enthalpy are accounted for directly and the corresponding entropy accounting is handled indirectly. The model contains the same inputs and outputs as the engine and the order of calculation proceeds roughly from engine inlet to discharge.

6.4.1 Thermodynamic Accounting

The turbomachinery components are represented as functions of two variables for fixed geometry components and a third variable is included for variable geometry components. The input variables for the compression components are corrected speed, an arbitrary variable which defines the departure from the minimum loss line, and variable stator position (where applicable). The turbine input variables are corrected speed, an energy ratio, and variable stator position (where applicable). Each component representation provides the component corrected gas flow, the pressure ratio, and the corresponding temperature ratio. Component efficiency is implied by the output pressure and temperature ratios but is not calculated.

Each duct pressure loss is calculated as a function of duct corrected flow and the V-BI pressures are obtained from the equations of conservation of mass, momentum, and enthalpy. Burner enthalpy rise is a product of fuel flow and burner efficiency. Burner efficiency is obtained from the burner inlet temperature, pressure and corrected airflow. Nozzle flow areas are obtained from choked-flow or unchoked relationships depending upon the nozzle pressure ratio. Gas enthalpy is obtained as a function of gas temperature and fuel-air ratio and gas entropy calculations are

avoided by the direct pressure and temperature ratio calculations.

The component representations were derived from the steady-state component operating characteristics of Figures 8 through 12. Since this model is intended to be a precursor for a subsequent real-time model for piloted simulation, a minimum computing time approach was used. Conventional table look-up and interpolation techniques were replaced by a polynomial representation approach. A leaps-and-bounds procedure was used to identify the best functional form for each component. The individual coefficients were then determined to minimize the mean square error.

Elemental table-like functions are used for some components. Nozzle characteristics, for example, have one function for choked flow and a second function for unchoked flow.

6.4.2 Iteration Techniques

Internal variables which must be known or assumed in order to complete the cycle calculation are designated as iteration variables. An equal number of dependent variables must also be available which can be calculated by two independent physical processes. The differences between the two calculation results represent the iteration errors. The iteration errors are functions of the iteration variables and an error partials matrix can be calculated from a series of perturbations of the iteration variables. The partials matrix represents a linearization of the functional relationships at a specific operating point. The iteration procedure must adjust the iteration variables to minimize the error vector. This is accomplished by the iteration algorithm which computes an adjustment vector from the product of an iteration matrix and the error vector and then subtracts the adjustment vector from the previous iteration variable vector.

In a non-real time model, the error partials matrix can be calculated for each individual operating point and inverted to obtain the iteration matrix. In order to achieve a real-time capability, the dynamic model must use a predetermined iteration matrix to permit a single pass per calculated

time step. The iteration matrix can be a constant matrix or its elements can be scheduled as a function of one or more of the engine variables. The iteration matrix will bear some relationship to the inverse of the error partials matrix.

There are two central problems to be solved in order to make this type of iteration work effectively. First, the error partials matrix must be well conditioned. This must be accomplished by a careful selection of iteration variables and an even more careful selection of error variables. These variables must be selected or designed for linear independence. A measure of linear independence is a condition number defined as the ratio of the maximum singular value to the minimum singular value of the error partials matrix. If the error partials matrix is A, then the singular values are the positive square roots of the eingenvalues of the A^TA matrix. For the current engine model which has a 5x5 matrix for the H and V modes, and a 6x6 matrix for the T mode, the iteration procedure works well only when the condition number is less than 20. This is not a hard limit, however, since slow convergence has been achieved with condition numbers as high as 150. Extremely rapid convergence has been achieved with condition numbers below 15.

The second central problem involves the scaling of the errors or the iteration variable increments so that the engine error matrix is relatively constant for the important coefficients. The variables and errors should be ordered so that the most important coefficients are on the diagonal. Important coefficients should not vary by more than 4:1 and preferably less than 2:1.

The following procedure was used to develop an iteration matrix from the available error partials matrices:

- The maximum value of the diagonal elements over the set of operating points (cycle data used in the regression fitting) were selected for the matrix diagonal.
- The minimum value of the off-diagonal elements were selected for the matrix off-diagonal terms. Diagonal terms which reversed sign over the operating regime or which were less than .1% of the magnitude of the diagonal were set to 0.

- The matrix was inverted and then all small off-diagonal terms of this inverse were set to 0. The resulting matrix is used as the iteration matrix.

An iteration matrix was developed for each individual model operating mode (H, V, T1 and T2).

6.4.3 Model Structure

The non-linear transient engine model has been structured for implementation on a hybrid computer with 16 bit fractional arithmetic (EAI P-100). All variables have been scaled to operate in the range of -1 to +1. A detailed description of the model structure is contained in Appendix C showing the functional form of each equation. This description uses the following nomenclature:

P	Total Pressure
Ps	Static Pressure
T	Total Temperature
H	Total Enthalpy per Pound of Air
STP	Stator Position
WA	Air Flow
W	Gas Flow
E	Iteration Error

Station designations are illustrated in Figure 25 and are used to modify the above variable names. An X following the station designation indicates an alternate computation of a variable for the purpose of calculating an iteration error. An R following the station designation indicates a corrected variable.

7.0 SIMULATION STUDIES

7.1 Flight Trajectory Simulation

The simplified pilot and aircraft models of Section 6.2 were used to conduct preliminary simulation studies of the initial phase of the Vertical-

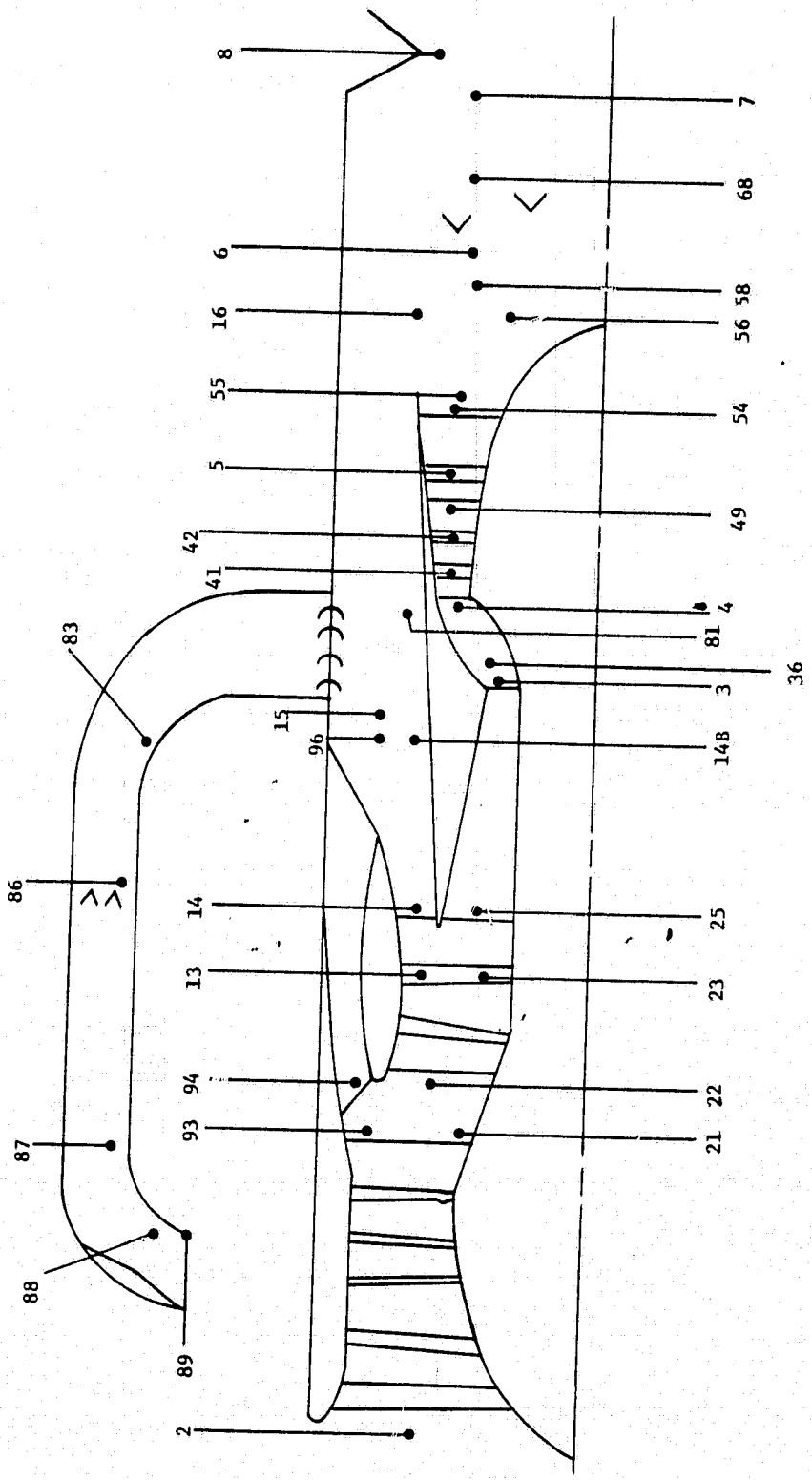

Figure 25. RALS/VCE Engine Station Designations

to-Horizontal transition process in order to determine thrust requirements during transition.

Figure 26 contains the results of a VTH transition simulation from hover to a final airspeed of 105 knots for a final pitch angle of 2.9°. The acceleration required 17 seconds to reach the final velocity and resulted in an essentially zero incidence angle for the final 7 seconds of the trajectory. RALS and ADEN thrust requirements to fly this trajectory are illustrated in Figure 27 along with the corresponding thrust vector angle. The intent of the thrust vector control was to schedule the nominal RALS and ADEN thrust split to maintain a zero propulsive pitching moment throughout the transition process. This would be achieved by scheduling the flow split between the primary and remote systems and corresponding nominal RALS and ADEN augmentor fuel flows as a function of Thrust Vector Angle Demand (TVA). The Pitch Rate (PR) demand would impose additional RALS and ADEN fuel flow/thrust modulation requirements which should be within the $\pm$ 12% modulation capability of the current baseline engine. As indicated in Figure 27, the actual thrust modulation requirement (FGMOD/FG) exceeded the $\pm$ 12% baseline capability near the tail-end of the trajectory.

Examination of the aircraft model and the aerodynamic derivatives of the pitch acceleration with respect to the forward velocity revealed the source of the problem. Figure 28 illustrates the assumed variation of this parameter with forward velocity. The current aircraft model aerodynamics are limited to small perturbations about the initial airspeed and, consequently, can equate the derivative of the pitch acceleration (∂PITCH"/ ∂V) to (∂PITCH"/XIVEL) where XIVEL is the difference between instantaneous and initial forward velocity. This equality holds for small forward velocities but not over the velocity range of the VTH transition process. Further development of the aircraft model will be required to resolve this problem so that a more realistic assessment of propulsion modulation requirements can be obtained.

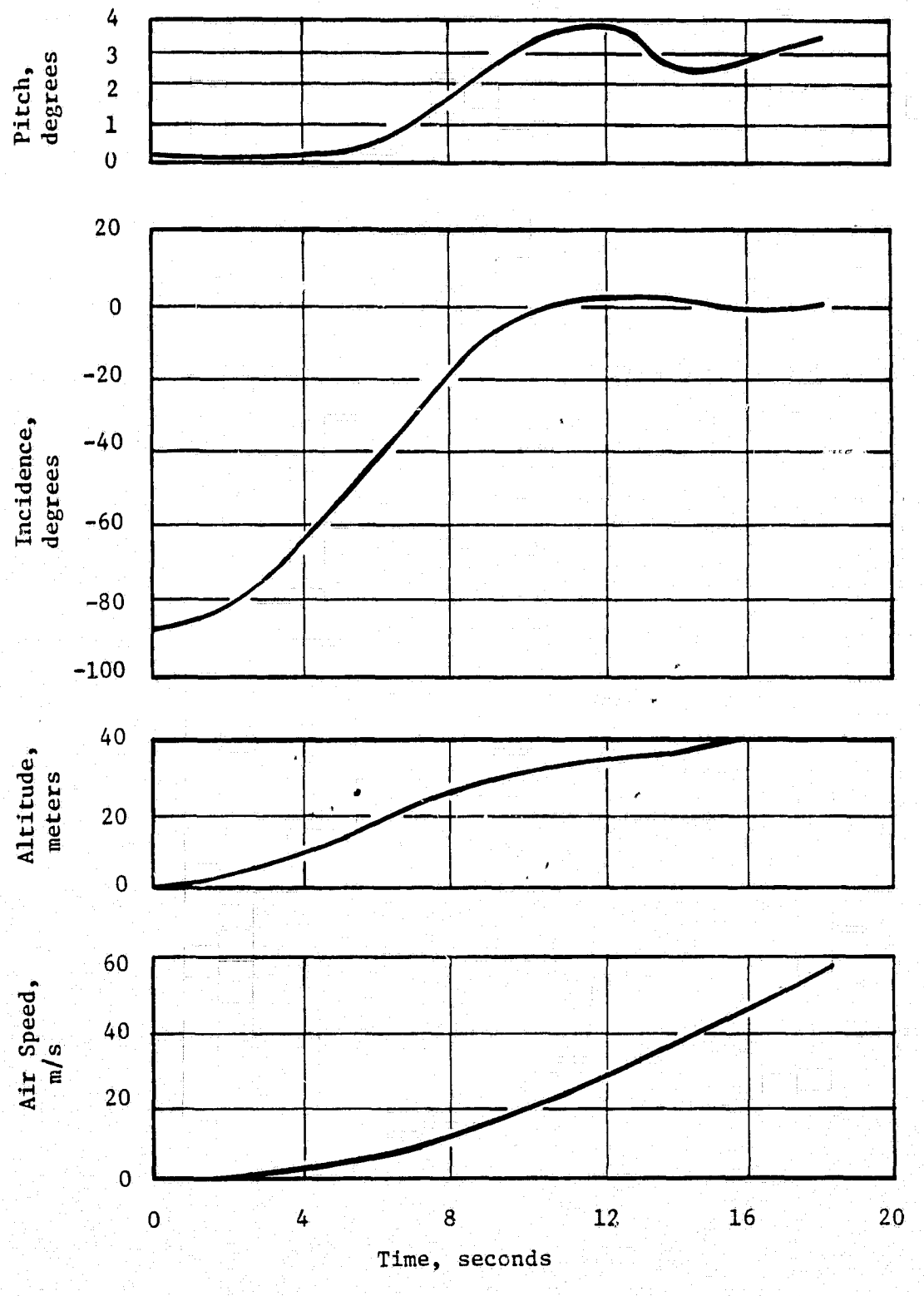

Figure 26. Typical VTH Transition Trajectory

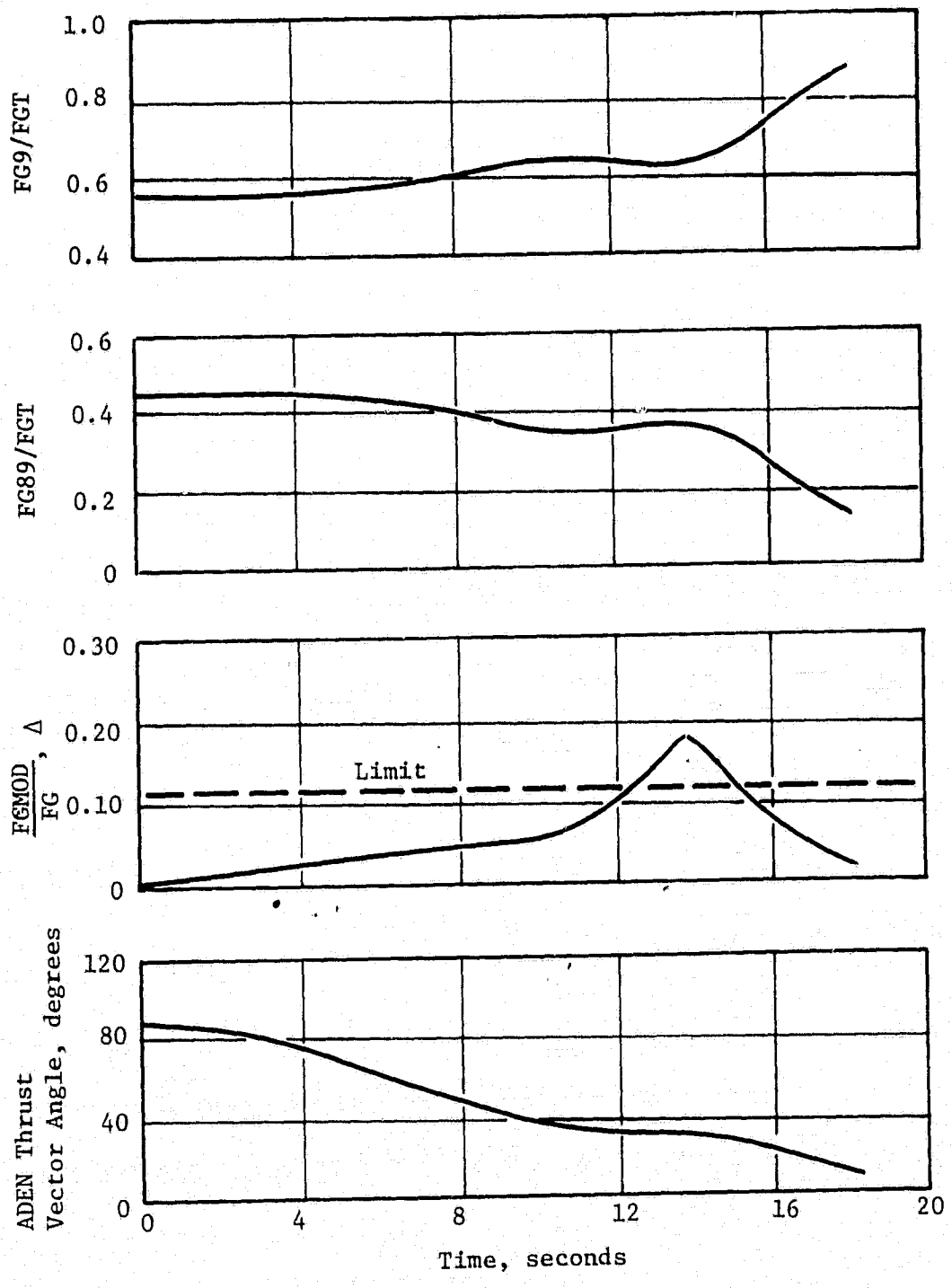

Figure 27. Typical VTH Thrust Requirements

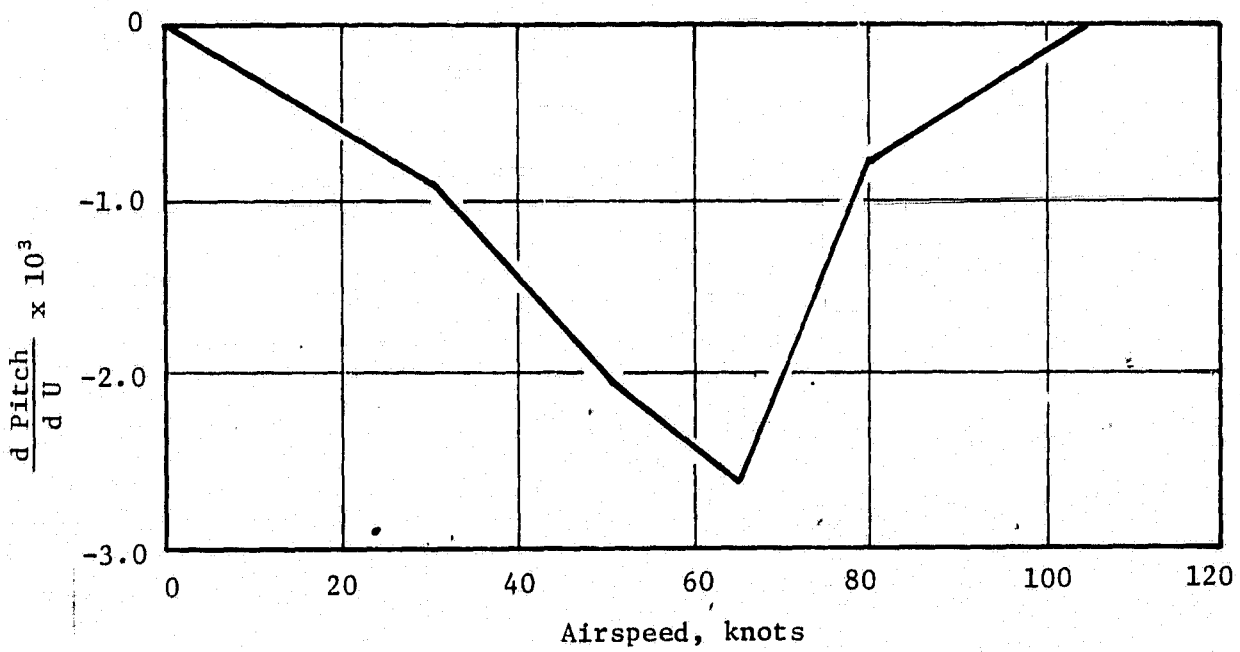

Figure 28. Aircraft Pitch Acceleration Due To Forward Motion

7.2 Engine Transient Simulation Results

The Phase II hybrid computer simulation studies consisted of the incorporation of two major modifications to the Phase I simulation program:

- The incorporation of a mode-switching digital transition regulator that would handle the V, T, and H operating modes along with the VTH and HTV transition paths.
- The incorporation of an iterative non-linear transient model of the baseline engine which represented operation along the above transition paths.

The initial modification to the Phase I simulation involved the replacement of the analog engine controller by its digital equivalent. The digital controller was then used with the Phase I Linear Engine Model and the non-linear actuator, augmentor, and nozzle models to reproduce the Phase I simulation results. This modification was successfully checked-out in the Takeoff Mode and the digital controller coding was used as the basis for coding the transition regulator.

The next modification involved the replacement of the current digital controller by the digital transition controller. The digital controller required the following inputs:

- TRNDIR - This input specified the type of flight transition path. A negative value of TRNDIR resulted in the selection of the VTH transition and a positive value the selection of the HTV path.
- FCD - This input represented the Flight Control Demand and defined a specific operating point along the specific VTH or HTV path defined by TRNDIR. Specific controller proportional and integral gains were obtained from the built-in gain schedules corresponding to the above inputs.
- ZEROIC - This third external input permitted the initialization of the digital integration process.

This version of the controller was restricted in that it did not permit switching between single and four-loop controllers along the HTV transition and it did not permit reassignment of manipulated variables

along either transition path. The digital transition controller was then checked-out with the Linear Engine Model for operation at Takeoff and Landing. The Takeoff check-out was successful but difficulties were encountered at Landing. Program priorities did not permit the effort necessary to resolve these problems at this time.

The Phase II non-linear engine model was then checked-out on the hybrid computer as a separate program. Static check-outs (no dynamics) were calculated for two VTH operating points (T/O and MH) and for three HTV operating points (FID, RALS, and L). A number of small problems were identified and corrected.

The digital controller was then modified to include mode switching logic as well as the logic needed for the reassignment of the variables A88 and STP22. Note that A88 is used as a closed-loop manipulated variable at high remote flow rates and is replaced as a manipulated variable by STP22 at low flow rates. The coding in this latest version of the controller contained MIN/MAX statements to limit the outputs of the digital integrators as well as numerous look-up tables for establishing upper and lower limits on the variables and for providing values for the corresponding open-loop schedules. Coding was also added to accommodate a noisy FCD signal in order to avoid erroneous manipulated variable or mode switching. A special program was developed for exercising the many logic paths available in the controller.

The revised digital controller was then combined with the non-linear engine model in order to obtain the final Phase II engine and control model. An initial attempt was made to simulate the total VTH transition from Takeoff (T/O) to Maximum Horizontal (MH). This run was unsuccessful and was abandoned. The linear simulation was utilized to generate open-loop response data that could be compared with the open-loop hybrid simulation data in order to identify specific problems that could resolve the overall simulation problem. The integral portion of the proportional/integral controller was disabled in both simulations in order to obtain steady state responses. The magnitudes and signs of the linear open-loop responses were then compared with those of the hybrid simulation. This procedure identified a number of problems and led to modifications of the feed-forward gains and

of the nozzle area schedules (XA8 and XA88). These changes produced hybrid simulation responses that were consistent with the linear simulation results.

The closed-loop hybrid simulation of the VTH transition was tried again and was found to work well at Takeoff. Additional problems occurred as FCD was varied to move the simulation towards Maximum Horizontal. An attempt was made to run at MH but was also unsuccessful. The data from these experiments was, however, used to modify the non-linear engine model to permit successful simulation runs in the Initial Condition Mode over the entire VTH transition path from Takeoff to Maximum Horizontal. This simulation could, however, be run in the Operate Mode only at the Takeoff point. No attempt was made to check-out the simulation over the HTV transition path which was substantially more complex with requirements for mode switching as well as reassignment of manipulated variables.

Figure 29 summarizes the results of the current hybrid simulation at Takeoff. The closed-loop control variables were XN2, T5, PS3, and XM93 and the corresponding closed-loop manipulated variables were A8, WF36, STP49, and A88. The open-loop manipulated variables included STP22 which received its scheduled value from the controller and AE16 and AE80 which received their scheduled values directly from table look-up. Note, however, that all three open-loop variables were functions of FCD. The responses shown are due to a step input of the fan speed (XN2) demand and its corresponding interactions with the T5, PS3, and XM93 loops. This data from the non-linear mode switching hybrid simulation compared favorably with the prior Phase I results using an elementary multi-variable controller and the Linear Engine model. The fan speed dynamics were sluggish and asymmetrical. The slow dynamics resulted from improper time scaling of the digital integration whereas the asymmetry was most likely the result of the increased non-linearity of the simulation.

8.0 CONDITION MONITORING

Traditionally, engine condition monitoring systems have evolved in parallel with the engine design with little forethought being given to objectives or to the ability of the system to satisfy these objectives.

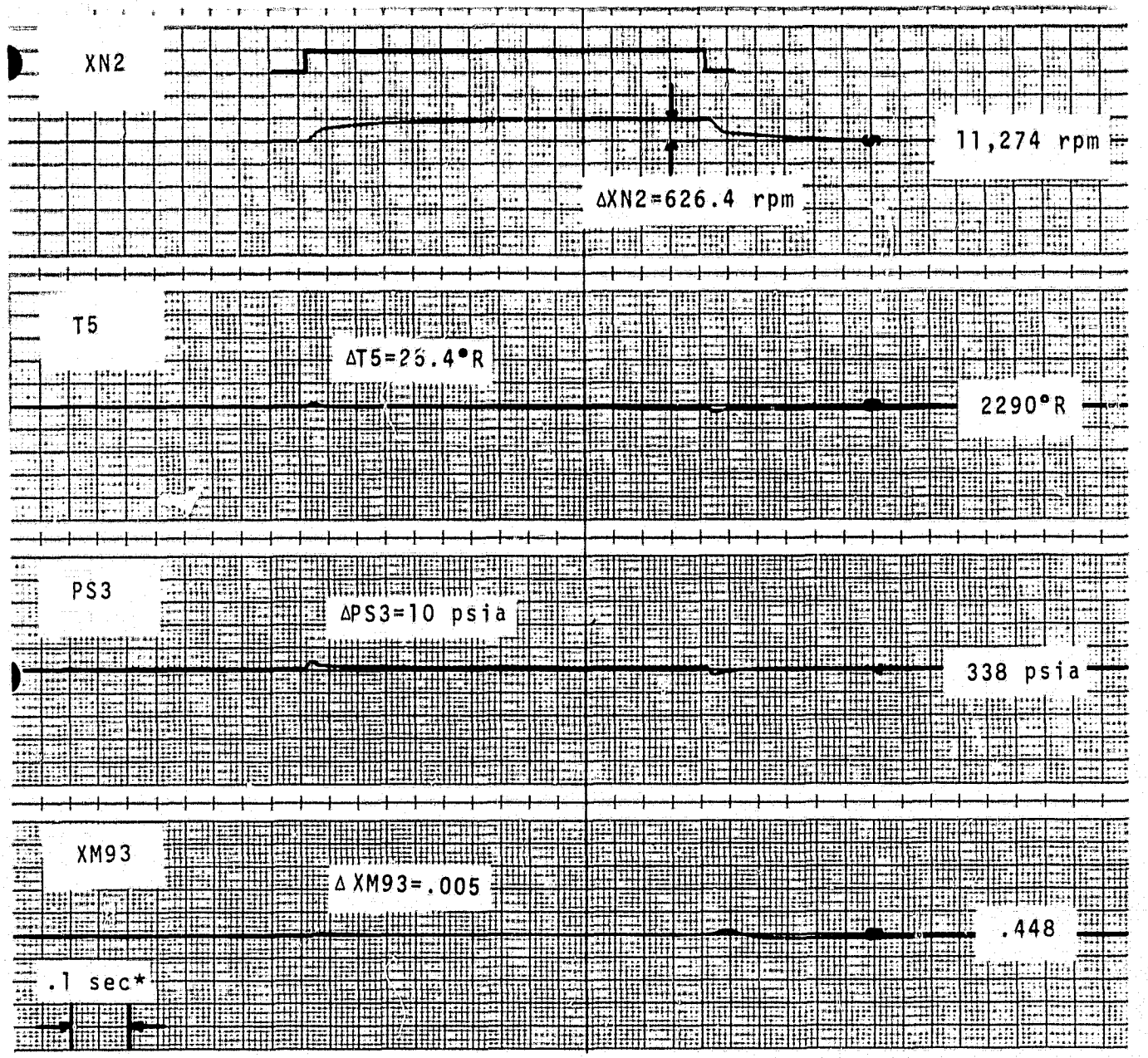

Figure 29. Hybrid Simulation Response To Fan Speed Demand at Takeoff

The approach has been to select instrumentation for the engine and then (via analysis and test/field experience) to determine what, if anything, the instrumentation can do to further condition monitoring objectives. In spite of this development approach, condition monitoring systems have performed useful functions on aircraft/engine systems. This has been possible primarily because engine designs have changed slowly, and lessons learned from previous experience have been successfully incorporated into new condition monitoring designs.

The V/STOL aircraft, however, is a radical departure from preceding aircraft designs and, consequently, it is expected that a condition monitoring system will serve new roles in V/STOL. To effectively fulfill these new roles, the condition monitoring system must be "designed" rather than evolved.

The specific condition monitoring tasks for the current phase of this investigation are to formulate a design strategy and to develop analytical tools required to support the design plan. The resulting design strategy is described in Section 8.1, and analytical tools are described in Sections 8.2 - 8.4. It is expected that the design plan will be carried out in future phases of the V/STOL development program.

8.1 Design Plan

Briefly, General Electric's design strategy for a V/STOL condition monitoring system is:

1. Define objectives for the condition monitoring system, initially in terms of capabilities or activities, but ultimately as one or more quantitative parameters (denoted objective functions) which can be estimated from measured data. Associated with each of these objective functions would be an accuracy or repeatability needed to satisfy the objective.

2. Develop a list of possible condition monitoring measurements which could be made in support of these objectives. For each of the potential measurements, realistic estimates of their accuracies and/or repeatabilities would be obtained.

3. Determine a list of possible engine/control hardware changes that could influence the ability of the aircraft to achieve its

mission or which could affect the measurements and thereby jeopardize the condition monitoring objectives (examples are engine component degradation or control schedule misrigging). For each of these potential influences, a reasonable range for the probable variation would be estimated.

4. Augment the V/STOL cycle model so that it can compute the condition monitoring objective functions and the condition monitoring measurements, and so that each of the possible engine/control hardware changes is modeled in terms of its effect on the cycle. This augmented cycle model can then be used to generate linear influence coefficients (derivatives) which define the effects of each of the hardware parameters on the measurements and the objective functions.

5. Develop a general algorithm which can be used to estimate the objective functions from any arbitrary subset of the prospective measurements. This algorithm can be used to identify the objective function accuracies/repeatabilities based on a given instrumentation complement.

6. Evaluate the ability of selected subsets of measurements to achieve the original condition monitoring objectives and, on this basis, select one or more instrumentation complements which achieve the objectives and are potentially cost effective. If specific objectives are not achieveable, then an analysis can be performed to determine whether improved measurement accuracy can lead to the ability to accomplish the goal, and if so, what level of improvement is required.

After one or more condition monitoring designs have been developed using the full cycle deck, a study would be conducted to estimate the computer resources needed to implement these systems in service. This study would focus on model simplification since this is the area of greatest potential payoff. As a result of this analysis the compatibility of the condition monitoring system with the control computer would be determined.

The following paragraphs elaborate on these design steps and indicate the scope of each effort.

8.1.1 Identification of Condition Monitoring Objectives

Typical objectives for an engine condition monitoring system include detection of limit exceedances, go/no-go decisions for ensuing flights, recognition of sudden shifts in performances, extrapolation of performance

trends to plan scheduled maintenance, modular fault isolation to permit more cost effective maintenance, identification of out-of-tolerance control schedules together with indication of required trim adjustment, etc. For the V/STOL aircraft, the go/no-go decision, takes on added complexity because of the transition from vertical to horizontal flight. This maneuver is not present for standard aircraft and will require careful review to choose proper condition monitoring objectives. For example, the pilot must be certain that a stall will not be encountered during this transition and, consequently, compression stall margins will be important objective functions for the condition monitoring system.

8.1.2 Condition Monitoring Measurements

A second step in the design process is the selection of a candidate list of possible condition monitoring measurements. This candidate list will include temperatures and pressures at key locations within the engine, rotor speeds, fuel flows, static pressure taps at locations where airflow is calculatable, variable geometry position settings, etc. For each of these prospective measurements, a model must be developed relating the measurement to the cycle representation of the engine so that the cycle deck will be capable of predicting the measurement. The accuracy and repeatability of the measurement must also be estimated.

8.1.3 Engine/Control Hardware Changes

Yet another list to be compiled as part of the condition monitoring design process is a list of the engine and control hardware changes that can occur to alter the performance of the aircraft and/or the objective functions. Some examples of items to be included on this list are component efficiency degradations; compressor pumping capacity changes; mis-rigged control schedules; parasitic flow changes; pressure losses due to turning, mixing, etc.; stall line degradation; re-ingestion, etc. The effort requires the identification of as many of these hardware problems as possible whether they represent long-term changes (such as the component efficiencies) or short-term fluctuations (such as re-ingestion). These hardware effects must also be incorporated into the engine cycle

deck so that their effects on the measurements and the objective functions can be determined. It is also necessary to estimate reasonable limits to the hardware variations for subsequent analyses.

8.1.4 Generalized Algorithm Development

The algorithm is the tool that will be used to estimate the objective functions from the measurements in the presence of hardware variations (and measurement errors). Our choice for an algorithm is a maximum likelihood estimator such as that described in References 3 and 4. In order to develop a specific algorithm, it is necessary to perform the following steps:

1. Select the measurements that will be used to calculate the objective functions (this will be a subset of the possible measurements).
2. Select the hardware changes (a subset of those present) that are to be estimated from the available measurements. These are analogous to state variables of References 3 and 4.
3. Use the cycle deck to produce a linear model which relates the measurements and the objective functions to the hardware changes.
4. Using the weighted least squares approach defined in References 3 and 4, a maximum likelihood algorithm is thus produced which will provide a best estimate of the objective functions given the available measurements and the selected state variables.

In order to produce the general algorithm that is needed to evaluate several proposed instrumentation sets, all that is needed is the generation of a complete linear model for all measurements and objective functions. A specific algorithm is then simulated by substituting nominal values for those state variables that are not to be estimated and using only the measurements that are to be available.

8.1.5 Evaluation of Instrumentation Sets

In order to evaluate a particular instrumentation set, the procedure is to select the set of state variables to be estimated, and then use the associated algorithm to perform an accuracy analysis for the objective functions. For any specific objective function, there will be some particular subset of state variables to be estimated from the measurements

that will yield a best accuracy for that objective function. In other words, the best accuracy for the objective function will be attained when some of the state variables are estimated from the data while others are assumed to hold their nominal value. Thus a search scheme will be established to choose state variables that will provide a good estimate of the objective functions (since there are several objective functions, some trade-offs may be desirable).

Because of the anticipated scope of this effort, it will not be feasible to evaluate all possible instrumentation combinations. Thus certain basic sets will be selected for analysis which will include all of the measurements which are expected to be in the basic engine parts list, plus some additional measurements that might be condition monitoring items. These selected sets will be evaluated and in addition the impact of adding/deleting certain additional measurements to the sets will be evaluated. In the present effort, those objective functions which relate to the transition from vertical to horizontal flight will be emphasized.

8.1.6 Other Condition Monitoring Tasks

Having selected some representative instrumentation sets for further consideration, additional analysis will be performed to evaluate the computer resources needed to incorporate the algorithm into an onboard system. The algorithm described above expects all of the data to be obtained at a single test condition (altitude, Mach number, type day, humidity, power setting). In practice, the data will be obtained at many different test conditions. Thus, a model of the engine is needed as part of the condition monitoring software. The size of the software is largely dependent upon the required complexity of this model (to provide the needed accuracy). Thus, if more instrumentation error can be tolerated (with the objectives still being met), a simpler, less exact model is possible. The simplification can pay off in both computer size and processor resources. For those functions which logically apply to an onboard system (for example, module fault isolation is more logically a ground based activity whereas go/no-go is an onboard activity) an

analysis will be performed to estimate the onboard computer resources required and specifically to evaluate compatibility with the control computer.

8.2 Maximum Likelihood Estimation

The primary problem of V/STOL engine condition monitoring is that variables such as thrust, compressor stall margin, and attitude control ability, as well as hardware performance parameters such as efficiency, flow capacity, and leakages cannot be directly measured during flight. However, properties of the engine such as pressure, temperature, shaft speed and stator position can be measured. Thus values of parameters which cannot be measured must be estimated by means of an analytical model of the system and available measurements.

An additional complexity is that measurements are difficult to interpret due to engine fluctuations and measurement error or noise. To solve this problem a statistical approach is needed.

Several potential approaches to solving this problem were considered. Of these, maximum likelihood estimation was selected as the most promising, primarily because it makes use of the greatest amount of information. In addition to considering the measurements themselves, this approach can integrate the following factors into the solution:

1) variances and covariances of the measurement error
2) nominal, "expected" levels for the hardware performance
3) variances and covariances of the hardware performance parameters

Given this information, maximum likelihood estimation distributes the original discrepancy (between the measured values and expectations based on moninal hardware levels) between measurement errors and deduced deviations of the hardware from nominal expectation. The resulting solution is the most probable solution given all of the available information.

8.2.1 Measurement and Objective Function Models

In the most general cases, the maximum likelihood estimation problem is non-linear requiring the application of a numerical optimization procedure to determine the solution. However, the linearized version, which assumes Gaussian probability distributions and requires the use of a linear engine model, is computationally simple and convenient. The linear requirement is readily accomplished by centering the analysis at the expected performance level, and the solution accuracy is not significantly impaired if actual hardware deviations are sufficiently small.

The linear model for the measured variables, z, may be written as

$$z = Hx + v \tag{8.1}$$

and a model for the objective functions is

$$y = Gx \tag{8.2}$$

where

z is an mxl measurement vector
H is an mxn model matrix
x is an nxl state variable vector
v is an mxl measurement error vector
y is a pxl objective function vector
G is a pxn model matrix

The vector, x, represents the hardware condition of the engine and includes parameters such as component efficiencies, flow capacities and leakages. The vector, y, represents objective function variables such as thrust and compressor stall margin which cannot be directly measured. The G and H matrices are linear approximations to the engine model at the expected flight condition. To preserve the linearity z, x and y should be considered as representing deviations from the expected flight conditions.

The measurement error vector, v, is assumed to be a zero mean Gaussian error whose variability is represented by the (mxm) covariance matrix

$$R = \mathrm{cov}(v) \tag{8.3}$$

Finally, the state vector, x, even though constant during measurement, is assumed to belong to a population of known statistical properties. Specifically, x is assumed to be Gaussian with mean $\bar{x}$ and (nxn) covariance matrix

$$M = \text{cov}(x) \tag{8.4}$$

8.2.2 Estimation Model

Given the above definitions, it can be shown (see References 3 and 4) that the most probable estimate, $\hat{x}$, is given by the expression

$$\hat{x} = Kz \tag{8.5}$$

where the gain, K, is given by

$$K = PH^T R^{-1} \tag{8.6}$$

and

$$P = (M^{-1} + H^T R^{-1} H)^{-1} \tag{8.7}$$

This algorithm is straightforward and the solution is readily obtained if H, M, and R are known. After $\hat{x}$ is calculated, the estimates of both the measured variables and the objective functions can be computed from

$$\hat{z} = H\hat{x} \tag{8.8}$$

and

$$\hat{y} = G\hat{x} \tag{8.9}$$

If v and z are random variables, then x, z and y are random variables with expected values of $\bar{x}$, $H\bar{x}$ and $G\bar{x}$, respectively. It can be shown that the covariance of the associated estimate errors are

$$\text{cov}(\hat{x}-\bar{x}) = P \tag{8.10}$$

$$\text{cov}(\hat{z}-H\bar{x}) = HPH^T \tag{8.11}$$

$$\text{cov}(\hat{y}-G\bar{x}) = GPG^T \tag{8.12}$$

It has also been shown in the literature that the maximum likelihood estimator is the optional estimation with the covariances given by Equations (8.10-12) being the smallest (minimum error variance) of all possible linear estimation techniques.

8.2.3 Optimal Filter

As successive sets of measurements become available for a system, the maximum likelihood estimation algorithm can be applied sequentially to successively improve estimates. This process is called filtering, and the recursion equations for the algorithm after the ith measurement became

$$x_i = x_{i-1} + K_i(z_i - z_{i-1}) \tag{8.13}$$

$$K_i = P_i H^T R^{-1} \tag{8.14}$$

$$P_i = (P_{i-1}^{-1} + H^T R^{-1} H)^{-1} \tag{8.15}$$

$$z_i = Hx_i \tag{8.16}$$

It can be shown that the error covariance, P_i, and the filter gain, K_i, monotonically approach zero in the estimation sequence.

8.2.4 Example

Consider the simple gas turbine used to generate net power, P_w, as illustrated in Figure 30. The expressions for pressure and temperature ratio shown in Figure 30 were derived from a straightforward thermodynamic analysis assuming one half of the turbine power is required by the compressor, the working fluid is a perfect gas, and a net power level of $P_w = 2WC_pT_o$.

A computer subroutine was constructed for Monte Carlo simulation of the simple gas turbine model. The compressor and turbine efficiencies were considered to be state parameters with true values of 0.845 and 0.895, respectively. The pressure and temperature ratios were considered to be measured variables with Gaussian measurement noise at the 1% level. That is:

$$z(1) = (P1/Po) + 0.3RN(1)$$

$$z(2) = (T3/To) + 0.3RN(2)$$

where RN(i) is a standardized normal random variable generated by a random number subroutine.

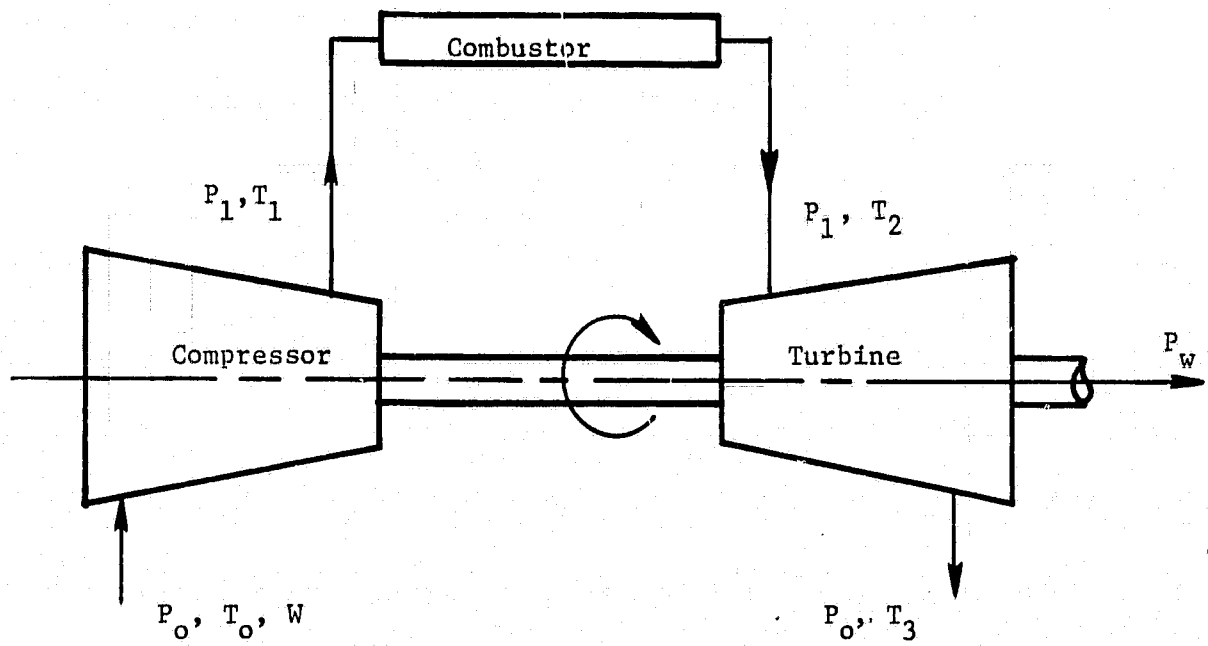

Specify Net Power Level: $\frac{Pw}{WCpTo} = 2$

Then:

Pressure Ratio $\equiv \frac{P_1}{P_o} = [\ 1 + 2\eta_c\ ]^{3.5}$

Temperature Ratio $\equiv \frac{T_3}{T_o} = \frac{2}{\eta_c \eta_T} [1 + 2\eta_c\ (1 - \eta_T)]$

Where: $\eta_c \equiv$ Compressor Efficiency

$\eta_T \equiv$ Turbine Efficiency

Figure 30. Simple Gas Turbine Model.

A filter subroutine was constructed using Equations (8.13-16). The H matrix was determined by taking derivatives of the measured variables with respect to the state parameters. That is,

$$\frac{\partial(P1/Po)}{\partial \eta_c} = 7(1+2\,\eta_c)^{2.5}$$

$$\frac{\partial(P1/Po)}{\partial \eta_t} = 0$$

$$\frac{\partial(T3/To)}{\partial \eta_c} = -\frac{2}{\eta_t\,\eta_c^2}$$

$$\frac{\partial(T3/To)}{\partial \eta_t} = -\frac{2}{\eta_c\,\eta_t^2}(1+2\,\eta_c)$$

The expected values of compressor and turbine efficiency were estimated as 0.85 and 0.90, respectively. After substituting these values into the derivative expressions, the following H matrix was obtained:

$$H = \begin{bmatrix} 83.851 & 0 \\ -3.076 & 7.843 \end{bmatrix}$$

The initial estimate of the state parameters (efficiencies) were assumed reliable at the 1% level. Thus,

$$M = \begin{bmatrix} 1.E\text{-}4 & 0 \\ 0 & 1.E\text{-}4 \end{bmatrix}$$

The variability of the measurement noise was also specified at the 1% level. Thus,

$$R = \begin{bmatrix} 9.E\text{-}2 & 0 \\ 0 & 9.E\text{-}4 \end{bmatrix}$$

Simulated measurements from the Monte Carlo subroutine were input to the filter subroutine for 60 successive flights (estimations), and the results are plotted in Figures 31 through 35. The true values for the simple gas

turbine system are plotted as square sumbols, and simulated "measured" values of pressure and temperature are plotted as diamond symbols. Note that simulated measurement noise causes the "measured" values to be randomly scattered about the constant true values in Figures 31 and 32.

Estimated values are plotted as triangular symbols. Note that the estimates converge to the true values in Figures 31 through 34, and the estimated values of state parameters (efficiencies) in Figures 33 and 34 are within 0.1% of the true values after about fifteen estimations. This result agrees with the predicted standard deviation of the estimate errors (square roots of the trace elements in the computed P covariance matrix) plotted in Figure 35.

8.3 Suboptimal Filters

A significant deficiency of the filter algorithm described in Section 8.2.3 is that state parameters are assumed to be constant during the measurement sequence. Filter estimates can follow small changes in state parameters, however, they will lag large changes. In some condition monitoring applications the estimation algorithm must be able to follow large changes in the values of state parameters. Two methods to adjust the optimal filter process in order to increase its gain are described in the following sections.

8.3.1 Fictitious Process Noise

The system model described in Section 8.2.1 can be adjusted to include random fluctuations of the state parameters. Such fluctuations are called process noise and are modeled as:

$$x_i = x_{i-1} + w$$

where w is the nx1 process noise vector assumed to have a zero mean Gaussian distribution with variability represented by the (nxn) covariance matrix

$$Q = \mathrm{cov}(w) \qquad (8.17)$$

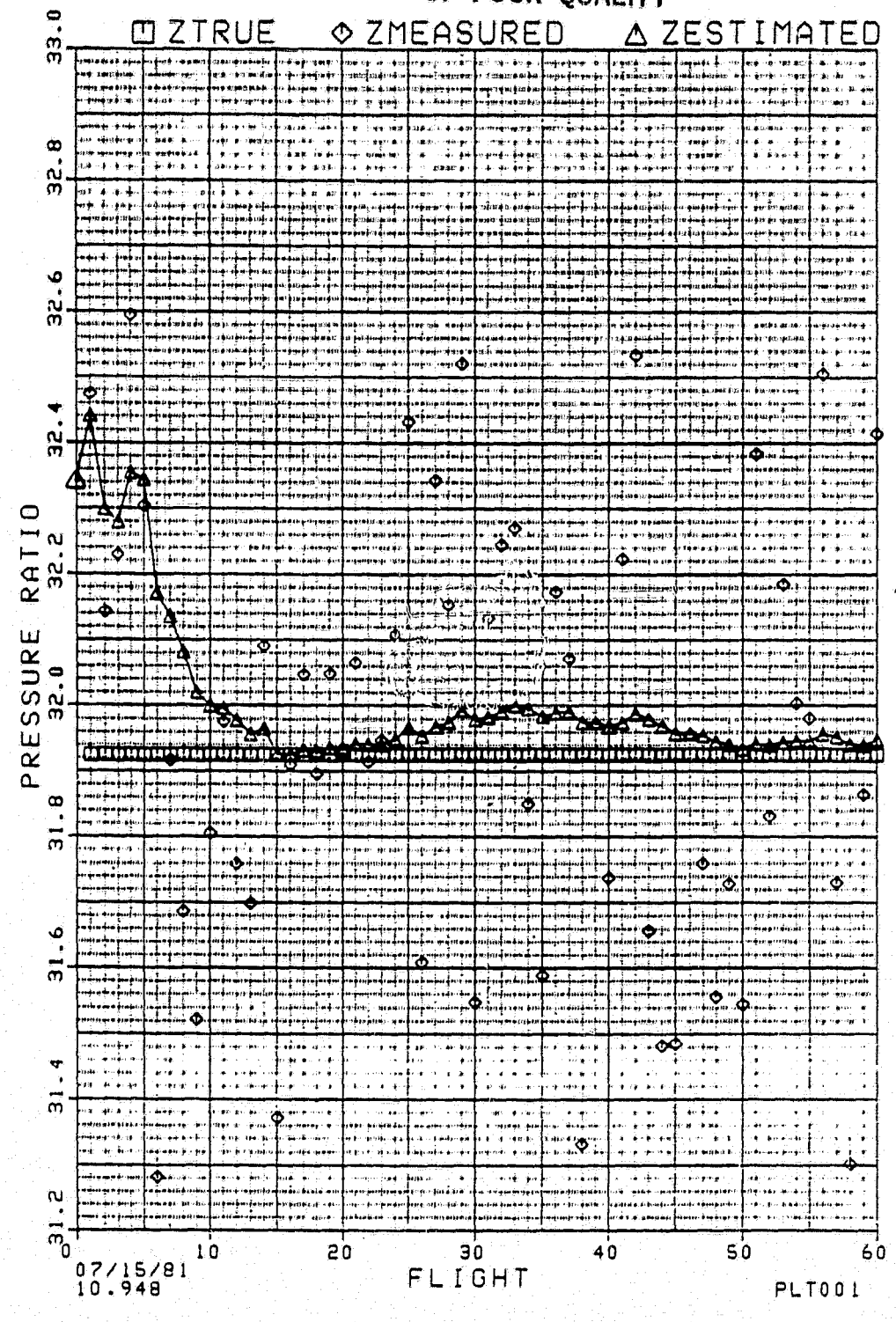

Figure 31. Pressure Ratio Variations

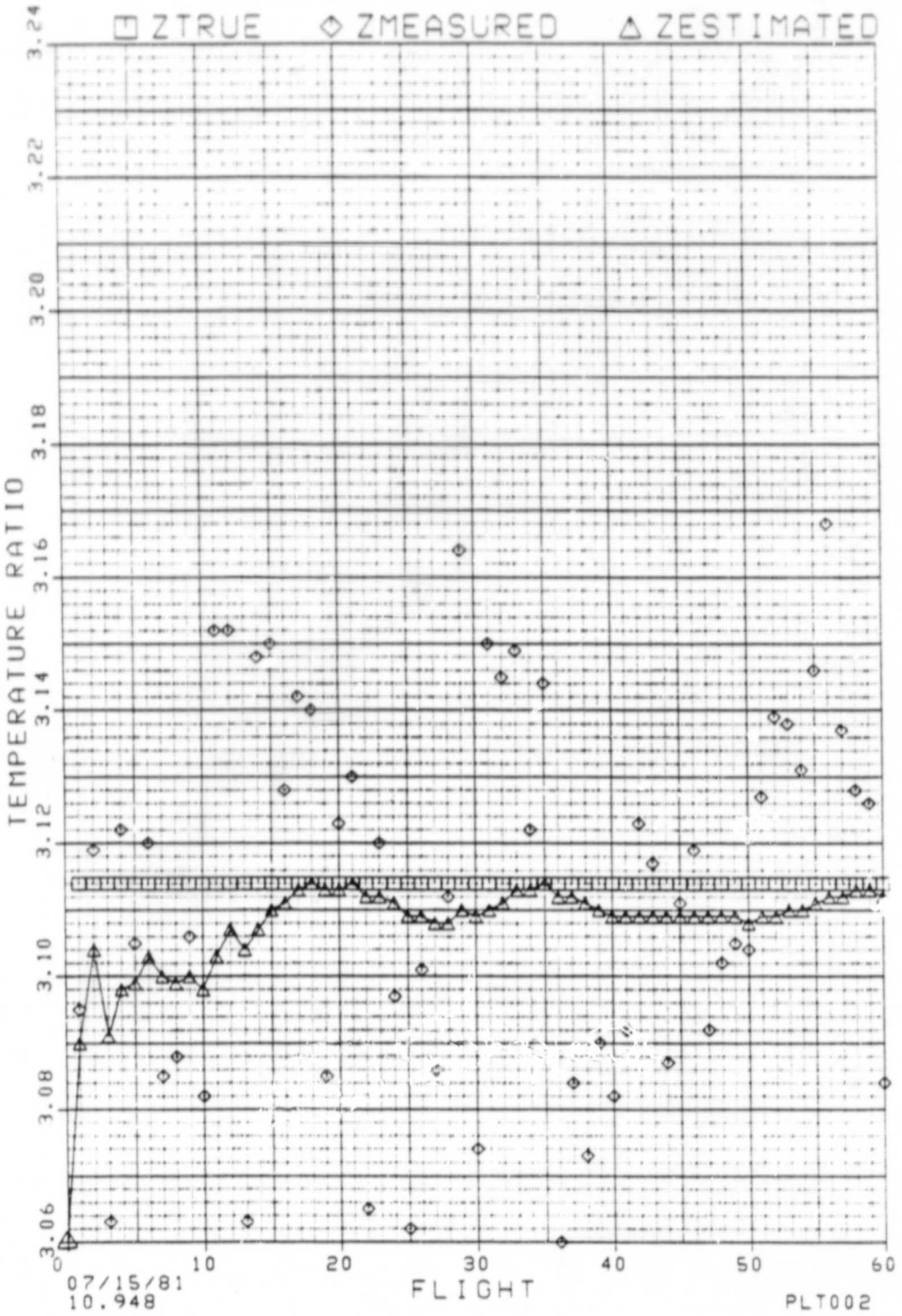

Figure 32. Temperature Ratio Variations

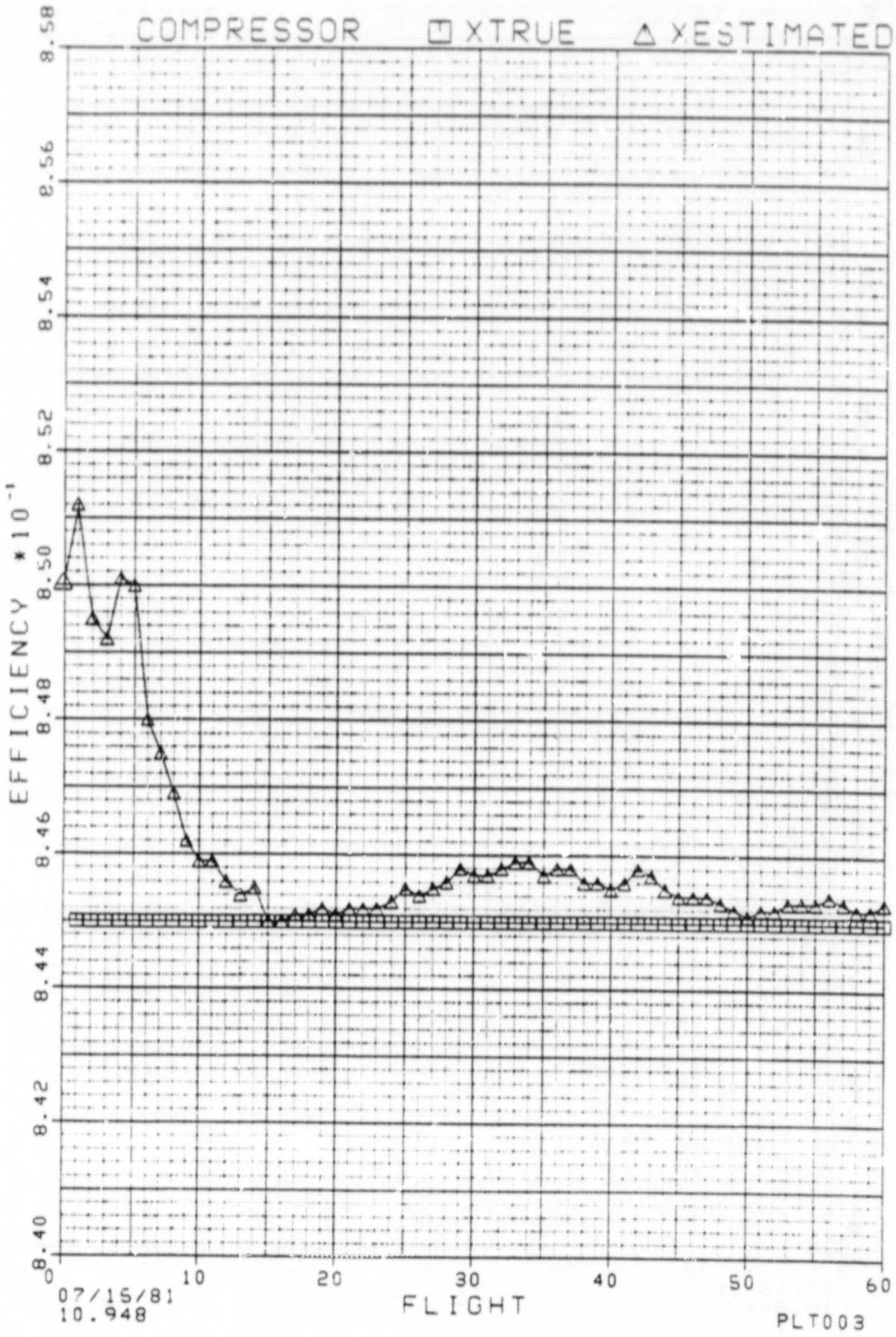

Figure 33. Compressor Efficiency Variations

C-2

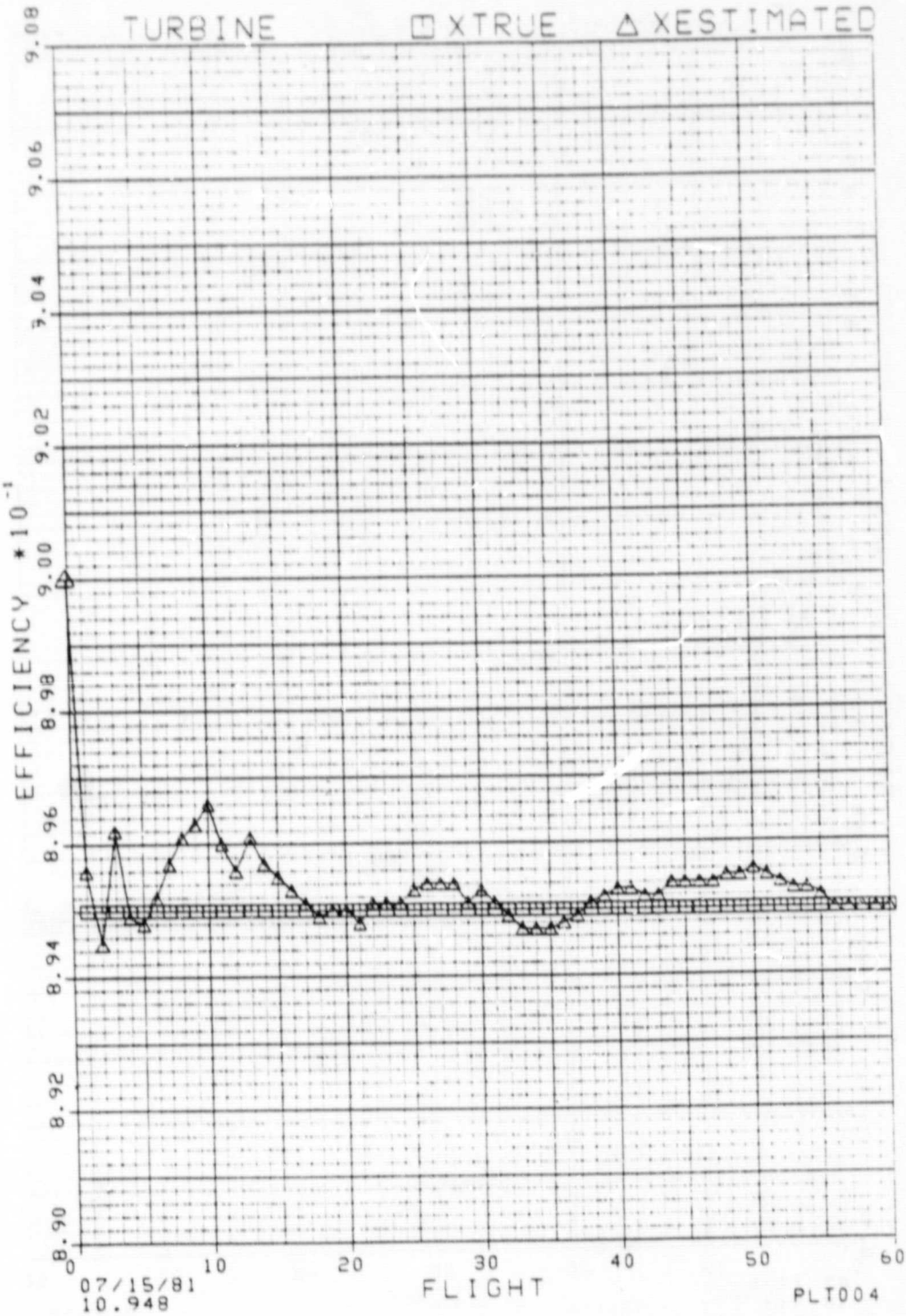

Figure 34. Turbine Efficiency Variations

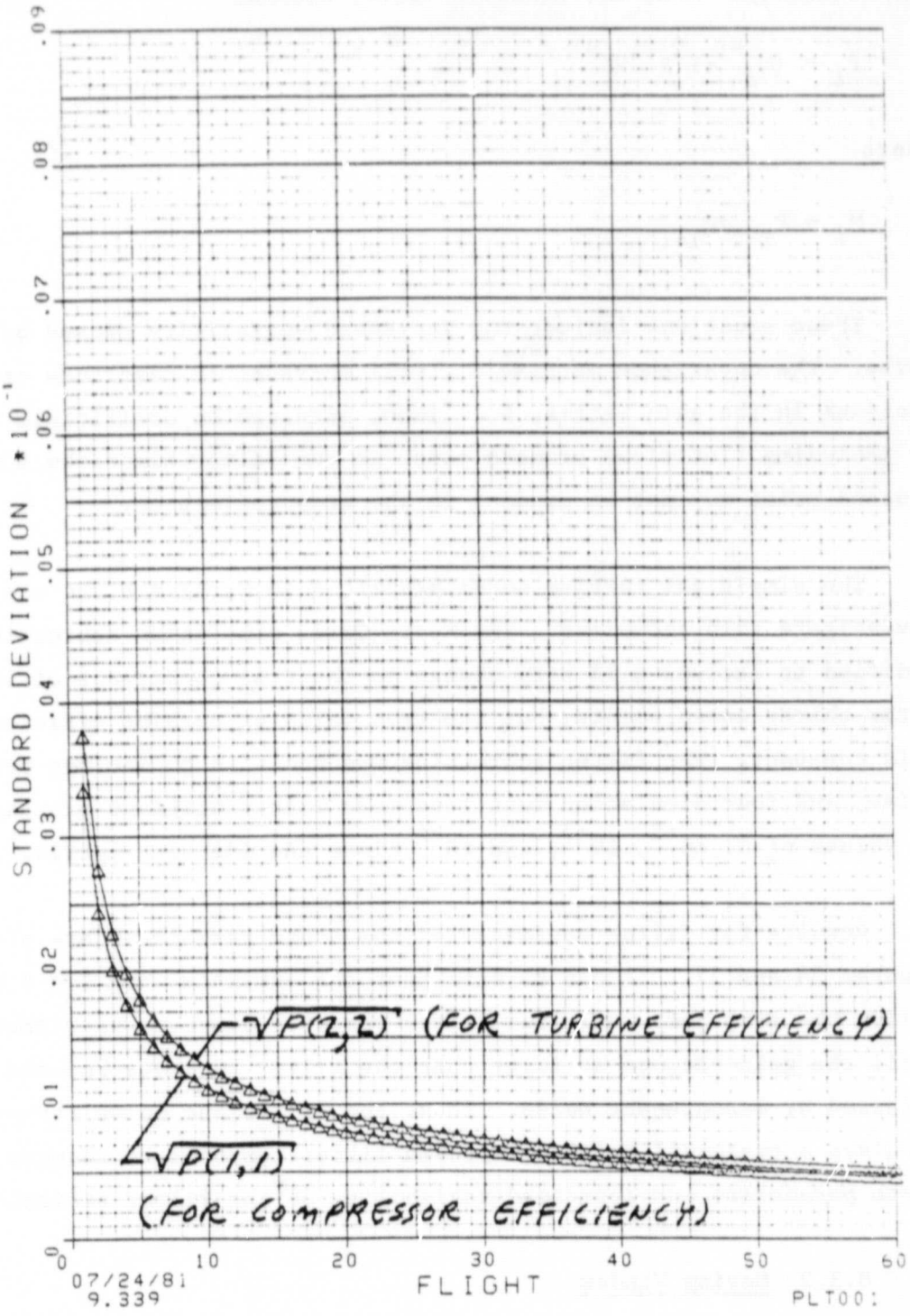

Figure 35. Predicted Standard Deviation Of The Estimated Errors

The addition of process noise caused the optimal filter algorithm to change only slightly. That is, Equation (8.15) becomes

$$P_i = (M_i^{-1} + H^T R^{-1} H)^{-1} \tag{8.18}$$

where

$$M_i = P_{i-1} + Q_{i-1} \tag{8.19}$$

These equations include the increased variability caused by process noise. The covariance matrix, P_i, will increase in magnitude causing an increase in the gain matrix, K_i. Thus, gain can be artificially increased by including fictitious process noise in the filter algorithm even though process noise may not be present in the measured system.

The simple gas turbine model described in Section 8.2.4 was used to investigate this technique. The Monte Carlo simulation subroutine was modified to include a 1% step change in the true compressor efficiency after thirty measurements, but the true value of turbine efficiency was held constant. The filter subroutine was modified to include process noise, and four simulation runs were made with fictitious process noise at values of 0, 10^{-8}, 10^{-7}, and 10^{-6} times the identity matrix.

Results for filter estimates of the state parameters are plotted in Figures 36 and 37. It can be seen that the estimate with Q = 0 does not follow the step jump well, but filter response improves as Q increases until the gain becomes so large that the filter estimate becomes adversely affected by measurement noise. Thus, the fictitious noise technique involves a trade-off between improved filter response to changes in the state parameters and increased variability of the filter estimates.

8.3.2 Moving Window

A disadvantage of the fictitious process noise technique is that extra information must be supplied to the filter algorithm prior to estimation. An alternative approach which reduces the significance of prior information is the moving window concept.

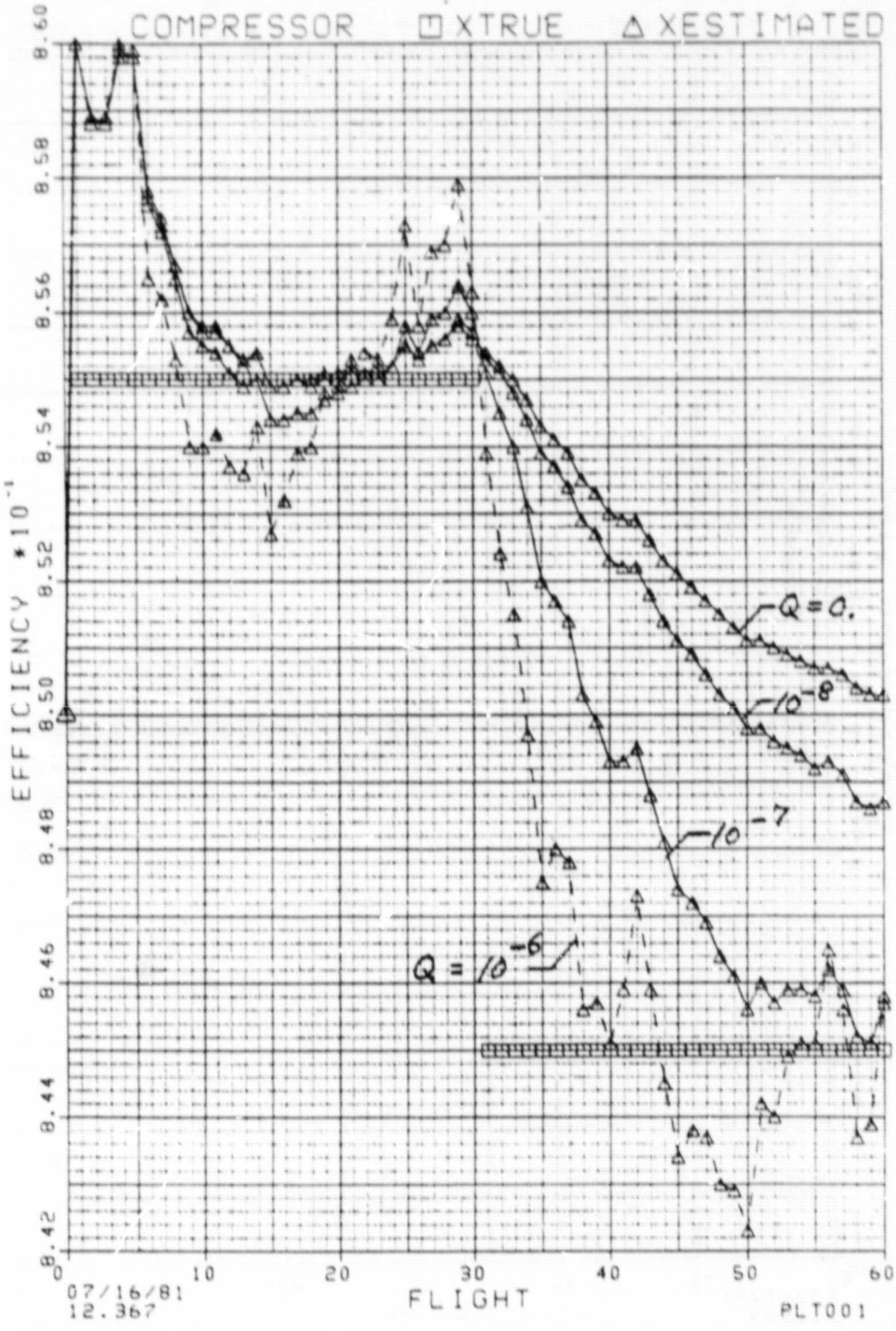

Figure 36. Compressor Efficiency Variations With Process Noise

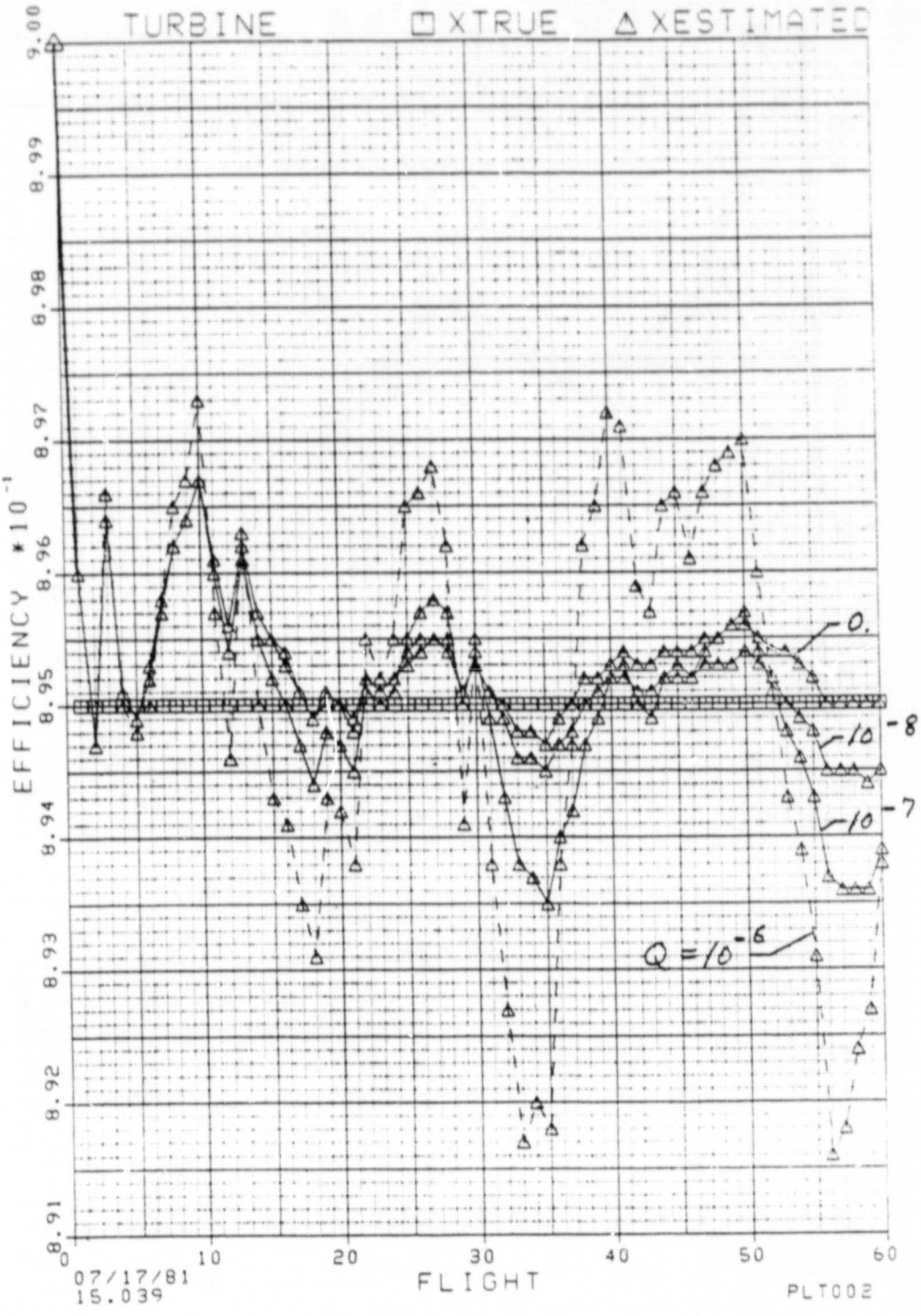

Figure 37. Turbine Efficiency Variations With Process Noise

Measurement error statistics are determined by using a sample of the most recent N measurements to estimate the variance of the data. That is, after the ith measurement,

$$(\bar{Z}_j)_i = \sum_{k=i-N+1}^{i} (Z_j)_k/N$$

$$(\sigma_j^2)_i = \sum_{k=i-N+1}^{i} \left[(Z_j)_k - (\bar{Z}_j)_k\right]^2/(N-1)$$

N is chosen large enough to get a reasonable estimate of the true measurement covariance and small enough that instrumentation and hardware changes are negligible in the interval.

The filter gain and response to state parameter changes can be increased by using a finite memory modification to the filter algorithm. That is, the recursion equation for the estimate covariance will include information based upon only the most recent N measurements, and Equation (8.15) of the filter algorithm is replaced by

$$P_i = (P_{i-1}^{-1} + H^T R_i^{-1} H - H^T R_{i-N}^{-1} H)^{-1} \qquad (8.20)$$

Thus, if R_i is constant, then P_i and K_i will be constant after the Nth measurement and will not asymptomatically approach zero as in the optimal filter algorithm.

The simple gas turbine model described in Section 8.2.4 was used to investigate this technique. The Monte Carlo simulation subroutine was modified to include a 1% step change in the true compressor efficiency after thirty measurements, but the true value of turbine efficiency was held constant. The filter subroutine was modified to include the moving window equations, and three simulation runs were made with window sizes of N = 10, 20 and 30 measurements.

Results for filter estimates of the state parameters are plotted in Figures 38 and 39. It can be seen that the estimate with N=30 does not follow the step jump well, but filter response increases as N decreases until the gain becomes so large that the filter estimate becomes adversely

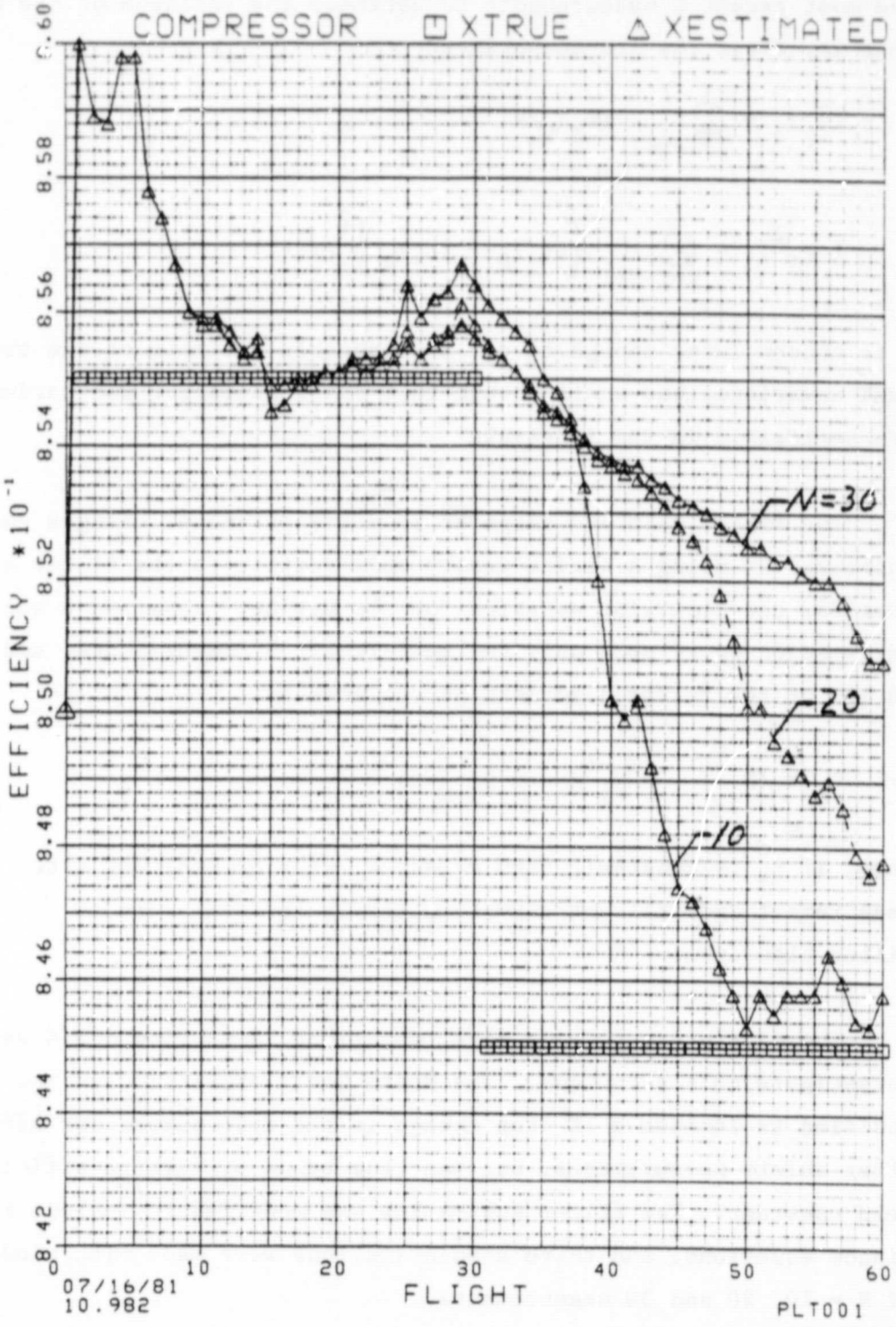

Figure 38. Compressor Efficiency Variations With Moving Window Concept

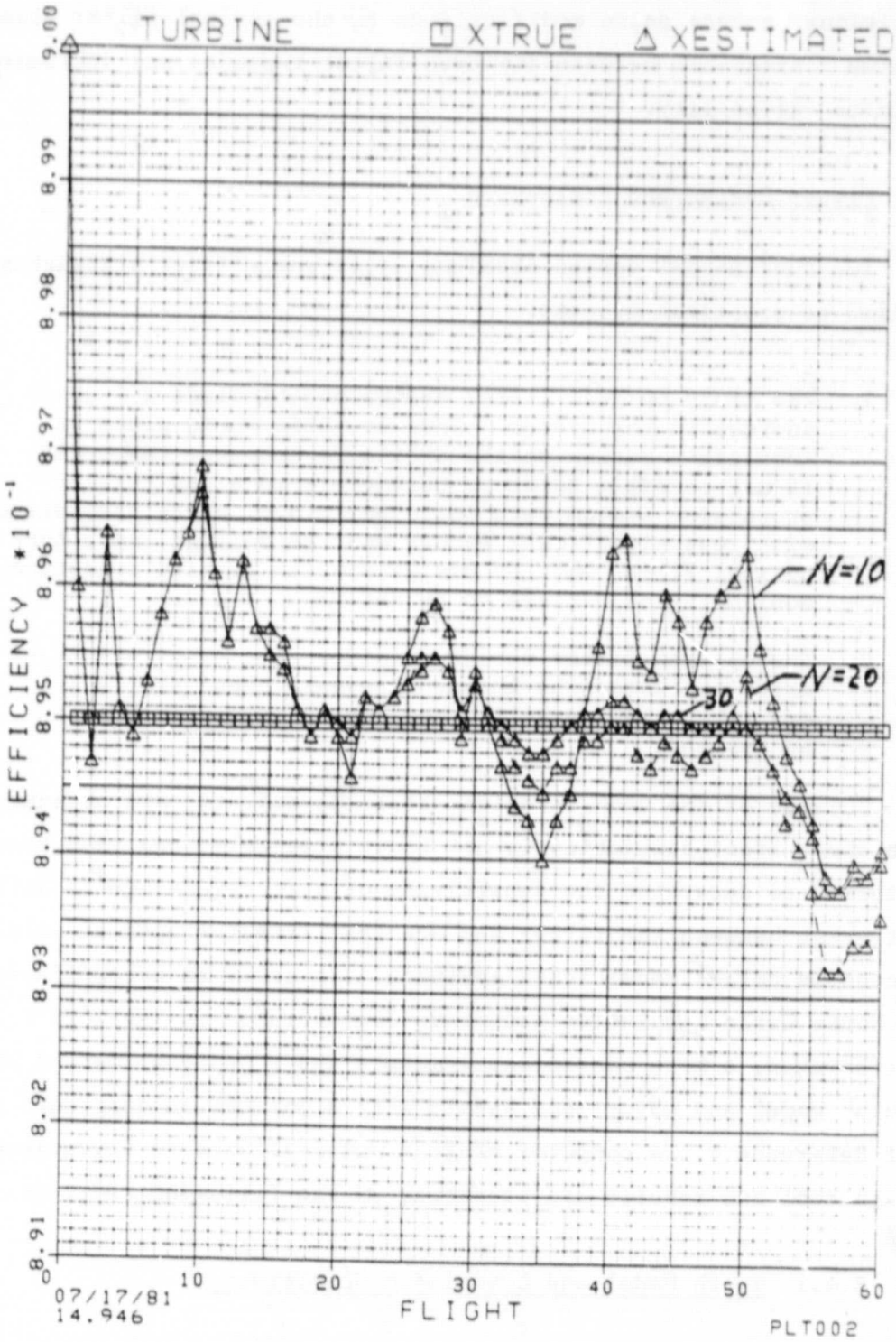

Figure 39. Turbine Efficiency Variations With Moving Window Concept

affected by measurement noise. Thus, both the moving window and the fictitious process noise modifications to the optimal filter algorithm involve a trade-off between improved filter response and increased estimate variability.

8.4 Filter Design and Evaluation

Two fundamental design problems arise when filter algorithms are applied to practical systems:

1. The truly optimal filter design must include all error sources in the system. However, this would place an impossible burden on the available computer resources if all possible hardware parameters in a gas turbine propulsion system were included. Thus, state parameters with less significant errors must be deleted and a sub-optimal filter must be designed which permits condition monitoring objectives to be met.

2. The optimal filter design requires that exact values of error statistics be known. However, these statistics are never known exactly, and approximate values must be assumed.

Because of the need to delete state parameters, and because information about error statistics is not known precisely, analyses should be performed to determine the sensitivity of a filter design to differences that exist between the filter and one that fits the optimal mold. This process is called sensitivity analysis. It could be accomplished using the Monte Carlo simulation technique demonstrated in Sections 8.2.4 and 8.3; however, a more convenient accurate and economical method using a "truth" model and covariance sensitivity algorithm is described in Chapter 7 of Reference 4. A computer program was developed to investigate this design tool and results are presented in the following sections.

8.4.1 Truth Model and Covariance Sensitivity

An equation for covariance of estimate error for the state vector is derived by substituting the basic measurement and estimation model equations (8.1, 8.13, 8.16) into the covariance definition. Thus,

$$P_i = \text{cov}(\hat{x}_i - x_i)$$

$$= \text{cov}\left[\hat{x}_{i-1} + K_i^* (z_i - \hat{z}_{i-1}) - x_i\right]$$

$$= \text{cov}\left[(\hat{x}_{i-1} - x_i) + K_i^* (Hx_i + v_i - H\hat{x}_{i-1})\right]$$

$$= \text{cov}\left[(I - K_i^* H)(\hat{x}_{i-1} - x_i) + K_i^* v_i\right]$$

$$\text{or } P_i = (I - K_i^* H) P_{i-1} (I - K_i^* H)^T + K_i^* R K_i^{*T} \qquad (8.21)$$

Equation (8.21) is the realistic estimate of the covariance of state estimate error for a filter with arbitrary gain. That is, it is valid for both optimal and suboptimal filter algorithms. The asterisk superscript is placed on the gain symbol, K_i^*, as a reminder of this fact.

The truth model sensitivity analysis is a very simple concept as illustrated in Figure 40. Assumed design values for an M-state filter model (P_o^*, R^*, H^*) are substituted into the filter covariance algorithm. In the absence of process noise, for example, Equations (8.14 and 8.15) or (8.14 and 8.20) with asterisk superscripts might be used. The resulting sequence of filter gains, K_i^*, together with the N-state truth model parameters (P_o, R, H), are substituted into the sensitivity covariance algorithm, Equation (8.21), to compute the realistic covariance matrix, P_i, if the design filter were used to process data from the truth model.

The filter-indicated covariance matrix, P_i^*, will always be optimistic and smaller (less accurate) than the realistic "truth" estimate, P_i. Thus, a true evaluation of a filter design can be made, and the consequences of design changes can be accurately determined.

8.4.2 Examples

Two applications of the truth model covariance analysis were carried out. The simple gas turbine model described in Sections 8.2.4 were assumed together with the optimal filter equations (8.13-8.16). The filter design assumed both measurement noise and initial uncertainty in parameter estimates to be at the 1% level.

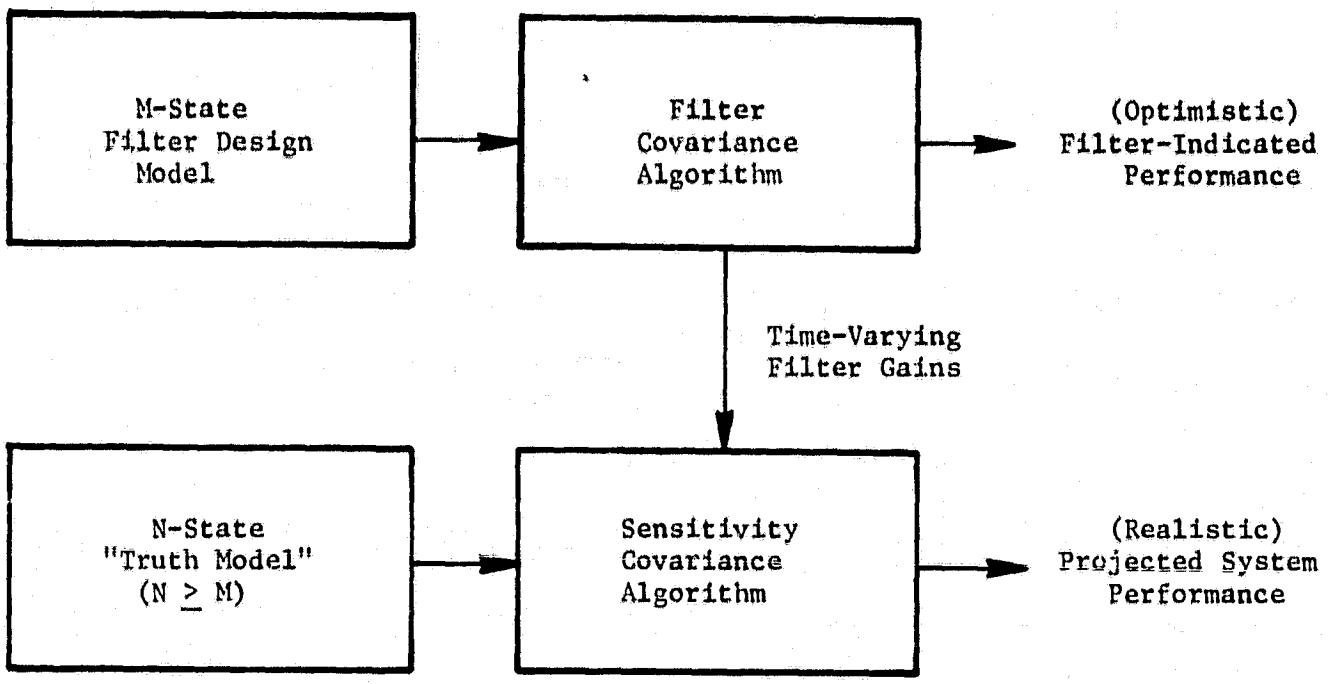

Objectives:

- Reduced State Analysis
- Sensitivity Analysis
- Error Budget Analysis
- Overall Performance Analysis

Figure 40. Truth Model Sensitivity Analysis Concept.

The first analysis consisted of a sensitivity analysis of the filter design to measurement noise. The resulting standard deviations of the estimated errors are shown in Table 12. Case 1 assumes the actual measurement error to be at the 2% level, and Case 2 assumes actual measurement noise at the 0.5% level. The truth model results show that the standard deviation of estimation errors would be almost doubled for Case 1 and almost halved for Case 2.

The second analysis consisted of a reduced state analysis of the filter design. The resulting standard deviation of the estimate errors are shown in Table 13. Case 1 assumes that the filter model has the same state parameters as the truth model; and the results are identical. However, Case 2 assumes no compressor efficiency error in the filter model, and Case 3 assumes no turbine efficiency error in the filter model.

Considering the first column of numbers in Table 13, the filter model predictions for the reduced state Cases 2 and 3 are smaller and apparently better than the results for Case 1. However, the filter predictions for Cases 2 and 3 are unrealistic, and should not be compared! Rather, the realistic truth model predictions in the last column should be compared to each other. The truth model predictions for the reduced state Cases 2 and 3 are larger and, as expected, poorer estimation models than the model for Case 1. This reflects the fact that estimates for Cases 2 and 3 have larger uncertainty than Case 1, because a source of error was deleted in Cases 2 and 3.

It is expected that the truth model and covariance sensitivity algorithm will be a very useful analytical tool in carrying out the design plan defined in Section 8.1 of this report.

9.0 LONG-RANGE TECHNOLOGY PLAN

A long-range V/STOL propulsion control technology plan was developed under the Phase I program in order to identify data base and technology requirements for the design of integrated aircraft-engine control systems for supersonic V/STOL. Each individual technology program has been refined to focus on

TABLE 12. SENSITIVITY ANALYSIS OF MEASUREMENT NOISE

VARIABLE	STANDARD DEVIATIONS OF ESTIMATION ERRORS: FILTER MODEL PREDICTIONS	STANDARD DEVIATIONS OF ESTIMATION ERRORS: TRUTH MODEL PREDICTIONS
	(CASE 1: R = 4R*)	
COMPRESSOR EFFICIENCY	3.34E-3	6.37E-3
TURBINE EFFICIENCY	3.75E-3	7.06E-3
PRESSURE RATIO	2.80E-1	5.34E-1
TEMPERATURE RATIO	2.80E-2	5.34E-2
	(CASE 2: R = R*/4)	
COMPRESSOR EFFICIENCY	3.34E-3	1.96E-3
TURBINE EFFICIENCY	3.75E-3	2.26E-3
PRESSURE RATIO	2.80E-1	1.64E-1
TEMPERATURE RATIO	2.80E-2	1.64E-2

SPECIFIED PARAMETERS:

$\Phi = I$
$P_0^*(1,1) = P_0^*(2,2) = 1.E\text{-}4$
$R^*(1,1) = 9.E\text{-}2$
$R^*(2,2) = 9.E\text{-}4$

TABLE 13. REDUCED STATE ANALYSIS

VARIABLE	STANDARD DEVIATIONS OF ESTIMATION ERRORS: FILTER MODEL PREDICTIONS	STANDARD DEVIATIONS OF ESTIMATION ERRORS: TRUTH MODEL PREDICTIONS
(CASE 1: FILTER MODEL = TRUTH MODEL)		
COMPRESSOR EFFICIENCY	3.34E-3	3.34E-3
TURBINE EFFICIENCY	3.75E-3	3.75E-3
PRESSURE RATIO	2.80E-1	2.80E-1
TEMPERATURE RATIO	2.80E-2	2.80E-2
(CASE 2: NO COMPRESSOR EFFICIENCY IN FILTER)		
COMPRESSOR EFFICIENCY	0.	1.00E-2
TURBINE EFFICIENCY	3.57E-3	4.95E-3
PRESSURE RATIO	0.	8.39E-1
TEMPERATURE RATIO	2.80E-2	2.83E-2
(CASE 3: NO TURBINE EFFICIENCY IN FILTER)		
COMPRESSOR EFFICIENCY	3.18E-3	4.19E-3
TURBINE EFFICIENCY	0.	1.00E-2
PRESSURE RATIO	2.67E-1	3.51E-1
TEMPERATURE RATIO	0.98E-2	7.08E-2

SPECIFIED PARAMETERS:

$i = 1$
$P_0^*(1,1) = P_0^*(2,2) = 1.E\text{-}4$
$R^*(1,1) = 9.E\text{-}2$
$R^*(2,2) = 9.E\text{-}4$

specific work tasks and to be oriented towards the development of an engine and control system model which could be used in a piloted aircraft-engine simulation program. The overall program has been restructured to delete the control components and integration programs which were primarily hardware design oriented and to add a program for V/STOL engine condition monitoring. The following sections describe the individual programs and an overall plan which has been based on an essentially constant level-of-effort for each year.

9.1 Control Requirements

The control requirements program is concerned with the establishment of engine operating schedules and protection schedules, with parameter sensing requirements for implementing the schedules, and with corresponding design margin requirements for the selected scheduling concepts. Individual work elements include the following:

- Transition Controls - The transition controls represent the engine protection schedules which limit regulator action on large and/or rapid throttle transients. The transition control includes the accel fuel schedule which limits maximum fuel flow during throttle bursts to protect against compressor stall and the decel fuel schedule which limits minimum fuel flow during throttle chops to protect against combustor blow-out. It also includes protection against over-speed, temperature, and pressure during steady-state and transient operation. The transition control involves parameter sensing requirements and processing requirements for engine fan and core speed, compressor inlet temperature, compressor discharge pressure, and at least one turbine temperature.

- Augmentor Light-Off - Augmentor light-off controls are required for both the primary and remote augmentors. Each control includes fuel metering to individual pilot burner and combustion zones, flame detection, and nozzle pre-opening or internal geometry modulation to minimize internal pressure spikes.

- Power Management - Power management studies must be conducted to identify the specific sensed or computed engine parameters which should be scheduled against power lever angle and thrust vector angle demands for setting engine thrust magnitude and direction. Additional studies must identify the corresponding parameters (thrust setting parameter, corrected fan speed, corrected core speed, etc.) for scheduling each individual open and closed-loop demand schedule.

- Full-Range Control Schedules - Steady-state operating schedules must be developed for the power management parameters, closed-loop sensed variables, and open-loop manipulated variables across the full operating envelope (altitude, Mach number, and ambient temperature ranges) and the full operating range (power lever angle and thrust vector angle). Any special requirements for bleed compensation should also be defined for the high bleed operating regime (vertical and transitional flight regimes).

- Stall Protection - Any special requirements for fan and compressor stall protection during high pressure distortion or temperature re-ingestion should be identified and potential control solutions examined.

- Design Margins - The selected closed-loop control configuration and power management concept must be combined with available component quality and deterioration models and control tolerance models to establish corresponding design margin requirements on rotor speeds, temperatures, pressures, stall margins, etc.

9.2 Modeling and Simulation

The modeling and simulation program will be concerned with refining the current Phase II engine and aircraft models and with additional simulation studies to evaluate large throttle transients, special environmental effects, and stability characteristics over the full operating range. Individual work elements include the following:

- Engine Model - The current engine model must be expanded to include the inlet and nozzle effects model, transition controls, and the full-range control schedules. Potential techniques for improving engine model computer running time must be identified, tested, and evaluated.

- Aircraft Model - The aircraft model must be refined to include force and moment coefficients out to the .3 Mach number regime, a ram drag vector, and a capability for initiating transitions at .3 Mach in horizontal flight idle descent. The existing pilot model must also be refined to provide input demands to both the propulsion system and the flight control system during the transitional flight regime. Complete VTH and HTV transitions should be simulated in order to evaluate the current V/STOL control concept.

- Environmental Effects - Simulation studies must be conducted to determine the effects of inlet pressure distortion and temperature re-ingestion to the operating characteristics of the engine and control system. Requirements for special engine protection control logic must be identified.

- System Evaluation - An evaluation test plan must be developed and carried out to evaluate system response characteristics over the major flight operating regimes. These studies must include small and large throttle bursts and chops, bodes, and mode transitions to identify any potential operating limitations.

- Real Time Model - All significant run-time refinements must be integrated into the expanded engine and control model to produce a final system model which would be suitable for piloted simulation at NASA-Ames. The final model would be coded, checked-out, and transmitted to NASA.

9.3 Control Logic

The control logic program will be concerned with the integration of the individual sub-systems into an overall control system logic design, with the identification of input-output interface logic with the aircraft/flight control system, and with the identification of preliminary fault management requirements. Individual work elements include the following:

- Control System Model - Control system requirements for transition control, full-range operating schedules, and regulator gain schedules must be implemented in control logic and integrated with the regulator and feed-forward system logic into an overall control system model. Any special engine protection requirements or operating refinements would be added as required.

- STOL Operation - The control system model will be evaluated with respect to Short Takeoff and Landing (STOL) operations and any special control logic requirements will be identified, developed, and integrated into the control system model.

- Interface Logic - Interface logic must be developed for processing input demand and environmental signals from the aircraft/flight control system and for transmitting output signals on engine operating condition, available control margins, and essential flight safety information.

- Fault Managment - Fault management studies will be conducted to establish preliminary sensor and actuator FICA logic and to evaluate system effectiveness in the vertical, transition, and low flight speed operating region.

9.4 Condition Monitoring

A condition monitoring program plan was developed and has been described in Section 8.1. The initial phase of this plan was used as the basis for the condition monitoring studies summarized in Section 8.0. Subsequent condition monitoring studies are expected to be pursued under a separate program and, consequently, have been omitted from the overall technology plan.

9.5 Propulsion Control Technology Plan

The individual technology programs have been integrated into the overall propulsion control technology plan summarized in Figure 41. It represents a time-phased program which will lead to a real-time V/STOL propulsion and control system model suitable for piloted simulation studies by mid-1985. The indicated program maintains the current technical level-of-effort through each of the indicated program phases.

10.0 DISCUSSION OF RESULTS

Typical propulsion requirements were examined for a maximum gross weight transition from vertical takeoff to horizontal accelerated-climb and for a minimum gross weight transition from flight idle descent to vertical landing. Key operating points were identified along each transition process and were used to establish typical steady-state operating requirements. The overall thrust vector direction was rotated from the vertical to the horizontal direction by longitudinal deflection of the ADEN nozzle, by varying the rear VABI area to modulate the remote-to-primary flow ratio, and by modulating the RALS augmentor fuel flow to maintain a zero propulsive pitch moment about the aircraft. Nominal ADEN augmentor temperature was maintained to preserve height and pitch control capabilities. Operation at low remote flow rates required the use of a remote flow control valve to hold the RALS augmentor inlet Mach number in the stable combustion regime.

Steady-state and transient partial derivatives were calculated at each individual VTH and HTV operating point and were used to conduct control mode studies and to develop linear state-space models for the regulator design process. The mode studies indicated that a four-loop regulator design could be retained throughout most of the flight transition regime. Mode transitions were required from closed-loop A88 control to STP22 control at low remote flow rates and to a single-loop regulator for flight idle operation in the horizontal flight mode. The K/Q matrix technique (described in the Phase I report) was used to develop proportional and integral gain constants for the four-loop controller for each individual operating point. Linear regression was used to establish overall gain schedules for the VTH and HTV controllers as a

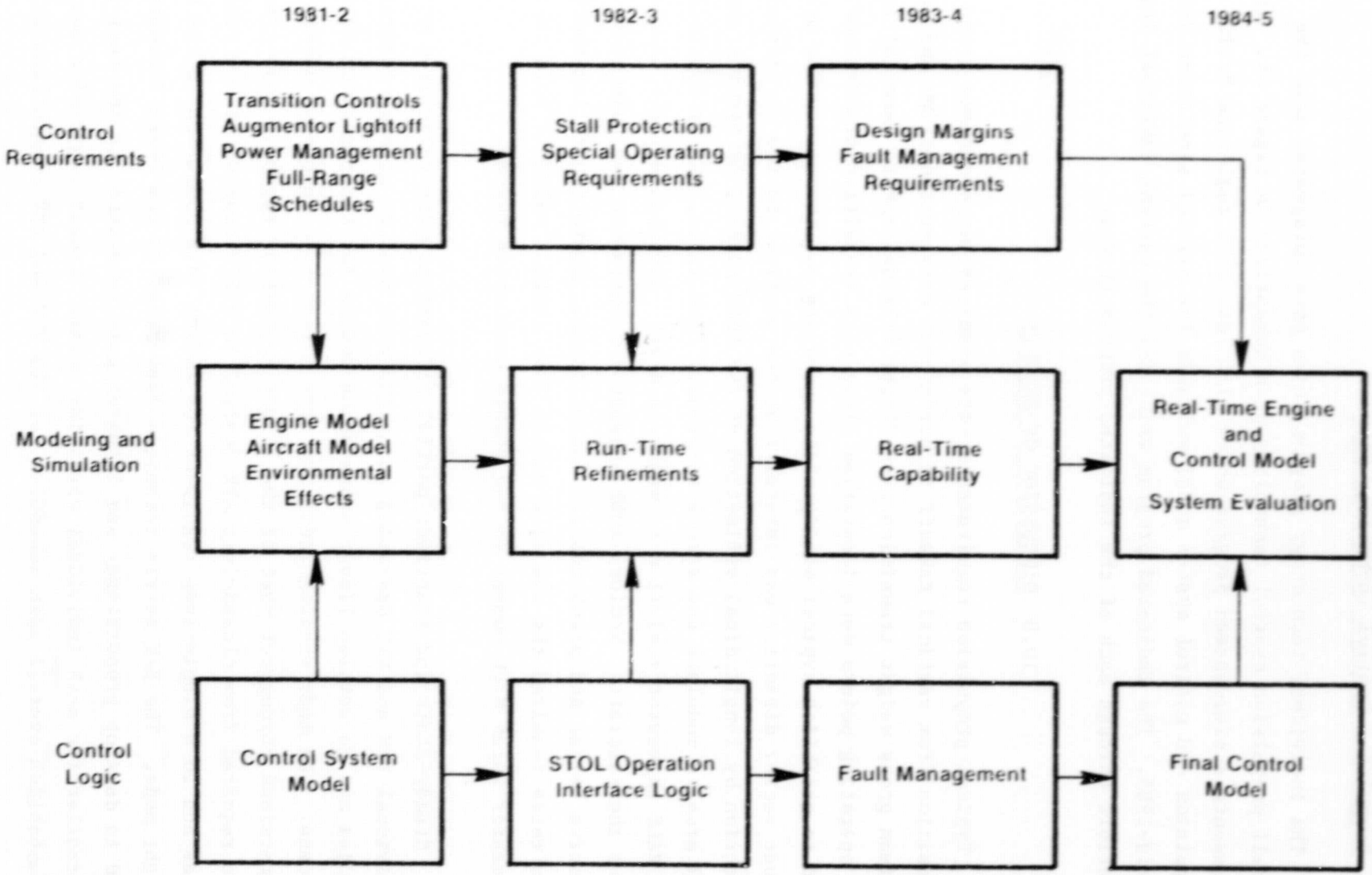

Figure 41. Long-Range Propulsion Control Technology Plan.

function of a preliminary flight control demand parameter. Simulation studies indicated acceptable response characteristics with relatively little cross-coupling effects for the application of simultaneous unit step demands to all four loops.

Mathematical models were developed for representing inlet and nozzle environmental effects, aircraft flight dynamics, and engine transient characteristics. The inlet and nozzle model provides corrections to nominal fan and compressor performance for inlet distortion and to the nozzle discharge coefficient for deflected nozzle operation. It will be incorporated into the engine model at a later date. The aircraft model was used to simulate the initial phase of the VTH transition in order to evaluate the zero propulsive pitch concept. Additional refinements to this model are needed to add the effects of the ram drag vector, combined aero and propulsive flight control, and a capability out to .3 Mach number. The engine modeling involved the development of a non-linear component-level regression model of available steady-state operating characteristics. The non-linear component model was combined with the Phase I non-linear models of the actuators, augmentors, and nozzles; with a modified version of the Phase I feed-forward system; and with the digital transition controller and its corresponding gain schedules. Subsequent non-linear simulation studies on the hybrid computer were successful in running individual operating points along the Vertical-to-Horizontal (VTH) transition trajectory in an initializing mode but were not successful in running transients along the VTH path. Corresponding simulations of the Horizontal-to-Vertical (HTV) transitions were not attempted because of the greater complexity of the HTV transition.

The simulation study results did, however, provide a partial validation of many of the design concepts and procedures employed in the development of the non-linear engine model and of the transition controller. Successful design concepts and procedures included the following:

- The use of multiple regression techniques for the development of an automatically scaled non-linear component-level engine model.
- The use of linear simulation studies for designing a multi-variable regulator with sufficient robustness for surviving the transition from the linear world to the non-linear world.

- The use of the linear simulation for generating test responses for checking the non-linear simulation.

- The concepts of mode-switching and reassignment of manipulated variables for handling regulator configuration changes.

The lack of success in simulating any significant transients along the VTH (or HTV) transition paths indicates a need for further development along the following lines:

- Better definition and/or refinement of the closed-loop and open-loop control schedules along the VTH and HTV transition paths.

- Better definition and refinement of the feed-forward schedules over the VTH and HTV transition flight paths.

- Further development and orchestration of checkout procedures utilizing linear and non-linear time-sharing studies in conjunction with the non-linear hybrid simulation studies.

Preliminary V/STOL engine condition monitoring studies were initiated to establish system design objectives, measurement requirements and evaluation criteria, and design techniques and procedures for developing a viable condition monitoring system. A simple gas turbine cycle was established as an analytical test vehicle and was used to evaluate a number of potential approaches for maximum likelihood estimation of engine health parameters which are not directly measureable (such as thrust and stall margin). Comparative results were obtained for a moving window approach and for an approach using fictitious process noise which is provided externally. A technique for evaluating reduced state models (which could be accommodated in the propulsion control system) against a truth model was also examined.

The long-range technology plan was re-structured and refined to focus specifically on propulsion control concepts and capabilities required for the development of a high fidelity real-time simulation capability which could be used in a piloted aircraft-engine simulation program. The revised plan describes individual sub-programs in the areas of control requirements, modeling and simulation, and control logic. The overall program assumes that the current level-of-effort would be maintained constant, and therefore, extends for four more years through the 1984-85 time period.

11.0 APPENDICES

11.1 Appendix A - Individual Regulator Response To Unit Step Demands

Appendix A contains time domain plots of the effects of simultaneous unit step demands on all inputs for the individual regulator designs of Tables 6 and 7. Figures A1-A6 contain the results for the individual VTH regulators, and Figures A7-A11 for the multi-loop HTV regulators. Note that, in all cases, multi-loop interactions appear to occur in about the first .25 seconds and that steady-state response is achieved by 2 seconds.

The following nomenclature has been used in Figures A1 through A22:

U1	Fan Speed (PCN2) Demand
U2	Turbine Discharge Temperature (T5) Demand
U3	Compressor Discharge Pressure (PS3) Demand
U4	Duct Mach Number (XM93) Demand
Y1	Fan Speed Response
Y2	Turbine Discharge Temperature Response
Y3	Compressor Discharge Pressure Response
Y4	Duct Mach Number Response

11.2 Appendix B - Scheduled Regulator Response To Unit Step Demands

Appendix B contains time domain plots of the effects of similar unit step demands for the VTH and HTV regulators based on the linear regression fits indicated in Tables 8 and 9. Figures A12-A17 contain the results at the individual operating conditions for the VTH transition, and Figures A18-A22 for the corresponding HTV operating conditions. These results indicate somewhat greater multi-loop interactions and, in some cases, longer time requirements to achieve steady-state conditions.

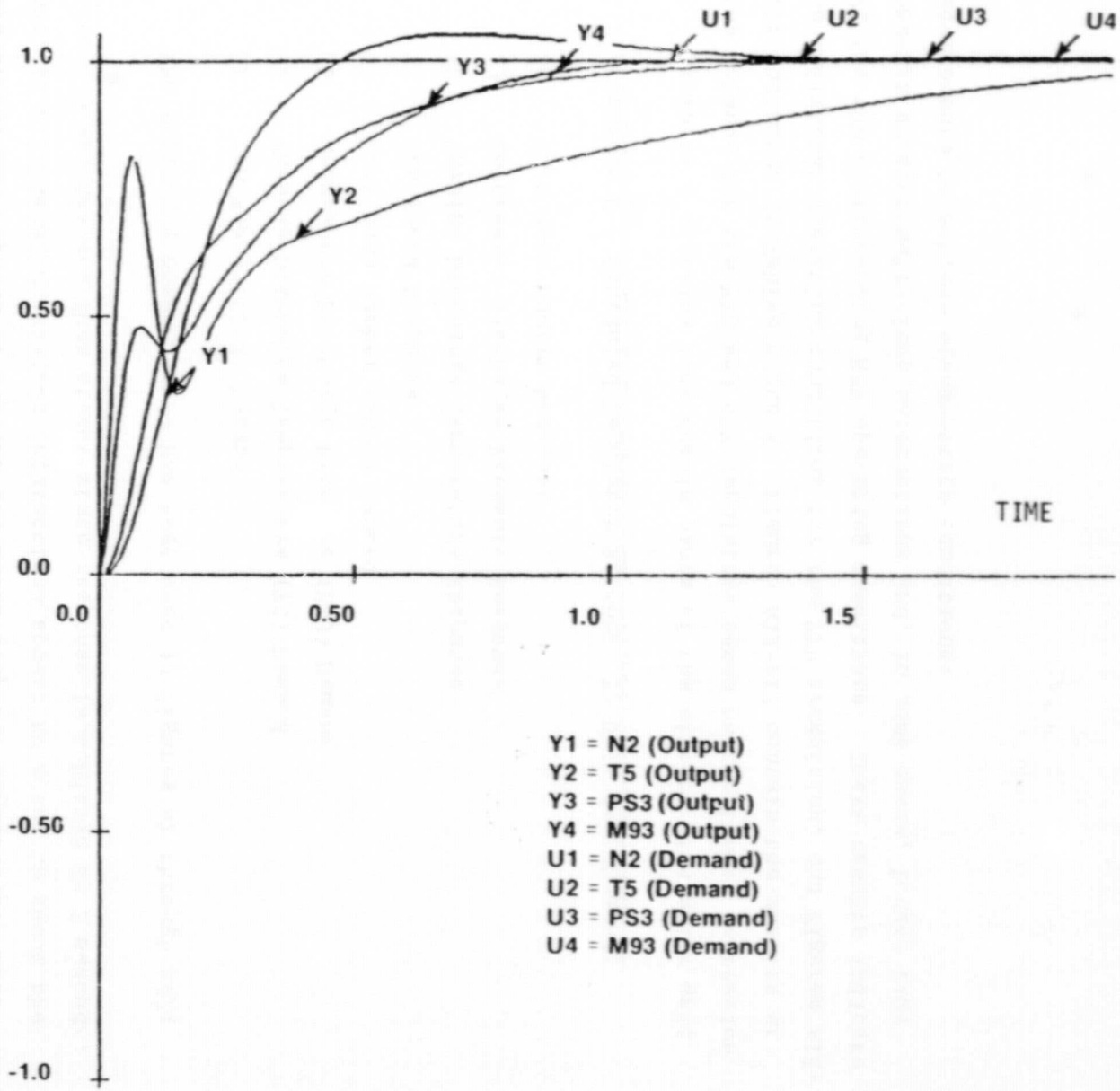

FIGURE A-1 RESPONSE TO UNIT STEP DEMANDS AT TAKEOFF

ORIGINAL PAGE IS
OF POOR QUALITY

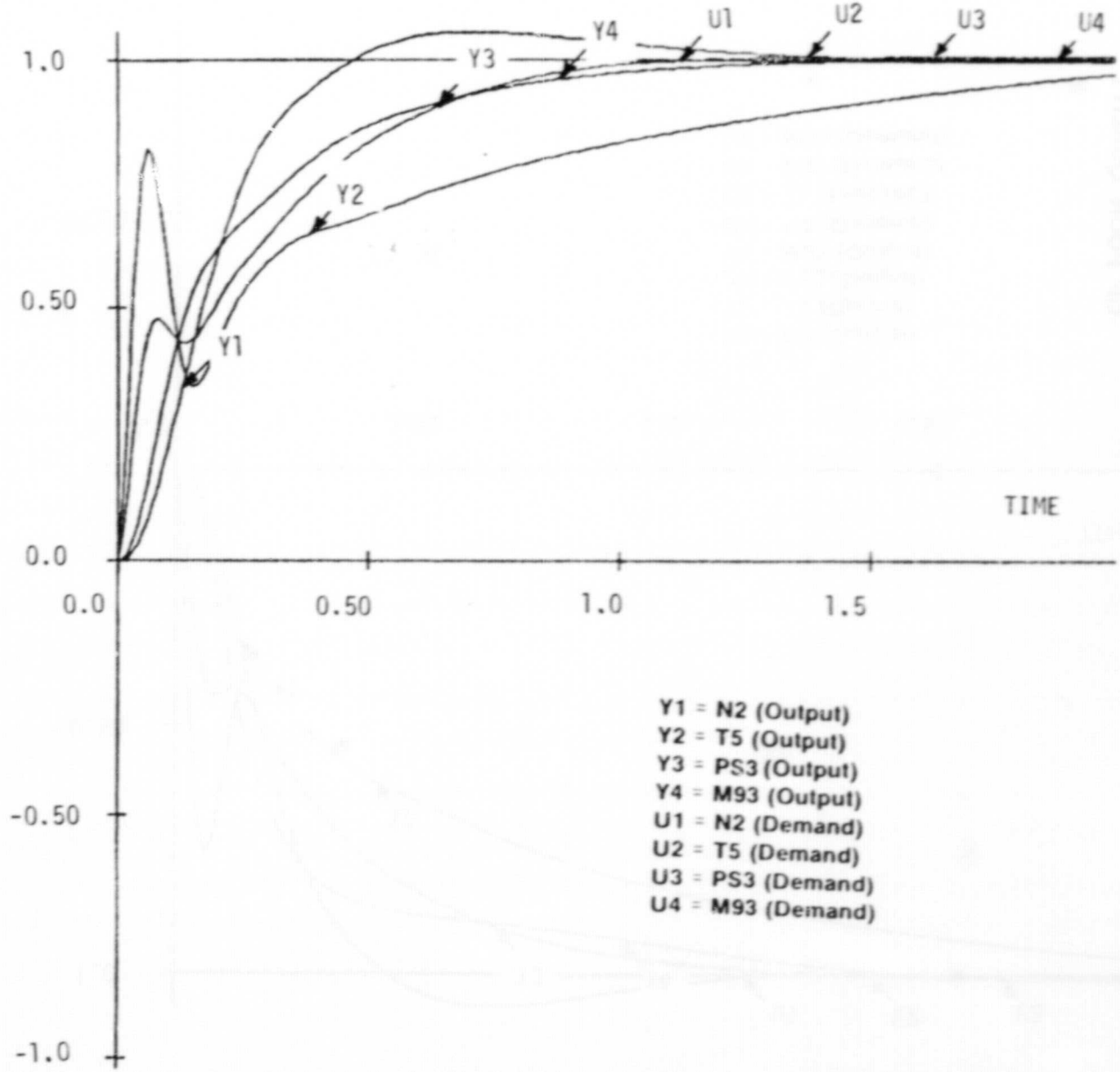

FIGURE A-2 RESPONSE TO UNIT STEP DEMANDS AT START TRANSITION

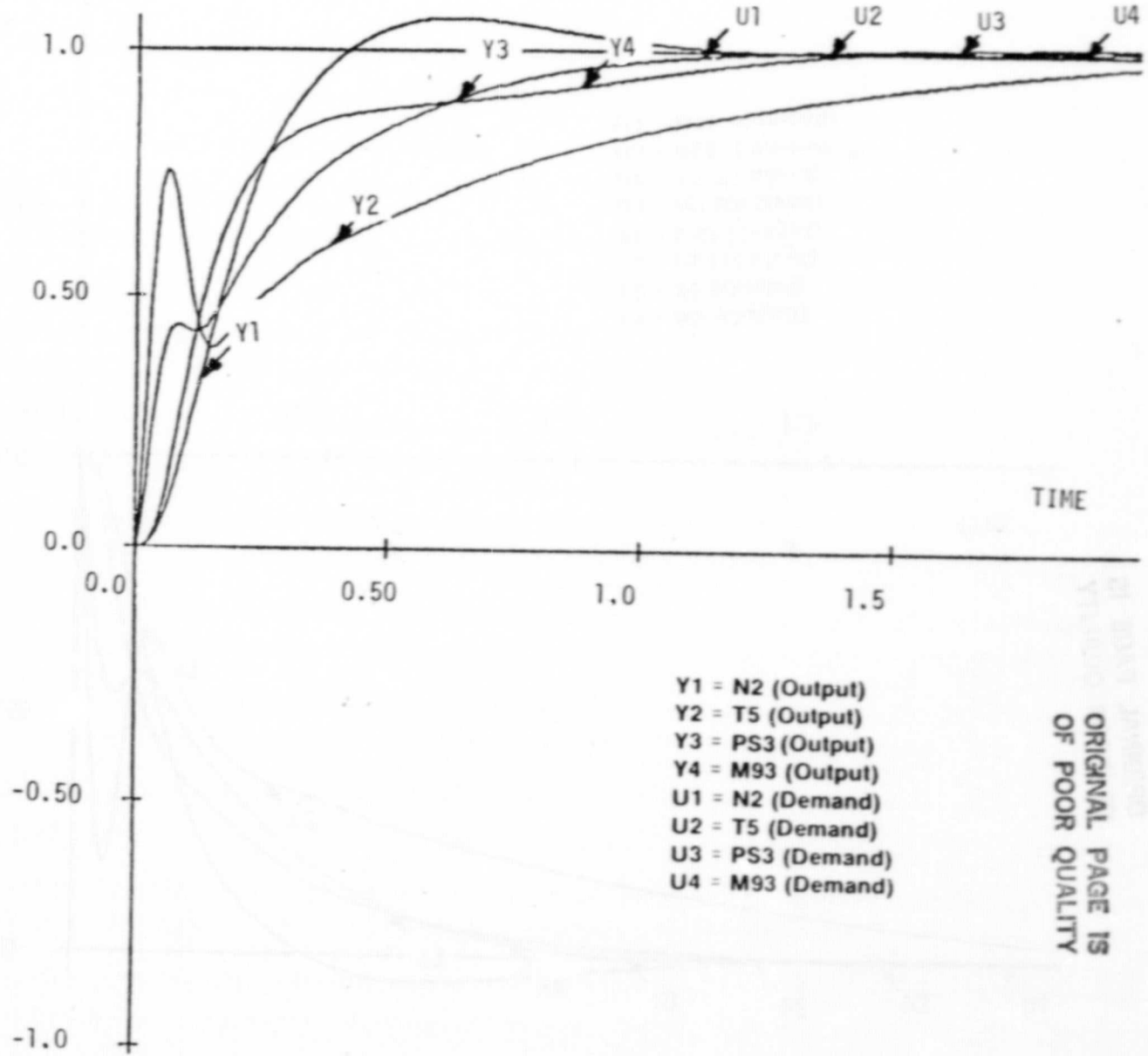

FIGURE A-3 RESPONSE TO UNIT STEP DEMANDS AT ACTIVATE RFCV

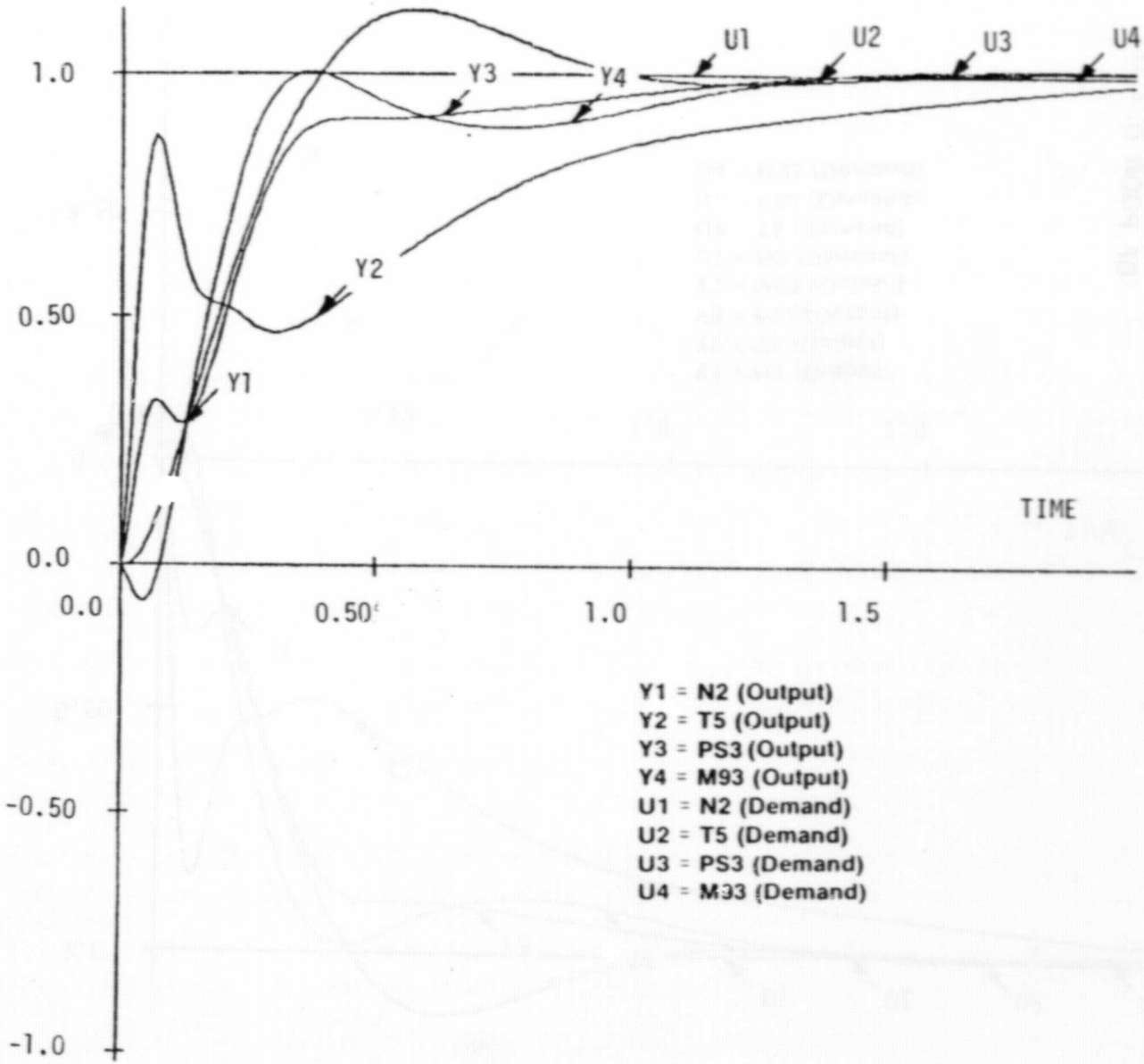

FIGURE A-4 RESPONSE TO UNIT STEP DEMANDS AT MID TRANSITION

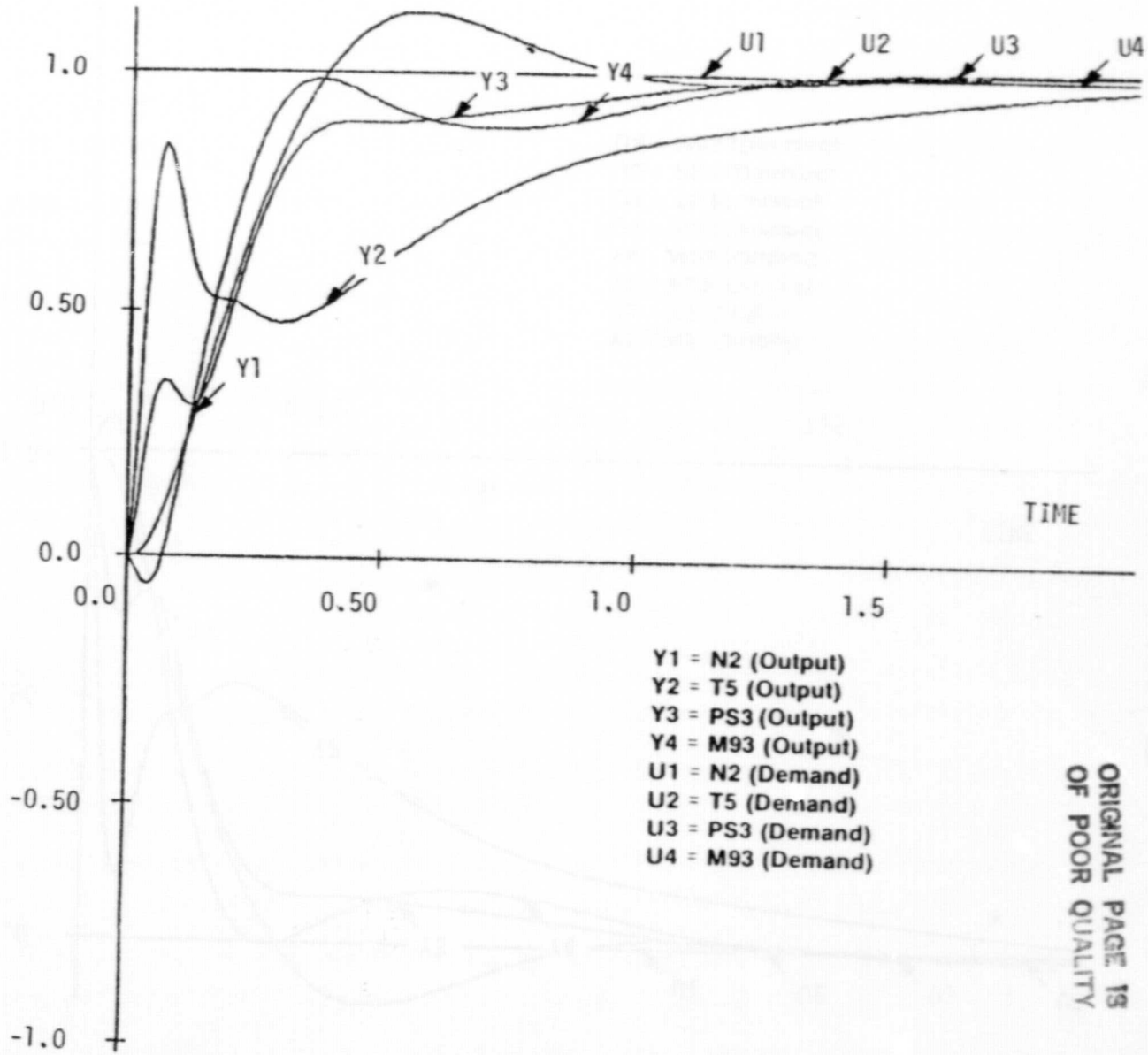

FIGURE A-5 RESPONSE TO UNIT STEP DEMANDS AT MINIMUM RALS

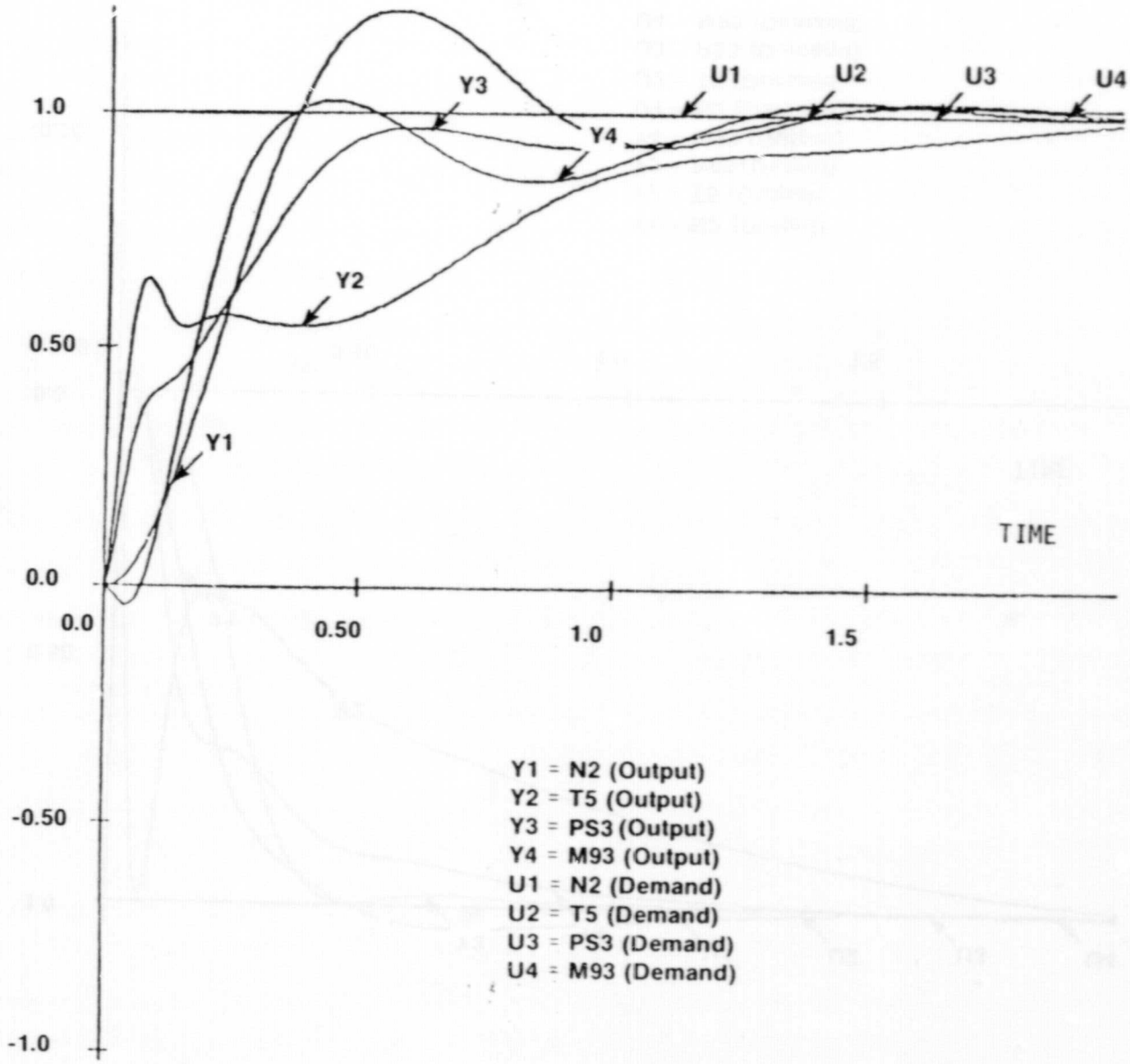

FIGURE A-6 RESPONSE TO UNIT STEP DEMANDS AT MAXIMUM HORIZONTAL

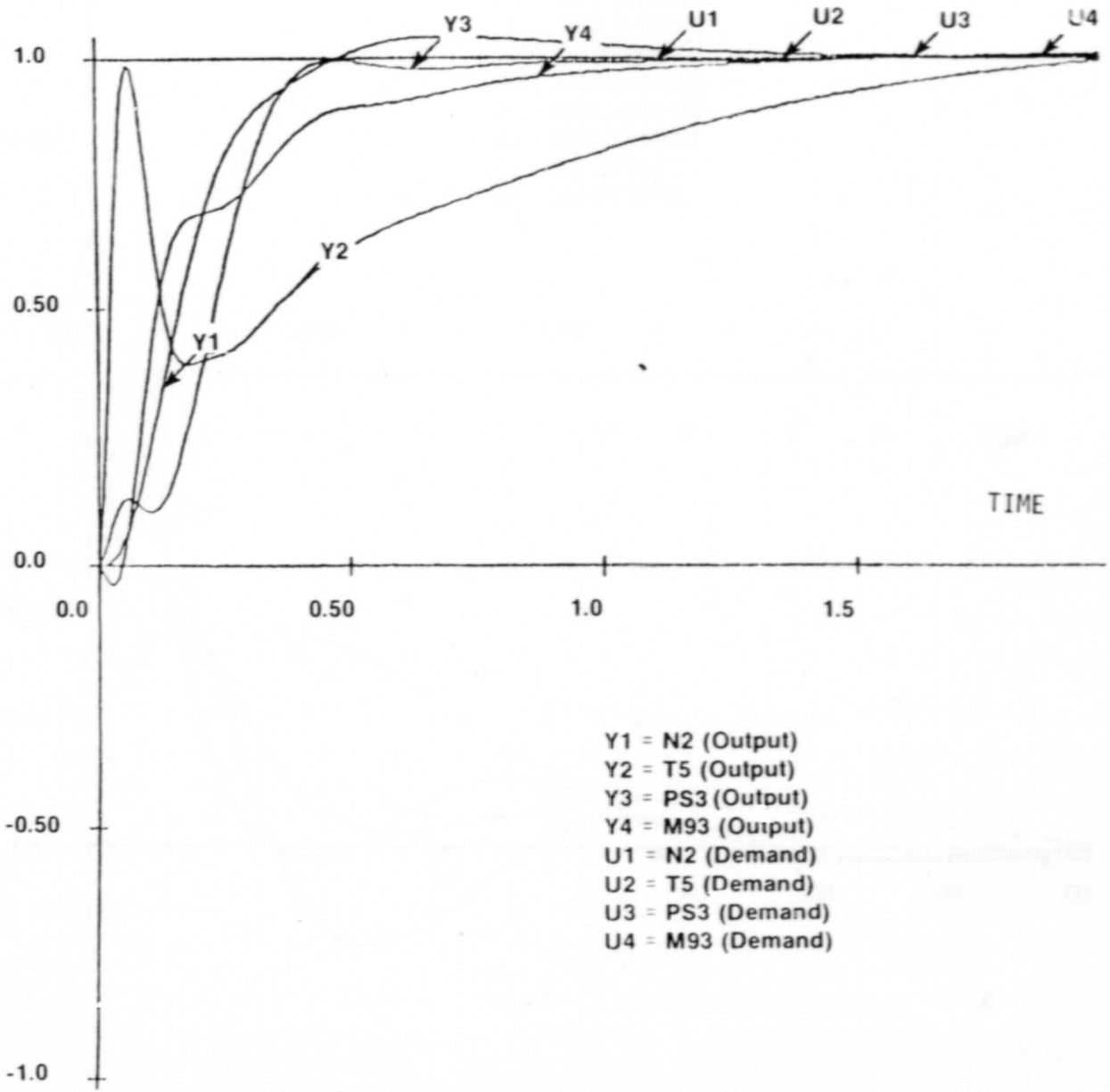

FIGURE A-7 RESPONSE TO UNIT STEP DEMANDS AT 30% RALS FLOW

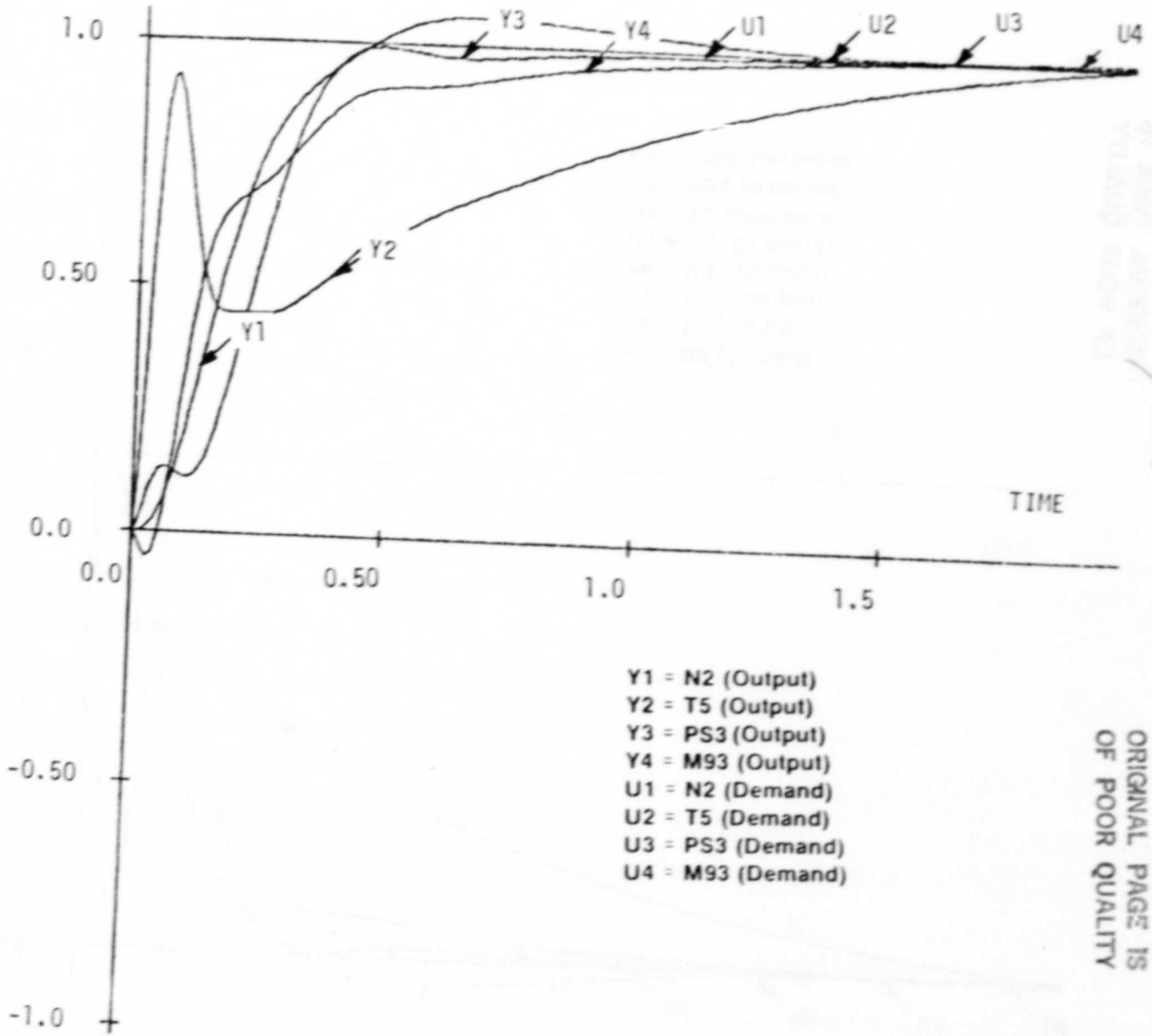

FIGURE A-8 RESPONSE TO UNIT STEP DEMANDS AT 60% RALS FLOW

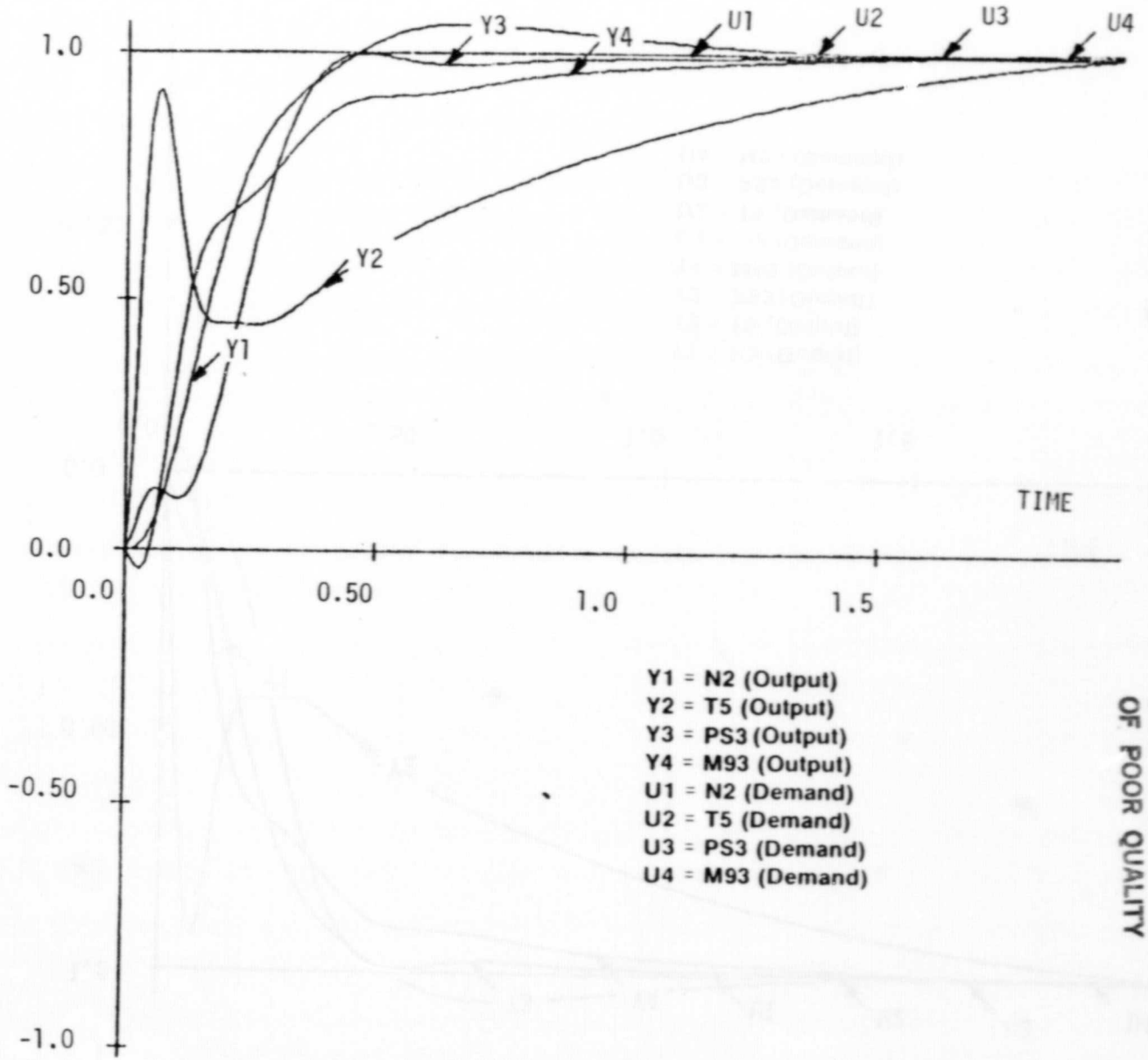

FIGURE A-9 RESPONSE TO UNIT STEP DEMANDS AT MINIMUM RALS (HTV)

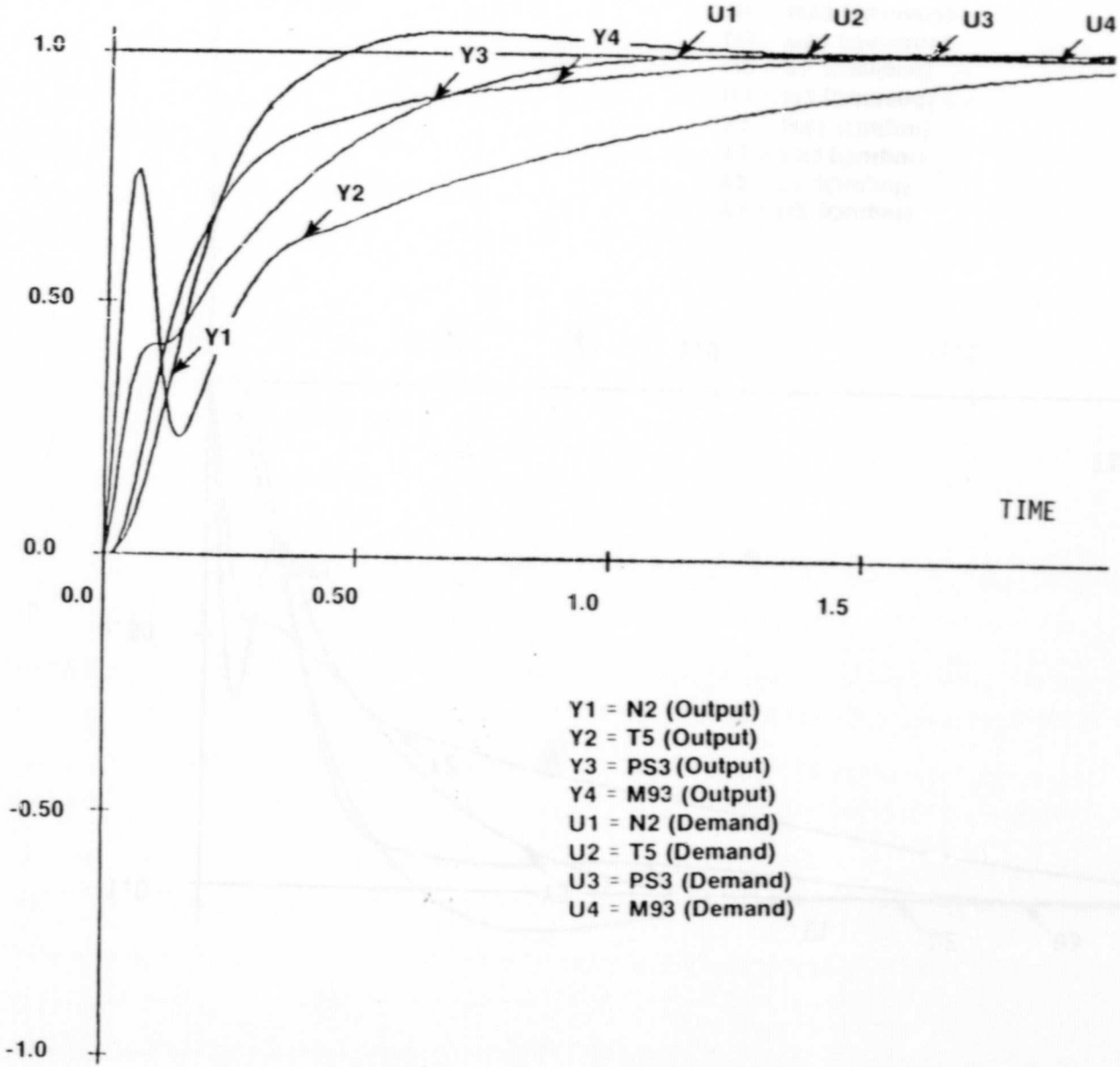

FIGURE A-10 RESPONSE TO UNIT STEP DEMANDS AT 80% RALS FLOW

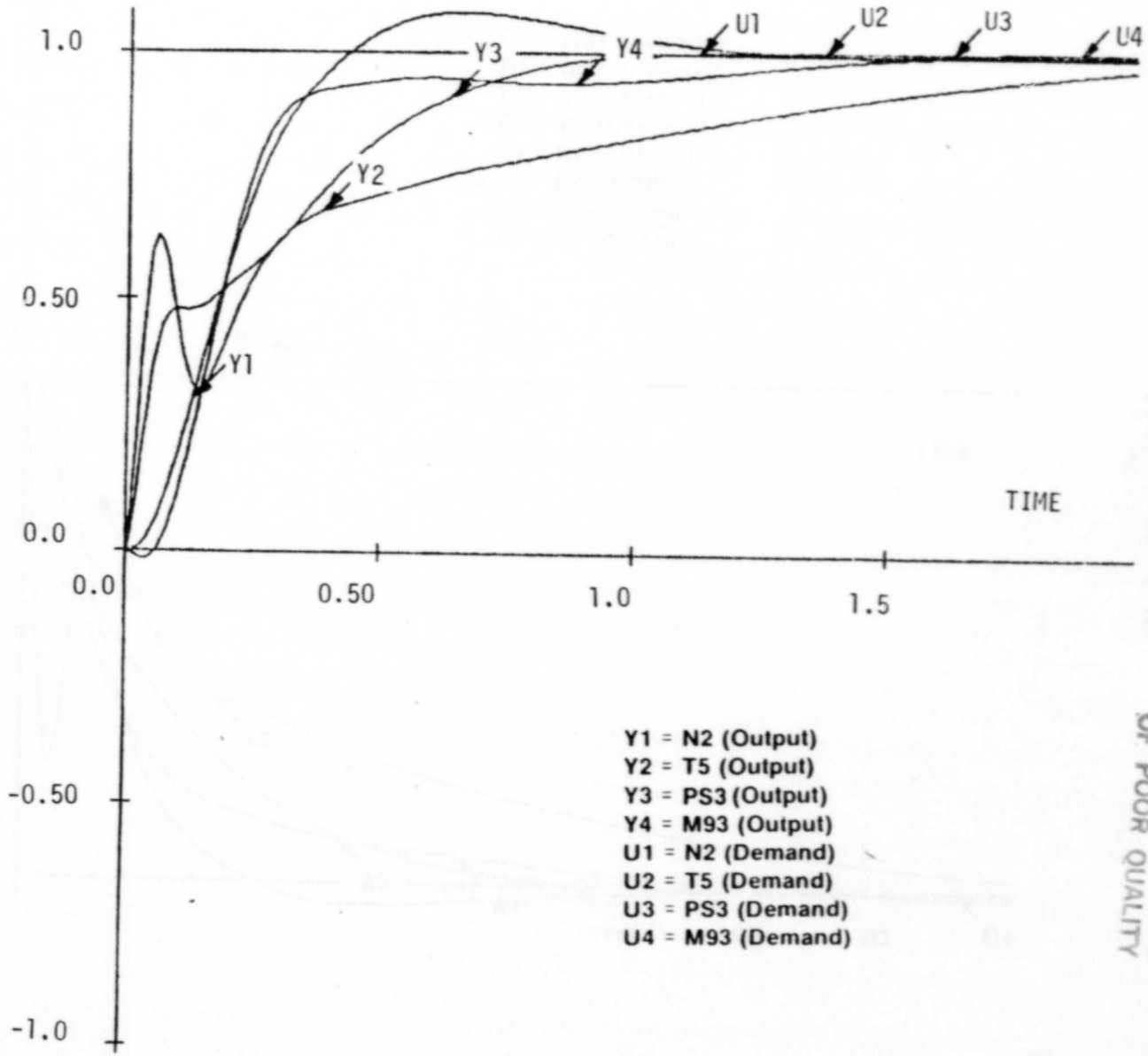

FIGURE A-11 RESPONSE TO UNIT STEP DEMANDS AT LANDING

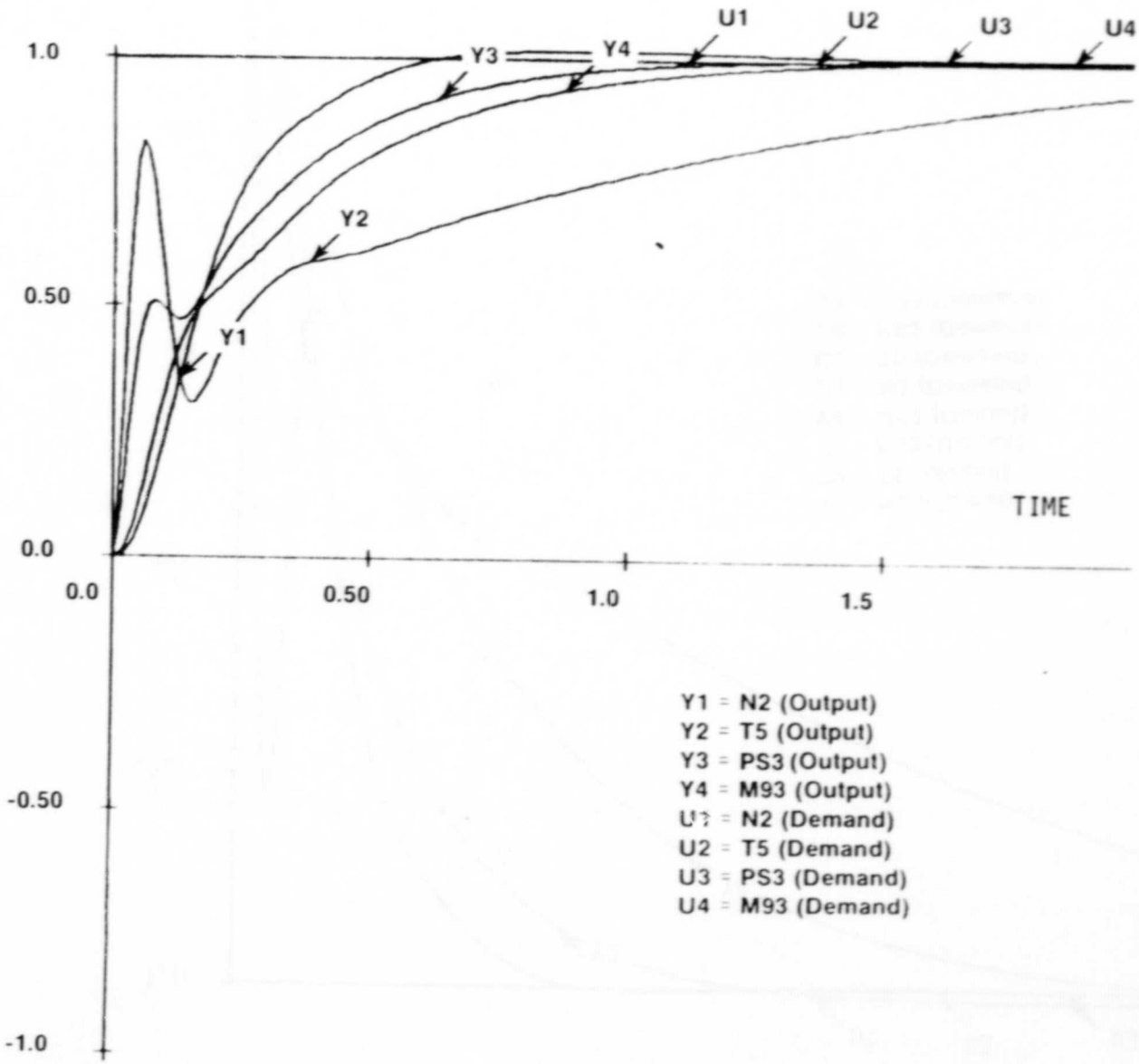

FIGURE A-12 SCHEDULED REGULATOR RESPONSE TO UNIT STEP DEMANDS AT TAKEOFF

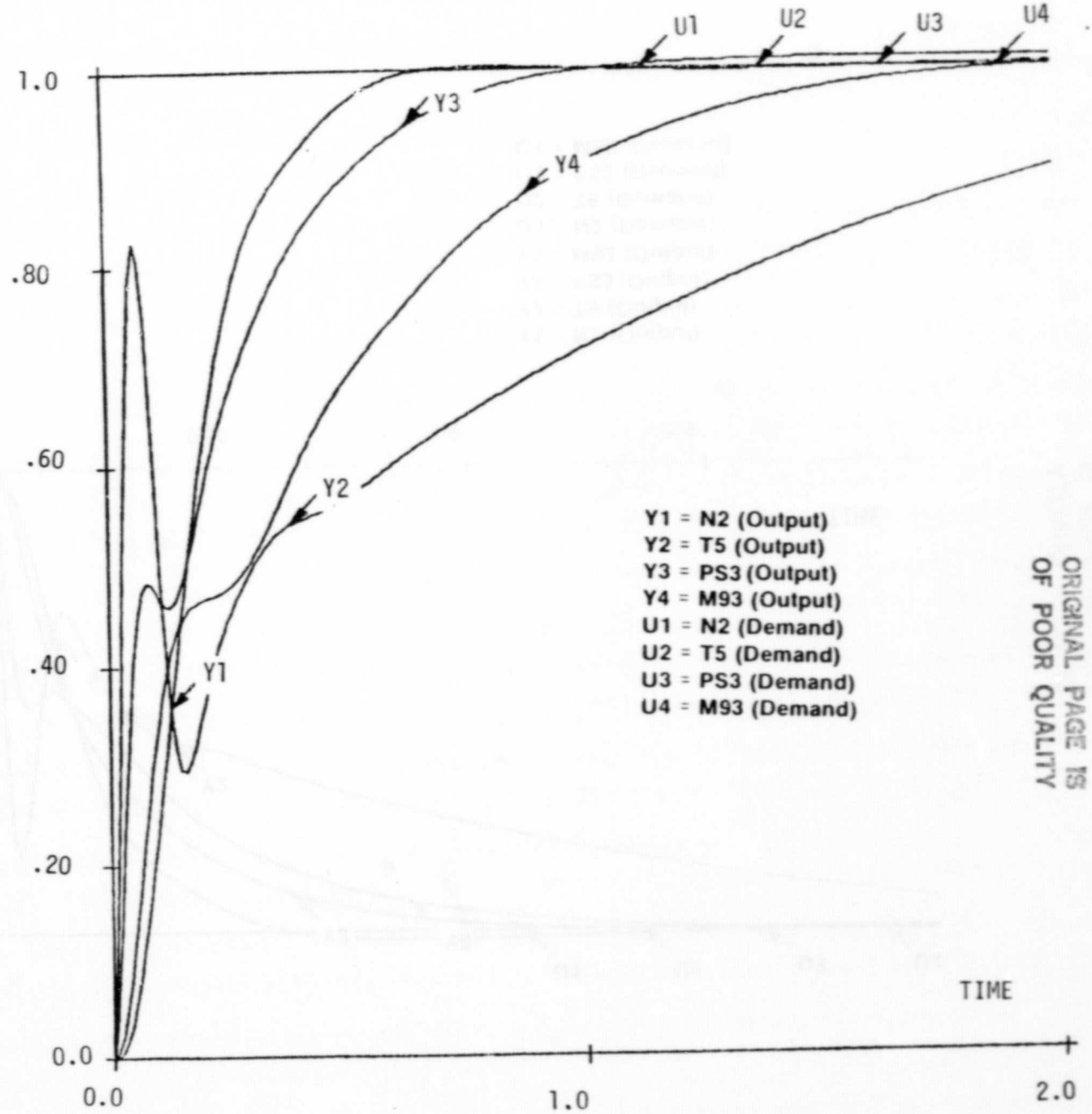

FIGURE A-13 SCHEDULED REGULATOR RESPONSE TO UNIT STEP DEMANDS AT START TRANSITION

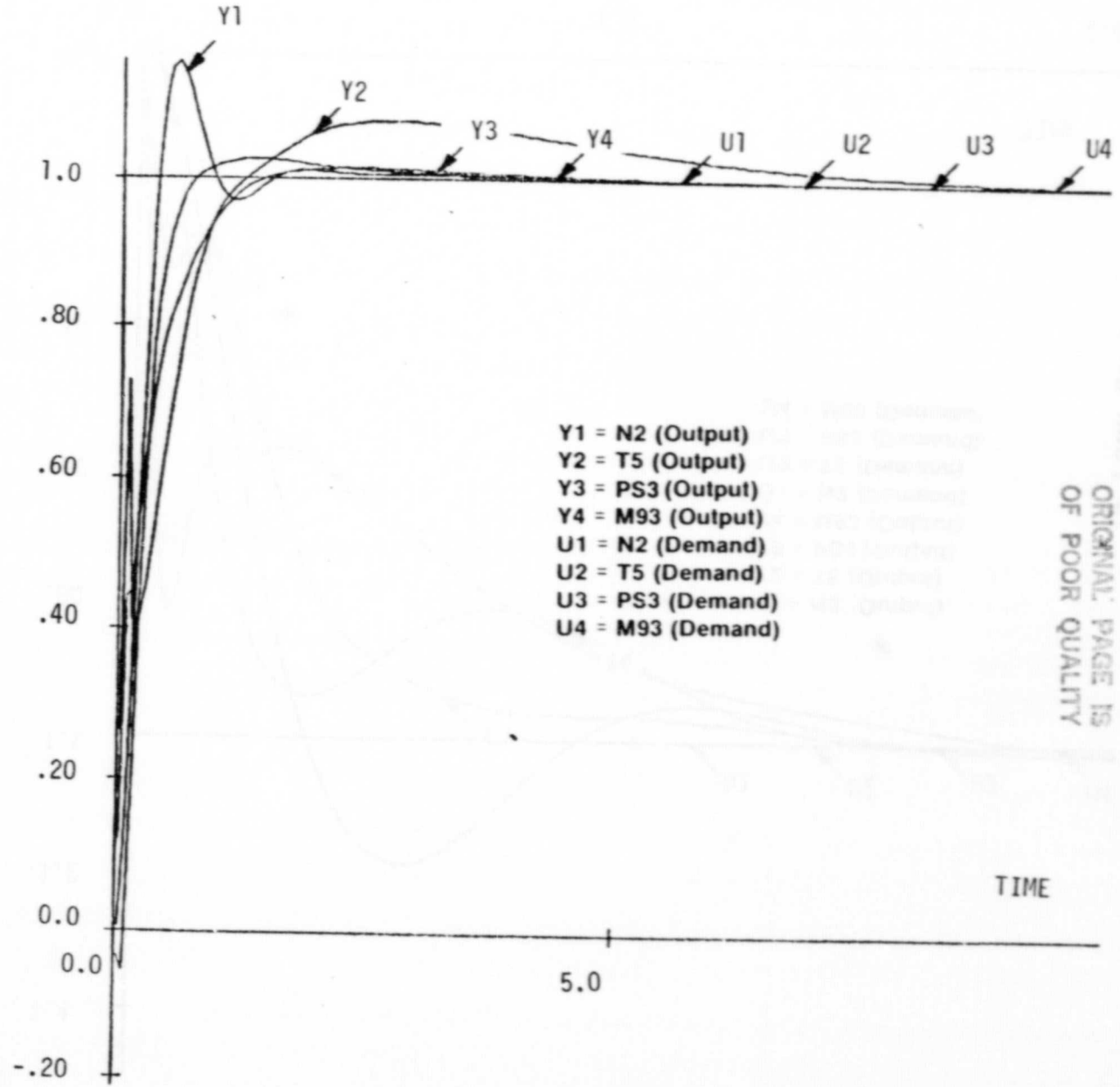

FIGURE A-14 SCHEDULED REGULATOR RESPONSE TO UNIT STEP DEMANDS AT ACTIVATE RFCV

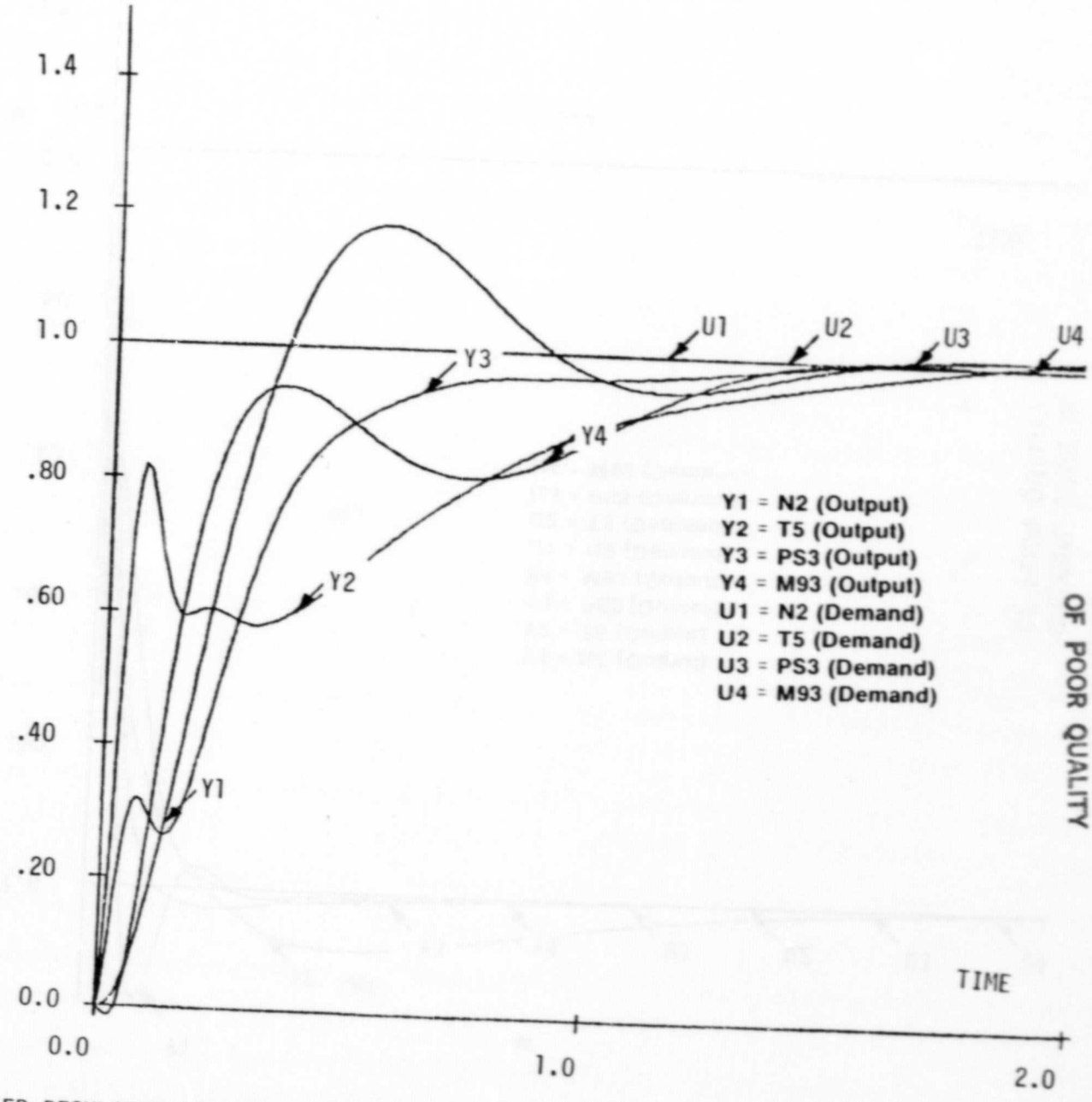

FIGURE A-15 SCHEDULED REGULATOR RESPONSE TO UNIT STEP DEMANDS AT MID TRANSITION

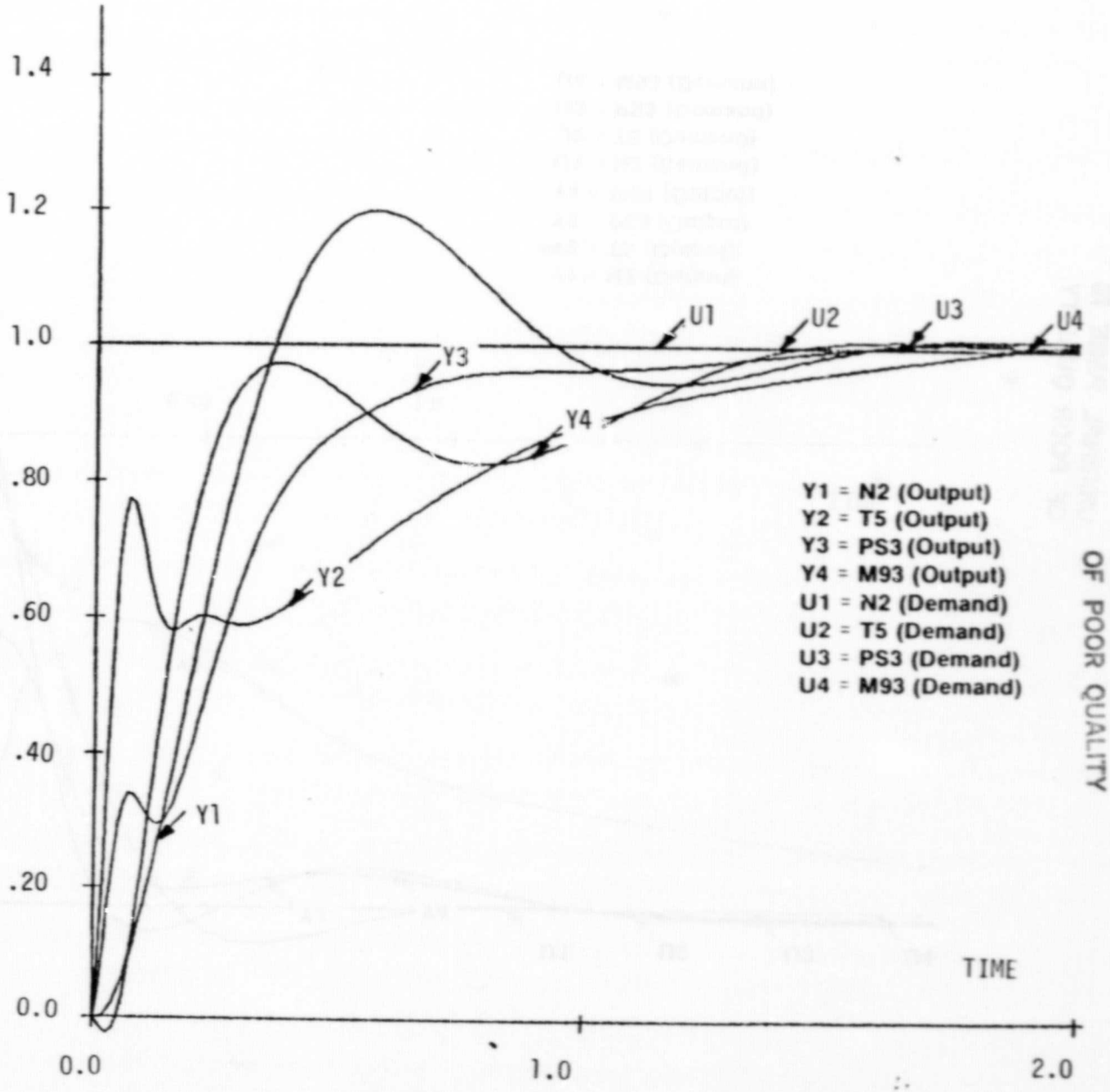

FIGURE A-16 SCHEDULED REGULATOR RESPONSE TO UNIT STEP DEMANDS AT MINIMUM RALS (VTH)

FIGURE A-17 SCHEDULED REGULATOR RESPONSE TO UNIT STEP DEMANDS AT MAXIMUM HORIZONTAL

30% RALS Response with Gain Schedules

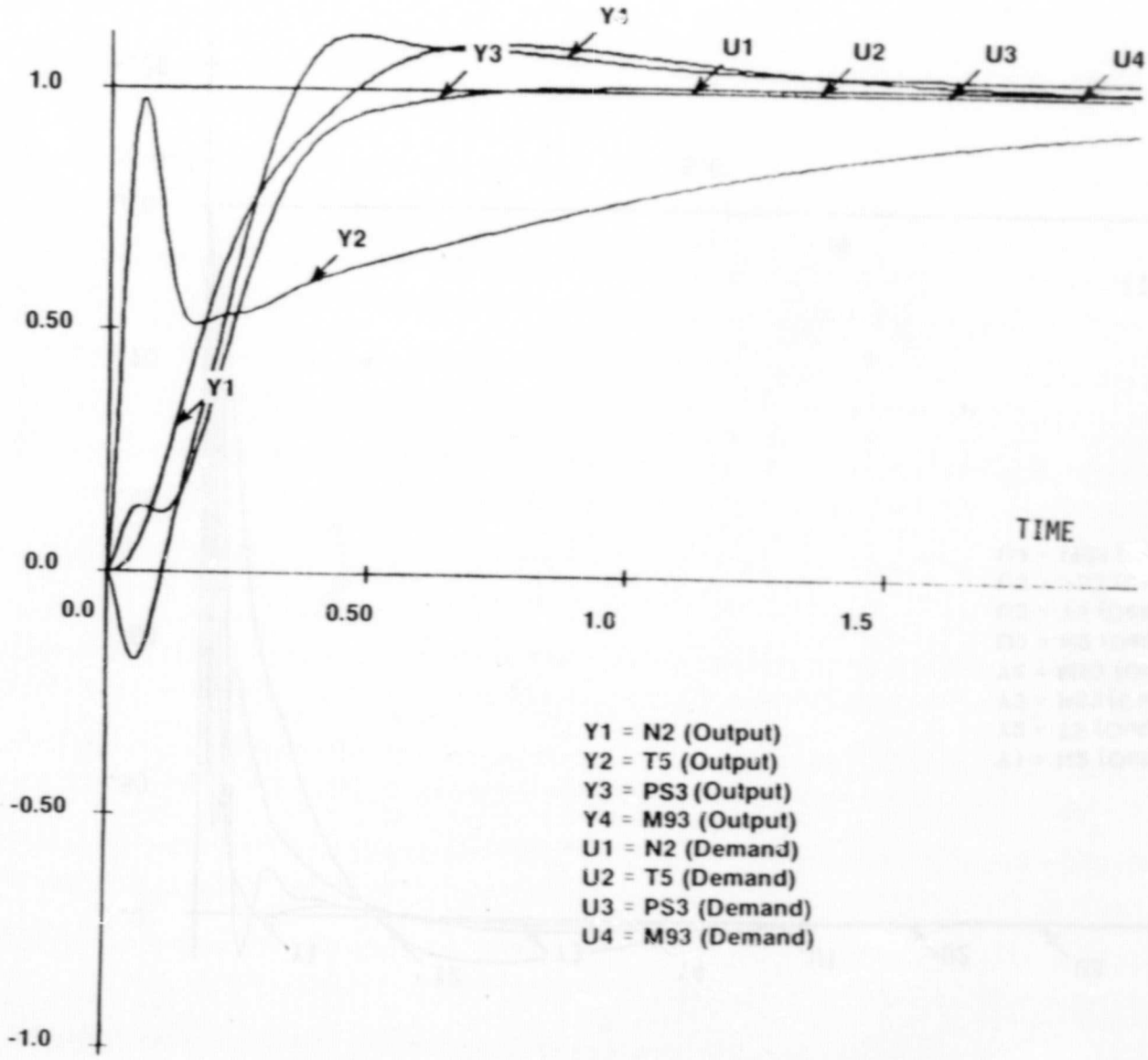

FIGURE A-18 SCHEDULED REGULATOR RESPONSE TO UNIT STEP DEMANDS AT 30% RALS FLOW

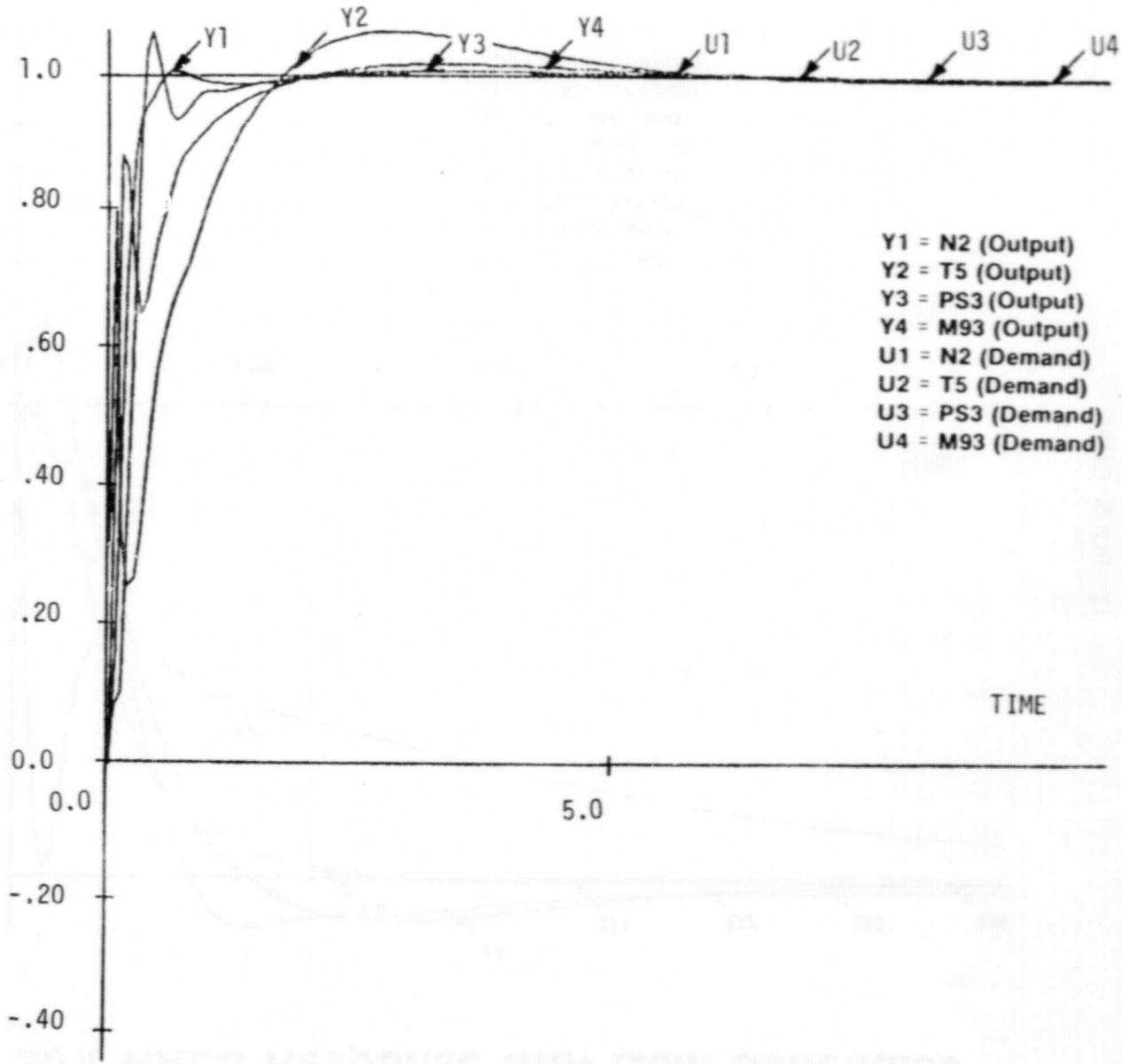

FIGURE A-19 SCHEDULED REGULATOR RESPONSE TO UNIT STEP DEMANDS AT 60% RALS FLOW

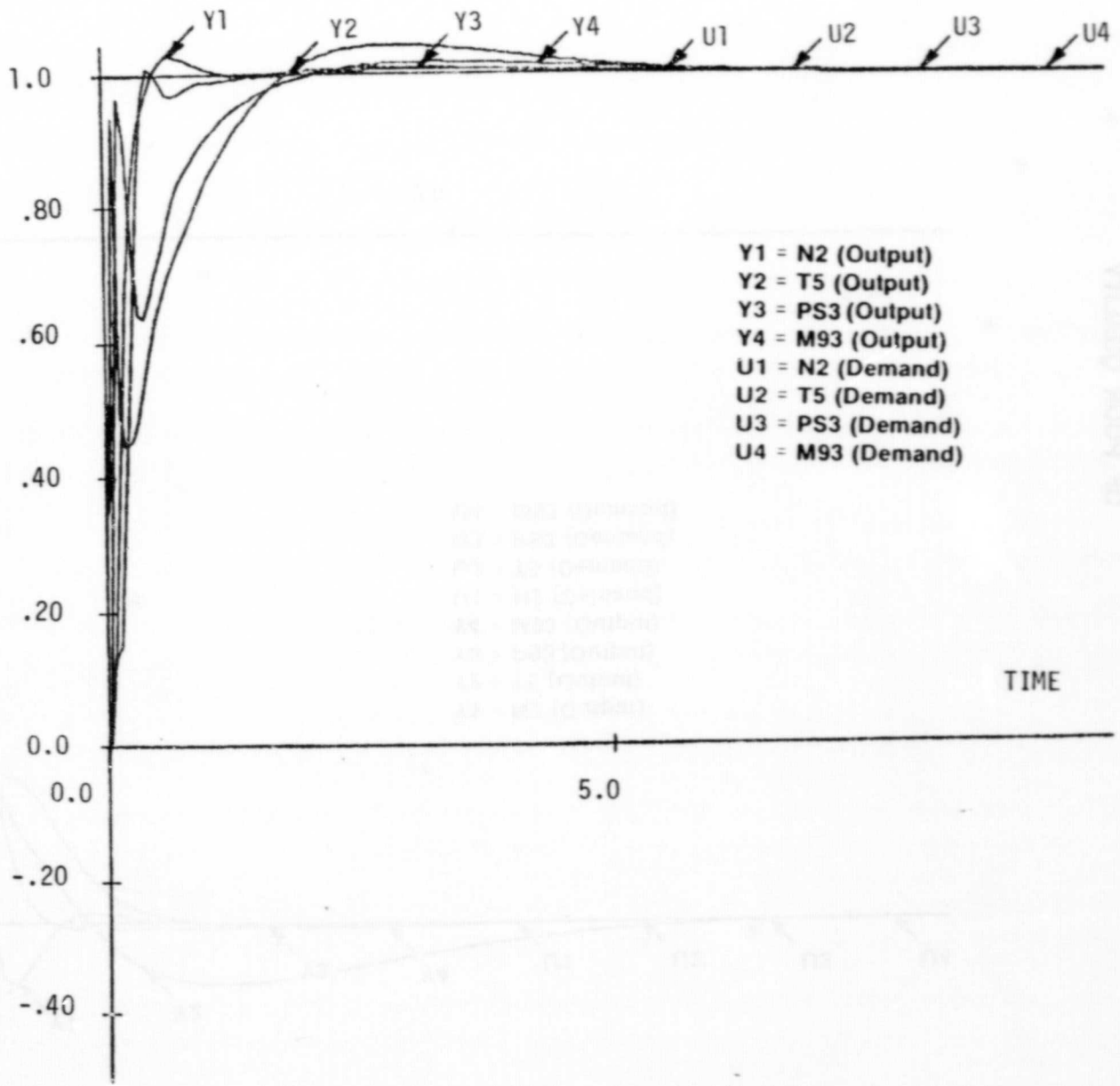

FIGURE A-20 SCHEDULED REGULATOR RESPONSE TO UNIT STEP DEMANDS AT MINIMUM RALS (HTV)

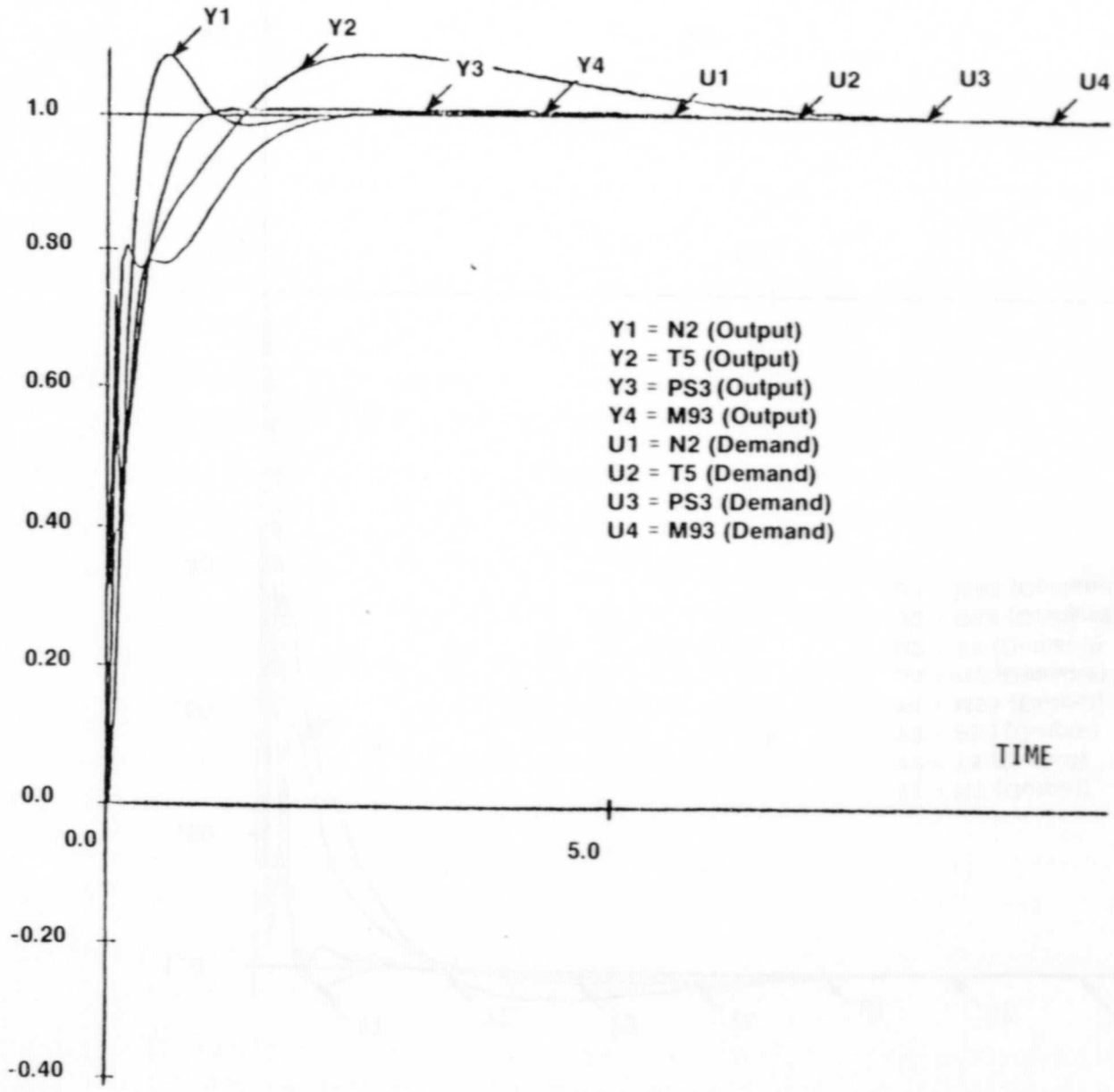

FIGURE A-21 SCHEDULED REGULATOR RESPONSE TO UNIT STEP DEMANDS AT 80% RALS FLOW

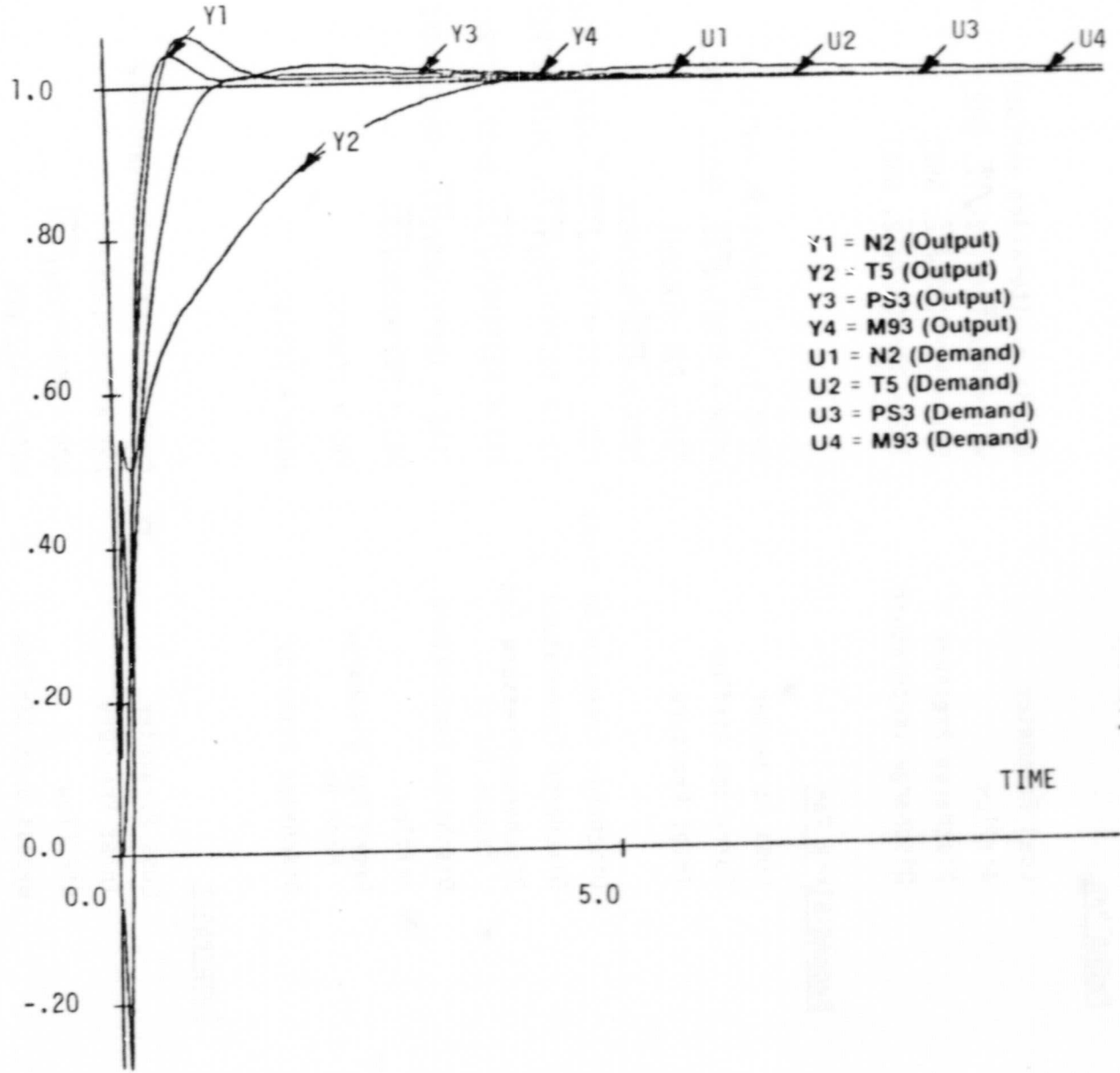

FIGURE A-22 SCHEDULED REGULATOR RESPONSE TO UNIT STEP DEMANDS AT LANDING

11.3 Appendix C - Non-Linear Transient Model

Front Fan

Loss Parameter	GH2 is an iteration variable
Airflow	$W21 = P2/\sqrt{T2} * f(N2/\sqrt{T2}, GH2)$
Discharge Pressure	$P21 = P2 * f(N2/\sqrt{T2}, GH2)$
Discharge Temperature	$T22 = T2 * f(N2/\sqrt{T2}, GH2)$

Second-Block Fan

Loss Parameter	GH22 is an iteration variable
Corrected Airflow	$W22R = f(N25/\sqrt{T22}, GH22, STP22)$
Inlet Pressure	$P22 = P21 * f(W22R)$
	$P22X = \sqrt{T22} * W2/W22R$
Discharge Pressure(to core)	$P23 = P22 * f(N25/\sqrt{T22}, GH22, STP22)$
Discharge Temperature	$T25 = T22 * f(N25/\sqrt{T22}, GH22, STP22)$
Discharge Pressure (to Bypass Duct)	$P13 = P23 * (N25/\sqrt{T22}, GH22, STP22)$
Discharge Temperature	$T14B = T25 * f(N25/\sqrt{T22}, GH22, STP22)$
Airflow	$W22 = P22 * W22R/\sqrt{T22}$
Front Fan Discharge Mach No.	$M93 = f(W22R)$
Discharge Enthalpy	$H14B = f(T14B)$

Compressor

Loss Parameter	GH25 is an iteration variable
Inlet Pressure	$P25 = P23/f(W25R)$
Air Flow	$W25 = W25R * P25/\sqrt{T25}$
Bypass Duct Airflow	$W14B = W22 - W25$
Discharge Pressure	$P3 = P25 * f(N25/\sqrt{T25}, GH25)$
Discharge Temperature	$T3 = T25 * f(N25/\sqrt{T25}, GH25)$
Inlet and Discharge Enthalpies	$H25 = f(T25)$
	$H3 = f(T3)$
Discharge Flow	$W3 = k * W25 - WB28$ (k reflects cooling air extraction and WB28 customer bleed extraction)

Compression Power

Front-Fan	PW2 = k1*T22*W2-k2*T2*W2
Second-Block Fan	PW22 = -k3*T22*W22+k4*H25*W25 +k4*H14B*W14B
Compressor	PW25 = k5*H3*W25-k6*H25*W25 -k7*H3*WB28
High Pressure Shaft	PWCMP = PW22+PW25

Cooling Flow Accountability

Combustor	WA36 = W3-k8*W25
HP Turbine	WA41 = WA36+k9*W25
	WA42 = WA41+k10*W25
LP Turbine	WA49 = WA42+k11*W25
	WA5 = WA49+k12*W25
Frame	WA56 = WA5+k13*W14B

Combustor

Compressor Discharge Pressure	PS3 = P3*f(W3$\sqrt{T3}$/P3)
Fuel-Air Ratio	FAR36 = k14*WF36/WA36
Efficiency	E4D36 = f(P3, W3$\sqrt{T3}$/P3, FAR36)
Discharge Enthalpy	H4 = H3+k15*FAR36*E4D36
Discharge Temperature	T4 = f(H4, FAR36)
Discharge Pressure	P4 = P3*f(W3$\sqrt{T3}$/P3, FAR36)

High Pressure Turbine

Gas Flow	W4 = WA36+k16*WF36
	W41 = W4+k17*W25
Nozzle Enthalpy	H41 = (WA36*H4+k18*W25*H3)/WA41
Fuel-Air Ratio	FAR41 = k19*WF36/WA41
Unbalanced Power Factor	PWX4Q is an iteration variable
Power	PW4 = PWCMP(1+PWX4Q)
Rotor Acceleration	DN25 = PWX4Q*PWCMP/N25
Energy Ratio	H41R = k20*PW4/(T41*W41)
Flow Function	W4R = f(N25/ T41, H41R)
Alternate Inlet Pressure	P4X = T4*W4/W4R)
Exit Pressure	P42 = P4X*f(H41R, N25/ R41)

Exit Gas Flow	W42 = W41+k21*W25
Exit Enthalpy	H42 = (WA41*H41-PW4+k22*W25*H3)/WA42
Exit Temperature	T42 = f(H42, WF36/WA42)

Low Pressure Turbine

Gas Flow	W49 = W41+k23*W25
Cooling Flow Enthalpy	HCL49 = k24*H3+k25*H25
Gas Enthalpy	H49 = (WA42*H42+k26-W25*HCC49)/WA49
Temperature	T49 = f(H49, WF36/WA49)
Unbalanced Power Factor	PWX48Q is an iteration variable
Rotor Acceleration	DN2 = (PWX48Q*PW2)/N2
Discharge Enthalpy	H5 = (WA49*H49-PW48+k27*W25* HCL49)/WA5
Energy Ratio	H49R = PW48/(T49*W49)
Flow Function	W42R = f(N2/$\sqrt{T49}$, H49R, STP49)
Inlet Pressure	P42X = 42*P42/W42R
Discharge Airflow	W5 = W49+k28*W25
Discharge Temperature	T5 = f(H5, WF36/WA5)

VABI

LPT Discharge Flow	W5R = W5*$\sqrt{T5}$/P5
Hot Stream Discharge Pressure	P56 = P5*f(W5R)
Gas Flow	W56 = W5+k29*W14B
Discharge Enthalpy	H56 = (WA5*H5+k30*W14B*H14B)/WA56
Discharge Temperature	T56 = f(H56, WF36/WA56)
Duct Discharge Pressure	P16 = P13*f(W13R)
Cold Stream Area	AE16 is an iteration variable
Hot Stream Area	AE56 = k31-AE16
Hot Stream Flow	W56RQA = W56* T56/(AE56*P56)
Hot Stream Static Pressure	PS56 = P56-f(W56RQA)

Gas Flow	W14Z = k32*W41B-k33*WA56
Remote Flow Ratio	WBL16Q is an iteration variable
Remote Airflow	W81 = W14Z*WBL16Q
Cold Stream Flow	W16 = W14Z-W81
Mixed Air Flow	WA58 = WA56+WA16
Mixed Enthalpy	H58 = (WA56*H56+W16*H14B)/WA58
Nozzle Gas Flow	WA7 = WA58+k34*WA56
Fuel-Air Ratio	FAR7 = k34*(WF6+WF36)/WA7
Mixed Gas Flow	W58 = WA58+K35*WF36
Nozzle Entrance Flow	W7 = W58+k36*WA56+k37*WF6
Cold Stream Flow	W16RQA = W16*$\sqrt{T14}$/(AE16*P16)
Cold Stream Static Pressure	PS16 = P16*f(W16RQA)
Mixing Plane Momentum	WV16 = W16*f(T14B, W16, W16RQA)/(P16*AE16) WV58 = W56*f(T56, W56, W56RQA)/(P56*AE56)
Mixed Velocity	V58 = (k38*WV56+WV16)/W58
Mixed Temperature	T58 = f(H58, WF36/WA58)
Mixed Static Temperature	TS58 = T48-k39*V58
Mixed Pressure	P58 = PS56*f(V58, TS58)

Afterburner

Fuel-Air Ratio Added	FAR68 = WF6/WA58
Efficiency	E68D6 = f(P58, FAR68, T58)
Discharge Enthalpy	H68 = H58+k40*E68D6*FAR68

ADEN Nozzle

Entrance Enthalpy	H7 = (WA58*H68+WA56*H14B)/WA7
Temperature	T7 = f(H7, FAR7)
Pressure	P7 = P58*f(V58, FAR68) P7X = f(W7*$\sqrt{T7}$/A8, PAMB)
Gross Thrust	F69 = W7*f(P7, T7)

RALS (Calculated only when W81 is greater than zero)

Alternate Remote Flow	W81X = k41*AE80*P16/$\sqrt{T14B}$
RFCV Flow	W80RQA = W81*$\sqrt{T14B}$/(P16*AE80)
RFCV Discharge Pressure	P86 = P16*f(W80RQA, AE80)

Burner Fuel-Air Ratio	FAR86 = k42*WF86/W81
Burner Exit Pressure	P87 = P86*f(W81*$\sqrt{T14B}$/P86, FAR86)
Burner Exit Enthalpy	H87 = H14B+k43*FAR86
Burner Exit Temperature	T87 = f(H87, FAR86)
Nozzle Gas Flow	W87 = W81+k44*WF86
Alternate Nozzle Pressure	P87X = f(W87*$\sqrt{T87}$/A88, PAMB)
Gross Thrust	FG89 = W87*f(P87, T87)

Iteration Errors

E4 = P4-P4X	V, H, and T Modes
E42 = P42-P42X	V, H, and T Modes
E22 = P22-P22X	V, H, and T Modes
E7 = P7-P7X	V, H, and T Modes
E87 = P87-P87X	Used in E8187
E16 = PS16-PS56	H and T Modes
E81 = W81-W81X	Used in E8187
E8187 = MIN(E87, -E81)	V and T Modes

11.4 Appendix D - Nomenclature

Symbol	Description	Engr. Units
ADEN	Augmented Deflected Exhaust Nozzle	
ADL	ADEN Deflection Angle (longitudinal)	degrees
AR	Nozzle Aspect Ratio	
A/RFCV	Activate Remote Flow Control Valve (VTH Transition)	
A8	ADEN Throat Area	$inches^2$
A27	VABI Cold Stream Area	$inches^2$
A88	RALS Nozzle Throat Area	$inches^2$
a11-a44	Regulator Proportional Gain Coefficients	
b11-b44	Regulator Integral Gain Coefficients	
BNG	RALS Nozzle Deflection Angle (Transverse)	degrees
Cd	Nozzle Discharge Coefficient	
CFGR	Nozzle Thrust Coefficient	
Cp	Specific Heat at Constant Pressure	BTU/lb/°R
ETA	Fan Efficiency	
FCD	Flight Control Demand Parameter	
FG	Gross Thrust	lbs.
FG8	ADEN Gross Thrust	lbs.
FG88	RALS Nozzle Gross Thrust	lbs.
FG89	RALS Nozzle Gross Thrust	lbs.
FGT	Total Gross Thrust	lbs.
FID	Flight Idle Descent (HTV Transition)	
FN	Net Thrust	lbs.
FRAM	Ram Drag	lbs.
G	Model Matrix (Objective Function)	
H	Model Matrix (Measured Variables)	
HTV	Horizontal-to-Vertical Transition	
H41R	Low Pressure Turbine Energy Ratio ($\Delta H/T$)	BTU/lb/°R
H49R	High Pressure Turbine Energy Ratio ($\Delta H/T$)	BTU/lb/°R
ID	Inlet Distortion Level	
K	Gain	
K/Q Matrix	Regulator Design Procedure	

Symbol	Description	Engr. Units
L	Landing (HTV Transition)	
M	Flight Mach Number	
M	State Vector Covariance Matrix	
MH	Maximum Horizontal (VTH Transition)	
M/R	Minimum RALS Operation (VTH Transition)	
M/T	Mid-Transition (VTH Transition)	
N	Number of Measurements	
P	Filter Matrix	
PAV	Average Inlet Total Pressure	psia
PCN2	Per Cent Fan Speed	%
PCN25	Per Cent Core Speed	%
PIC	Proportional/Integral Controller	
PITCH	Pitch Attitude Angle	degrees
PLA	Power Lever Angle	degrees
PMIN	Minimum Inlet Total Pressure	psia
PR	Pitch Rate Demand	deg/sec.
PRE1	First Precompensator Matrix	
PRE2	Second Precompensator Matrix	
PS3	Compressor Discharge Static Pressure	psia
P_T	Total Pressure	psia
PT_j/P_0	Nozzle Total-to-Static Pressure Ratio	
P/P	Fan or Compressor Pressure Ratio	
P_0	Ambient Pressure	psia
P_1	Compressor Discharge Pressure	psia
P_W	Net Power Output	hp
P2	Inlet Total Pressure	psia
P3Q25	Compressor Pressure Ratio	
P13Q25	Rear-Block Fan Pressure Ratio	
P93Q2	Front-Block Fan Pressure Ratio	
Q	Process Noise Covariance Matrix	
R	Measurement Error Covariance Matrix	
RALS	Remote Augmented Lift System	
RALS	Minimum RALS Augmentation (HTV Transition)	
RDL	RALS Deflection Angle (Longitudinal)	degrees

Symbol	Description	Engr. Units
RDT	RALS Deflection Angle (Transverse)	degrees
RFCV	Remote Flow Control Valve	
SFC	Specific Fuel Consumption	lbs/hr/lb
SM2	Front-Block Fan Stall Margin	%
SM22	Rear-Block Fan Stall Margin	%
SM25	Compressor Stall Margin	%
STP22	Rear-Block Fan Stator Position	degrees
STP49	Low Pressure Turbine Stator Position	degrees
STOL	Short Takeoff and Landing	
SYS	Linear Engine Model	
S/T	Start Transition (VTH Transition)	
t	Time	seconds
TKOA	Linear Engine Model	
TKOIF	Sensor Matrix	
TKOIP	Actuator Matrix	
TKO2P	Controller Matrix	
TR	Thrust Ratio Demand	
TVA	Thrust Vector Angle Demand	
T/O	Vertical Takeoff (VTH Transition)	
ΔT	Augmentor Temperature Rise	°R
To	Ambient Temperature	°R
T2	Fan Inlet Total Temperature	°R
T3	Compressor Discharge Temperature	°R
T41	High Pressure Turbine Inlet Temperature	°R
T48	High Pressure Turbine Discharge Temperature	°R
T49	Low Pressure Turbine Inlet Temperature	°R
T5	Low Pressure Turbine Discharge Temperature	°R
V	Flight Velocity	meters/sec.
v	Measurement Error Vector	
VABI	Variable Area Bypass Injector	
VCE	Variable Cycle Engine	
V/STOL	Vertical and Short Takeoff and Landing	
VTH	Vertical-to-Horizontal Transition	
WF36	Primary Fuel Flow	lbs/hr.
WF6	Mixed-Flow Augmentor Fuel Flow	lbs/hr.
WF86	RALS Augmentor Fuel Flow	lbs/hr.

Symbol	Description	Engr. Units
WR	Corrected Air Flow	lbs/hr.
W2R	Front-Block Fan Corrected Air Flow	lbs/hr.
W22R	Rear-Block Fan Corrected Air Flow	lbs/hr.
W25R	Compressor Corrected Air Flow	lbs/hr.
x	State Variable Vector	
XIVEL	Forward Aircraft Velocity	meters/sec.
XM	Flight Mach Number	
XM13	Front-Block Fan Discharge Mach Number	
XM93	Rear-Block Fan Discharge Mach Number	
XN2	Fan Rotor Speed	RPM
XN41R	Corrected High Pressure Turbine Speed	RPM/$\sqrt{°R}$
XN49R	Corrected Low Pressure Turbine Speed	RPM/$\sqrt{°R}$
y	Measurement Error Vector	
z	Measurement Vector	
ZIVEL	Normal Aircraft Velocity	meters/sec.
ηc	Compressor Efficiency	
ηT	Turbine Efficiency	
θF	ADEN Deflection Angle (Longitudinal)	
θB	RALS Deflection Angle (Longitudinal)	
σ	Standard Deviation	
30 RF	30% RALS Flow (HTV Transition)	
60 RF	60% RALS Flow (HTV Transition)	
80 RF	80% RALS Flow (HTV Transition)	

Subscripts

CLEAN	Clean Flow With No Inlet Distortion
COMP	Compressor
D	Demand Values
DESIGN	Nominal Design Value
DIS	Flow With Inlet Distortion
FAN	Fan
IN	Fan Inlet

Symbol	Description	Engr. Units
OUT	Fan Discharge	

Superscripts

^	Most Probable Estimate
-1	Matrix Inverse
T	Matrix Transverse

11.5 Appendix E - References

1. Brown, H., V/STOL Propulsion Control Analysis Phase I (Tasks 1 through 3), NASA CR-165207, February 1981.

2. Lebacgz, J.R., Redfore, R.C., and Beilman, J.L., An Experimental Investigation of Control-Display Requirements for a Jet-Lift VTOL Aircraft in the Terminal Area, NADC-76099-60, July 1978.

3. Bryson, A.E., Jr., and Ho, Y.C., Applied Optional Control, Hemisphere Publishing Corp., New York, 1975, Chapter 12.

4. Gelb, A., Editor, Appplied Optimal Estimation, M.I.T. Press, Cambridge, Mass., 1974, Chapters 4 and 7.